1996

Optimization of a 100-KSI yield-strength high-performance steel (HPS) for infrastructural applications

Anthony Bernard Magee
Lehigh University

Magee,
Anthony Bernard

Optimization of a 100-KSI Yield-Strength High-Performance...

June 2, 1996

OPTIMIZATION OF A 100-KSI YIELD-STRENGTH HIGH-PERFORMANCE STEEL (HPS) FOR INFRASTRUCTURAL APPLICATIONS

by

Anthony Bernard Magee

A Thesis

Presented to the Graduate and Research Committee

of Lehigh University

in Candidacy for the Degree of

Master of Science

in

Materials Science and Engineering

Lehigh University

May 1996

This thesis is accepted and approved in partial fulfillment of the requirements for the degree of Master of Science.

May 2, 1996

Date

Dr. R.D. Stout
Thesis Advisor

Dr. J.H. Gross
Thesis Advisor

Dr. S.K. Tarby
Faculty Advisor

Dr. D.B. Williams
Chairperson of the Materials Science and Engineering Department

Acknowledgments

The author would like to acknowledge Lehigh University's Center for Advanced Technology for Large Structural Systems (ATLSS) for facilitating and funding the work conducted in this thesis. ATLSS is a NSF Engineering Research Center directed by Dr. John W. Fisher. My graduate education was funded by the Oak Ridge Institute for Science and Education (ORISE).

I am eternally grateful to two of Lehigh University's most honorable Distinguished Senior Research Fellows; Dr. Robert D. Stout and Dr. John H. Gross who guided my efforts with patience, high standards and fine example. I would also like to thank Dr. Peter Likins, Dr. Alan Pense, Dr. John W. Fisher, Mr. Henry Odi, Dr. David B. Williams, Dr. S. Kenneth Tarby, Dr. John E. Bower, Dr. Behzad Bavarian (CSUN), Dr. Roger Di Julio (CSUN) and Dr. Eric Kaufmann for their support and expertise.

Special thanks are due to Dave Schnalzer (Bro. Dave), John Hoffner (John-John), Peter Bryant, Jack Gera, John "J.P." Pinter, Jack Williams, Dave Ackland and Lehigh's Instructor of the Year 1996 "Uncle Arlan" Benscoter for their technical support. Thanks are also due to Thomas "T.J" Todaro for being a wonderful mentor; and to my summer 1995 intern Lysa Chizmadia.

I would like to thank my beloved mother, the late Novel Jean Taplin-Magee to whom this work is dedicated. Special thanks are due to the entire Taplin Family, the Bowers, Wayne L. Bethea, Aloria Lei Armstrong and her family for their support and understanding throughout my education.

Table of Contents

List of Tables

List of Figures

Abstract

The development of the 100-ksi grade steels is designed to contribute future high-performance steels (HPS). High-performance steels are defined as steels having better combination of characteristics than existing steels with respect to one or more of the following: strength, yield-tensile ratio, fracture toughness, ductility, weldability, uniformity, corrosion resistance and fatigue life. The purpose of this investigation is to develop a chemical composition and thermo-mechanical controlled processing (TMCP) for a 100-ksi yield strength steel that can be welded without preheat and with the strength and toughness of low carbon, low alloy 100-ksi steels previously studied by the Advanced Technology for Large Structural Systems (ATLSS) Center at Lehigh University. Modified A710-grade-A class-1, low carbon, Cu-Ni-Cr-Mo-Cb, copper precipitation hardened high-performance steels have been selected for study in this research. A thorough examination of the hardenability of these HPS was conducted via Jominy end-quench hardenability tests. Tempering studies were performed to evaluate the effect of tempering on hardness for various treatments and TMCP practices. The mechanical properties of these HPS were determined by tensile and Charpy V-Notch impact tests. Metallographic techniques, such as, light optical microscopy (LOM), scanning electron microscopy (SEM), and transmission electron microscopy (TEM) were employed to evaluate the microstructures, fractography and microanalysis of these high-performance steels. These low-carbon Cu-Ni steels, relatively lean in other additions offer combinations of yield strength and fracture toughness superior to present

commercial structural steels; with yield strengths exceeding 100-ksi and high Charpy V-Notch toughness down to -120F and lower.

1. Introduction

1.1 Purpose of Present Investigation

The purpose of this investigation is to develop a chemical composition and thermo-mechanical controlled processing (TMCP) for a 100-ksi yield strength steel that can be welded without preheat and with the strength and toughness of low carbon, low alloy 100-ksi steels previously studied by the Advanced Technology for Large Structural Systems (ATLSS) Center at Lehigh University.

Dynamic infrastructure applications such as buildings and bridges are fabricated from ASTM A36 (36-ksi minimum yield-strength), and ASTM A572 and A588 (50-ksi minimum yield-strength) steels. Today, there is a necessity to upgrade the quality of the infrastructure in the United States.[1-7] At ATLSS, prior research and development of high-performance steels (HPS) propose that substantial weight-savings and cost advantages could ensue if 70 to 100 ksi minimum yield-strength were employed.[9-13]

The significant factor in cost saving through use of HPS steel in construction is the reduction or elimination of preheat for welding, by significantly reducing the carbon content[12] Thermo-mechanical controlled processing (TMCP) studies showed the resulting loss in strength due to the reduction of carbon content could be off-set by controlled-rolling and direct quenching (CRDQ). It was also determined that controlled-rolling, air-cooling, and off-line heat treatment (CRAQ) also augmented toughness, however strength-gains were not as notable as those obtained by the CRDQ processing technique. [13]

The high strength steels currently accessible commercially are limited in usefulness due to the following conditions:[2,3]

1. the fatigue strength does not scale-up with the yield strength.

2. most of the steels average about 0.15% carbon, have high coarse-grain heat-affected-zone (HAZ) hardness when welded, and therefore require preheat to avoid hydrogen-assisted HAZ cracking.

3. many of the steels do not have sufficient notch toughness to meet the specifications for fracture-critical members.

4. the steels often have unacceptably high yield-strength and tensile-strength ratios.

5. the higher-strength thinner-section steels must exhibit improved corrosion to provide acceptable life cycles.

Various investigators[9-22] have addressed the foregoing limitations. At the Lehigh University Center for Advanced Technology for Large Structural Systems (ATLSS), a solution to the fatigue problem is being studied through improved design. Limitations 2, 3, 4 and 5 are being addressed through the development of new high-performance steels (HPS). This approach involves studies of chemical composition and thermo-mechanical processing (TMCP).[9-13]

Previous ATLSS investigations of chemical composition have included a broad range of carbon contents, alloying elements, and atomic strengthening mechanisms. These have indicated that the carbon content should be less than 0.09% to minimize susceptibility to heat-affected zone (HAZ) cracking and to optimize fracture toughness.[9] The ultimate objective is to develop suitable low cost, low alloy 100-ksi steels which could be utilized as High-Performance Steels and would meet the American Association of State Highway Transportation (AASHTO) and the ASTM requirements (Tables I and II). So far, the Cu-Ni precipitation-hardening type steels have shown the greatest promise for good strength and toughness in heavy sections. Table III demonstrates the metallurgical development of high-performance steels and their various applications.[12]

1.2 Background

Many bridges fabricated in the 1960's and early 1970's from A514/A517 steel have suffered from hydrogen cracks which occured during fabrication. Cracking has also been observed in A572 and A588 steel structures. The frequent occurrence of hydrogen cracking in high-strength steel has inhibited application. [8] Hydrogen cracking is most effectively avoided by using steel and weld metal with microstructures that are not susceptible. Susceptibility to hydrogen cracking increases significantly as the carbon content exceeds 0.1%.[2] The susceptible microstructures are typically martensite.[17] A number of low-carbon steels have been developed that are not susceptible to hydrogen cracking.

In the 1970's, microalloyed steels with low carbon content, high manganese levels and microalloy carbide and nitride formers were developed as construction materials with high-strength, good weldability[24-26], and good low-temperature toughness. Over the past decade, steels similar to ASTM A710 (low-carbon, age-hardenable steels) have gained increasing usage in shipbuilding, heavy-vehicle manufacturing, and offshore structure construction because of their excellent weldability and fracture toughness. These steels have become known as high-strength low alloy steels although their total alloy content is generally around 4%.[2]

Another method of increasing strength without increasing carbon and alloy content is controlled rolling, combined with on-line accelerated cooling, i.e., thermomechanical controlled processing (TMCP). The equipment required to make TMCP steels runs into a substantial capital investments, and so far the U.S. steelmakers have not deemed the potential market to be large enough to justify this investment.[2,13]

However, TMCP steels in the 50-ksi (350 MPa) to 80-ksi (600 MPa) yield strength range are widely produced in Japan and Europe and have found markets through- out the world. In fact, some of these steelmakers will supply TMCP plate and rolled shapes to fill orders that require only conventional structural steels, since it is no longer cost effective to produce both types of steel. Thus, if a large enough market can be developed, this high-performance steel can be produced at a cost which is equal or lower than the traditional steel of comparable strength.[2,10,13]

1.3 Thermo-Mechanical Controlled Processes (TMCP) at ATLSS

Thermo-mechanical controlled processing (TMCP) is defined as any combination of mechanical and thermal production processes intended to obtain preferred properties within a material. This is accomplished by controlling plastic deformation of a material within the hot-working temperature range. The ultimate goal is to improve mechanical properties beyond those normally achievable by conventional means. [11]

The three TMCP treatments investigated were as follows:

1. **HRAQ** - *Conventional Hot-Rolled and Air-Cooled, then off-line Quenched.*
2. **CRDQ** - *Control-Rolled using 2T practice to 1600°F and Direct Quenched.*
3. **CRAQ** - *Control-Rolled using 2T practice to 1600°F, Air-Cooled and Off-line*

Quenched.

Previous ATLSS investigations of thermo-mechanical controlled processing indicated the following:[9]

1. controlled rolling followed by direct quenching (CRDQ) increased the yield strength by 10 to 20 ksi, resulted in significant anisotropy, reduced the toughness in the transverse direction, and increased the yield-tensile ratio.

2. for certain compositions, controlled rolling followed by air cooling and off-line quenching and tempering (CRAQ) was observed to improve the strength-toughness relationship compared with conventional hot rolling followed by air-cooling and off-line quenching and tempering (HRAQ).

To evaluate these TMCP variables, the optimization study included HRAQ vs CRAQ vs CRDQ processing. Figure 1 schematically represents various examples of TMCP treatments.

2. Experimental Procedures

2.1 Melting and Rolling of Steels

Two different 500-lb heats of steel were vacuum-melted by the United States Steel Technology Center with the following compositions (Table IV):

U-Steel (*1" Plate Gauge*)

C	Mn	P	S	Si	Cu	Ni	Cr	Mo	V	Cb	Al
0.075	1.50	0.012	0.0046	0.25	0.96	0.75	0.50	0.50	0.058	0.025	0.034

V-Steel (*2" Plate Gauge*)

C	Mn	P	S	Si	Cu	Ni	Cr	Mo	V	Cb	Al
0.073	1.49	0.015	0.0050	0.23	0.95	0.75	0.50	0.50	0.059	0.022	0.035

The rolling of the steels was as follows:

1. ***1-inch-thick plate***: The steel ingot was rolled straight-away to a 3.5-inch slab, cut into three equal lengths and cross-rolled into a 1-inch plates using respectively HRAQ, CRDQ and CRAQ practices described above.

2. ***2-inch-thick plate***: The steel ingot was rolled straight-away to a 4.0-inch slab, cut into three equal lengths and cross-rolled to 2-inch plate using the aforementioned TMCP conditions.

2.1.1. Thermo-Mechanical Controlled Processing

Hot-Rolled Practice:

U-Steel - The 7-inch-thick ingot was rolled to a 3.5-inch-thick slab (12"wide x 39" long), cut into three 13-inch long pieces, and cross-rolled to 1-inch-thick plate as follows:

1. Cut A - Heat slab to 2275F, roll in 6 passes and finish at 1900F, and air-cool (HRA).

2. Cut B - Heat slab to 2150F, roll in 3 passes to 2 inches, hold to 1750F, control-roll in 4 passes to 1-inch at 1600F, and direct-quench at 50F/sec (CRDQ).

3. Cut C - Heat slab to 2150F, roll in 3 passes to 2 inches, hold to 1750F, control-roll in 4 passes to 1-inch at 1600F, and air cool (CRAQ).

V-Steel - The 7-inch-thick ingot was rolled to a 5-inch-thick slab (12"wide x 30" long), cut into three 10-inch long pieces, and cross-rolled to 2-inch-thick plate as follows:

1. Cut A - Heat slab to 2275F, roll in 4 passes and finish at 1900F, and air-cool (HRA).

2. Cut B - Heat slab to 2150F, roll in 2 passes to 4 inches, hold to 1750F, control-roll in 4 passes to 2-inch at 1600F, and direct-quench at 50F/sec (CRDQ).

3. Cut C - Heat slab to 2150F, roll in 2 passes to 4 inches, hold to 1750F, control-roll in 4 passes to 2-inch at 1600F, and air cool (CRAQ).

Figure 2 and 3 illustrate the respective rolling schedules involved in the processing of the high-performance steel.

2.2 Heat Treatment

Austenitizing - The hot-rolled plates were cut into convenient test sections and heat-treated as outlined in Table VII for steels U and V. The cooling rates were chosen to simulate those that would be expected in production as illustrated in Figure 4. The curves shown are the best current information for production facilities. Additional information is desired because of the limited number of such facilities in the United States. The cooling rates reported in Table VIII are based on the rate between 1472F and 932F (800C and 500C).

The *IQ Water* practice involved immersion quenching into mildly agitated water at 60F. The average typical cooling curves for immersion-quenched 1/2-, 1-, and 2-inch-thick plates are shown in Figure 8. The corresponding cooling rates are tabulated for plates cooled from 800C to 500C (1479F to 932F). For practical purposes, these rates are the same as the rates at 1300F (cooling from 1500F to 1100F), which are the rates published for the Jominy test. These rates are shown in Figure 4 for comparison with typical spray-quench production practices and in Figure 9 to illustrate their location with respect to distance from the quenched end of the Jominy test. As shown in Figure 4, this laboratory quenching practice agrees extremely well with that shown for typical production. Therefore, the cooling rates for 3- and 4-inch-thick plates are tabulated on Figure 9 and are identified by plate thickness on subsequent Jominy curves.

Spray Q involved spray quenching using four solid cone nozzles, 5.5 inches apart vertically and horizontally, and eight inches from the mid-thickness of a vertically suspended plate, using 60F water at 95 psi pressure. The rates were varied by using different flow-rate nozzle sets shown in Table V.

All plates were treated in the thickness indicated except for the simulation of production quenching of 4-inch plate, which was done at three different cooling rates - air-cooling a 1/2-inch plate (2F/sec.) and spray quenching a 1-inch plate using different nozzle sets to produce cooling rates of 5F/sec. and 9F/sec. The different rates represent different opinions on the best simulation for production quenching of a 4-inch plate.

At the U.S. Steel Technical Center facility, the "USS Spray" involved direct cooling from the rolling mill into a spray-quench runout table. All plates were cooled continuously to room temperature using the same cooling medium, except for the "CR+IAC" interrupted-accelerated-cooling practice which involved quenching from 1600F to 1050F followed by air-cooling to ambient temperature.

2.3 Quenching Practice

Steel plates processed via HRA and CRA processes were off-line austenitized at 1650°F and water quenched. The quenching of these plates were performed by means of *total immersion* or *spray* quenching on a spray quench facility (Figures 5 and 6), designed to simulate the cooling rates associated with commercial direct quench facilities. In the ATLSS spray quench facility, the cooling rate of the steel plates are controlled by varying nozzle size, spray pressure, nozzle to plate distance and nozzle quantity demonstrated in Table V.

2.4 Cooling Rate Studies

Cooling rates were measured on the 100-ksi yield strength steel plate of the targeted chemical composition. The steel plate specimens consisted of an 8 x 10 inch plate with varying thickness'; 0.5, 1.0 and 2.0-inch, respectively. The plate specimen was austenitized at 1650F, removed from the furnace, transported and placed in a vertical position within the spray quench apparatus and spray quenched (Figure 7). By imbedding a thermo-couple inside the center of each plate, cooling rate curves were traced and generated by an electronic x-y plotter connected to the thermo-couple. The cooling rate was calculated in the temperature range of 932F to 1472F.

2.5 Mechanical Property Tests

2.5.1 Tempering and Hardness Surveys.

A tempering survey was conducted on the test steels in each TMCP condition. This study served as a guide for determining the tempering temperature that would produced the optimum combination of mechanical properties. A series of small metallographic blocks were taken from the quenched plates and tempered between 1000F and 1350F. Hardness measurements were gathered from the small steel blocks and correlated to yield/tensile strength. The Wilson Series 500 Rockwell Hardness Tester was employed to measure all hardness values, via Rockwell C (HRc). HRc employs a brale diamond "C" indenter loaded by a minor load of 10 kg and a major load of 150 kg. The resulting tempering curves are shown in Figure 10 and 11 for the U and V steel treatments. The tempering curves were used to select appropriate tempering temperatures. Calculated Ae_3 and Ae_1 transformation temperatures for steels U and V are tabulated in Tables VI and VII, respectively. The details of the heat treatment for Steels U and V are summarized in Table VIII.

2.5.2 Tensile Tests

Standards taken from the ASTM E8-91 and A370 specifications were observed for all tensile experiments. Two standard steel tensile coupons were machined from each plate and tested in an ambient environment. For 1/2-inch thick test plates, standard 0.252-inch diameter tensile coupons were machined; and for 1 and 2-inch thick test plates, standard 0.505-inch diameter tensiles were machined. From each test, a plot of load versus displacement was generated and from these plots, the yield and ultimate strength per test was calculated. The percent elongation, percent reduction in the cross-sectional area, fracture stress and the yield-to-tensile strength ratio was also obtained.

2.5.3 Charpy V-Notch Impact Tests

For each steel condition, sixteen standard transverse Charpy V-Notch specimens were machined according to the ASTM E23-92 and A370 testing specifications and notched in the through thickness direction. For 2-inch-thick plate, specimens were machined from the plate and identified as top, top-middle, bottom-middle, and bottom specimens. The CVN specimens were tested between a temperature range -140F and +100F chosen to analyze the ductile to brittle transition-temperature behavior. In order to generate temperatures below room temperature (70°F), a liquid-nitrogen cooled ethanol bath was used. A hot water bath was used for temperatures above ambient conditions. For each specimen, the absorbed energy, lateral expansion and fracture appearance data was recorded.

2.5.4 Jominy End-Quench Hardenability Tests

In determining the hardenability of the special 100-ksi yield strength steel, three 1-inch-diameter by 3-inch-long cylinders Jominy end-quench specimens (per steel) were machined and tested according to ASTM A255-89. The Jominy bar specimens were austenitized in a furnace at 1650°F and held for one hour. The specimen was then water-quenched individually in a standard Jominy end-quench apparatus. After the bar was completely cooled, two opposing sides of the Jominy bar was ground to a flat surface. On the flat surfaces, hardness measurements were taken at 1/16 inch intervals for the first inch and in 1/8 inch intervals thereafter for the remaining length of the specimen. Hardenability curves were generated from the collected data as hardness vs. distance from quenched end of the Jominy bar. The specimens were then tempered at 1050F, 1150F, or 1250F and again hardness-tested.

2.7 Metallographic Evaluation

Jominy End-Quench Hardenability Test - One hardness-test flat on the end-quenched specimen for each steel was polished and etched and the microstructure at sixteenth-inch intervals for the first inch from the quenched end and at eighth-inch intervals for the second inch was photographed at a magnification of 1000X. Selected scanning-electron micrographs were also obtained.

Tempering Studies - The microstructure at 1000X of selected tempered specimens was obtained to illustrate the change in microstructure with tempering temperature.

Mechanical Tests - For each mechanical-test series, the microstructure at 1000X was obtained to characterize that test condition.

Transmission Electron Microscopy - Several selected specimens were thinned to permit internal examination of the steel for the presence of copper precipitates and dislocation effects.

All samples examined via light optical microscopy were well-polished and etched with a 50/50 mixed solution of 2% nital and 4% picral and observed at 1000x magnification.

2.8 Fractographic Evaluation

Typical fracture surfaces of selected tensile, and CVN specimens were observed via Amray 1810 Scanning Electron Microscope (SEM). This technique aided in detecting microvoid coalescence (ductile) and cleavage (brittle) characteristics present on fractured surfaces. The photographs were taken at various magnifications, approximately 20 mm working distance and 20 keV accelerating potential.

3. Results and Discussion

3.1 Jominy End-Quench Hardenability Results

Standard-Test Results - The results of the Jominy tests are shown in Figure 12. The microstructure and hardness at the various distances from the quenched end of the bar correspond to continuous-cooling rates (measured at 1300F) of about 500F/second at 1/16 inch for the quenched-end to 3.5 F/second at two inches from the quenched-end. These cooling rates encompass all the rates that occur at the midthickness of plates of any thickness through 4 inches when quenched in production facilities. Consequently, the curves are useful in estimating the microstructure and hardness and therefore the tensile strength to be expected. The cooling rates at 1300F at the center of 1-, 2-, 3-, and 4-inch thick plates quenched at an approximate severity of H = 1.5 (Figures 4 and 8) are shown along the abscissa of the Jominy plots. These are the approximate cooling rates to be expected when plates are quenched in standard roller or platen production facilities, which are also the same for the Laboratory "IQ Water" quench employed in the present study. The plateau hardness of 25 HR_C for the Steels U and V suggests that 4-inch-thick and thicker plate can attain a tensile strength of about 123-ksi and therefore a yield strength above 100-ksi. The calculated ideal critical diameter (D_I) was 3.04.

Tempered-Jominy-Test Results - Tempering the Jominy specimens permits analysis of the effect of reheating on the full range of microstructures that result from end-quenching. In the case of these Cu-Ni steels, tempering results in competition between softening due to carbide agglomeration and strengthening due to copper-particle precipitation. The effect of tempering the Jominy-test specimens for Steels U and V is shown in Figure 12. At 1050F, the previous plateau value of 25 HRc increases to 28/29 HRc as a result of copper precipitation strengthening. At 1150F and 1250F, the original plateau hardness is retained as a result of a lesser but significant copper precipitation strengthening and some vanadium strengthening above 1150F.

3.2 Mechanical-Property Testing

The mechanical-property tests were conducted to characterize these steels with respect to tensile and impact-toughness behavior. Of particular interest was the ability of the steels to meet a minimum yield-strength of 100-ksi in a minimum plate thickness of 2 inches with an aim of 4 inches. The determination of yield strength in the present tests was done in accordance with Section 7.5.1 Offset Method of ASTM E8 using the usual offset of 0.2%.

Tension- and Impact-Test Results - The results of tension and Charpy V impact test are listed in Tables IX and X, for Steels U and V, respectively. The strength and toughness properties are depicted in Figures 14, and 15, respectively. As illustrated in Figure 14, 1-inch-thick Steel U readily meets the 100-ksi minimum yield strength for all rolling practices after appropriate tempering. For conventionally rolled and air-cooled (HRA) and off-line austenitized specimens, tempering at 1250F produced the best combination of strength and toughness. This was also the case when the steel was control-rolled to 1600F, air-cooled (CRA), and off-line austenitized and then tempered at 1250F. When the plate was control-rolled to 1600F and immediately direct-quenched, the yield strength and tensile strength were increased by more than 10-ksi compared with the other two practices. However this treatment resulted in extraordinarily high yield-to-tensile-strength ratios approaching 1.0.

As also shown in Figure 14, the toughness of Steel U is extraordinary, and is characterized by very high energy absorptions in the fully ductile condition and by extremely low transition temperatures. It readily meets the AASHTO fracture-critical energy absorption of 30 ft-lb at -120F. This Cu-Ni type steel exhibits a better combination of strength and toughness than any existing structural steel.

As illustrated in Figure 15, the strength and toughness of the 2-inch-thick Steel V was similar to that of the 1-inch-thick steel, except that the toughness was not quite as good as that for the 1-inch-thick plate. As discussed in detail later, the 2-inch-thick plate cooled at a mid-thickness rate of about 20F/second compared with 50F/second for the 1-inch-thick plate, typical for production quenching facilities (Figure 4). Consequently, the 2-inch-thick plate transformed to lesser amounts of low-temperature transformation products. Nevertheless, the combination of strength and toughness is far better than that of any existing 100-ksi yield-strength structural steel.

Figure 16 illustrates the strength and toughness for Steel U when 1/2- and 1-inch-thick plates were cooled at rates similar to those at the mid-thickness of production-quenched 4-inch-thick plates. As shown in Figure 4, 9F/second is more typical for production quenching of 4-inch-thick plate than 5F/second or 2F/second, which resulted from air cooling a 1/2-inch plate, is ultraconservative and corresponds to plate much thicker than 4 inches. At a cooling rate of 2F/second, the yield strength averaged 98-ksi and the energy absorbed was 55 ft-lb at -40F. At 5F/second, the corresponding values were 114-ksi and 55 ft-lb, and at 9F/second were 108/112 ksi and 65/48 ft-lb at -40F when tempered at 1175F. The strength and toughness were quite good but depended on the actual cooling rate (2, 5, or 9F/second). These results confirm the Jominy data for the high hardenability steels, which indicated that they should be suitable for the most stringent bridge requirements in 4-inch-thick plate. It should be noted that as the thickness increased from 1- to 2- to 4-inch-thick plate, the yield-tensile ratio decreased significantly as a result of the decrease in low-temperature transformation products with decreased cooling rates. However, it should also be noted that the properties of the 4-inch were simulated using 1/2- or 1- inch plate, and therefore, the effect of thickness reduction during hot-rolling is not incorporated in the results.

Figure 16 also illustrates simulated interrupted accelerated cooling (IAC) of 1-inch-thick Steel U. The results suggest that IAC may be appropriate for producing an 80-ksi yield-strength steel after appropriate tempering. However, its use as-quenched is not recommended because its yielding characteristics were so erratic that reproducible yield-strength values could not be obtained. These results clearly demonstrate that a hardenability D_I value of 3.0 will ensure a minimum yield strength of 100-ksi and excellent toughness through 2 inches and possibly through 4-inches. It is therefore recommended that a minimum D_I of 3.0 be established for Cu-Ni steels of the type under study to ensure excellent toughness in plates through 4 inches thick when conventionally rolled and heat-treated. This level of hardenability is also estimated to be necessary for interrupted-accelerated-cooling to a minimum yield strength of 80-ksi and good toughness in plates through 4-inches thick.

Strength - Toughness Relationships - Of particular interest are the combinations of yield strength and Charpy notch toughness that can be obtained in these heats of Cu-Ni steel as a function of composition, section thickness, and thermomechanical treatment. Since the steels were selected as candidates for bridge constuction among numerous potential applications, it is appropriate to examine their performance at -40F, a temperature conservatively below the -30F AASHTO test temperature specified for 100-ksi yield-strength steels in Zone 3, the most severe environment. The rationale for the alloy design of the Cu-Ni HPS can be shown by referring to the Granville diagram (Figure 17) [17]. This diagram shows the susceptibility of a steel composition to heat affected zone (HAZ) cracking as a function of carbon content and carbon equivalent. Figures 18 and 19 present the range of strength-toughness combinations in Steels U and V.

From Figure 18a it is evident that Steel U exceeded the 30 ft-lb AASHTO requirement for all conditions studied. Water quenching from 1650F readily produced yield strengths above 100-ksi. Treatment simulating the quenching and tempering of 4-inch thick plate met yield-strengths of 90 to 98 ksi. The general decrease in the yield-strength-toughness levels was related to the respective decreases in cooling rate and low-temperature transformation product. However, the microstructure produced at the reduced cooling rates is suprisingly strong and tough. Figure 18b shows that the same composition in 2-inch thickness, Steel V, likewise exceeds 30 ft-lb at -40F in all treatments utilizing water quenching and appropriate tempering. As to be expected, tests in the longitudinal direction to rolling were somewhat tougher than those in the transverse direction, even though the plates were cross-rolled.

The extraordinary notch toughness of the U and V heats of the Cu-Ni steels is further illustated in Figure 19. The water-quench and temper treatments can generate 35 ft-lb transition temperatures below -120F and as low as -200F in the 1-inch-thick plate.

3.5 Metallographic Evaluation

3.5.1 Tempered Microstructures

Figures 20a through d and 21a through d, show selected microstructures from various tempering studies performed on Steels U and V, each. The selected microstructures represent the "As-Quenched" condition as well as thoses tempered at 1200F, 1250F, 1275F 1300F and 1350F, respectively. Figure 20a through c show various microstructures of the aforementioned tempering conditions performed on HRA, CRDQ, and CRA thermo-mechanical processes of Steel U. The "as-quenched" condition of each Steel U TMCP is shown in Figure 20d. The same heat treatments performed on Steel U specimens were conducted on Steel V specimens (Figure 21a through c). The *as-*

quenched microstructures of Steel V (HRA, CRDQ and CRA) are represented in Figure 21d. The appropriation of metallographic specimens is illustrated in Figure 22.

3.5.2 Jominy End-Quench Hardenability Microstructures

An evaluation of the microstructural changes occurring along the length of the Jominy specimens, beginning at the quenched-end, is illustrated in Figures 24a through d and selected SEM micrographs are shown in Figures 25a through c for Steel-U. Figures 26a through d, illustrates the microstructural changes occurring along the length of the Jominy specimens, beginning at quenched-end for Steel-V. Figure 26 (Steel-V) depicts the best representation of microstructural changes of the two steels of like-compositions. At 1/16-inch, the microstructure is fully martensitic. At 2/16-inch, a very small amount of granular bainite is present with the martensite.[29] From 3/16-inch, the amount of granular bainite increases until it reaches 100 percent at 6/16-inch. Granular bainite is described as packets of ferrite laths with inter-lath second phase particles of primarily martensite with some small amounts of retained austenite that has been significantly enriched in carbon content by the prior transformation products. From 7/16-inch on, the acicularity of the transformation products decreases very gradually with decreased cooling rate until the second-phase tends to break-down into smaller discrete particles in a ferrite matrix.[14,29] The second-phase particles also increase in size with decreased cooling rate, so that by 18/16-inch they are large enough to reflect light and begin to appear light in color. Except for some increase in size and decrease in number of the second-phase particles, the microstructures remains generally similar from 12/16- through 32/16-inch. This behavior is consistent with the relatively constant hardness over this Jominy distance range. These are very desirable types of microconstituents, which after tempering have an excellent combination of strength and toughness. Thus, the plateau of 28 to 25 HRc is desirable for a relatively high-hardenable steel.

3.5.3 Test Specimen Microstructures

For every specimen that was solution heat-treated and tested for mechanical properties, a representative microstructure is shown in Figures 26a through h for Steels U and V. Microstructures representing the various heat treatments performed on Steel U (1-inch thick plate) with respect to the HRA, CRDQ and CRA thermo-mechanical processes can be observed in Figures 26a through e. Figures 26f, g and h show the microstructures of Steel V (2-inch thick plate) for various heat treatments and HRA, CRDQ and CRA thermo-mechanical processes, respectively.

3.5.4 Transmission Electron Microscopy

Figures 27a through f, show various (thin foil) TEM microstructures depicting observations of copper precipitation formation within grain-boundaries and dislocation pinning within the grains.[30] Many different patterns of dislocation bands are present in each micrograph. In Figure 27g, the diffraction pattern illustrates the spots belonging to the face-centered cubic copper precipitates lying within the grainboundaries and iron matrix. [14,28,30]

3.5.5 Scanning Electron Microscopy

An evaluation of the fracture morphology studied on each of the steel conditions HRAQ, CRDQ and CRAQ was performed using scanning electron microscopy. SEM micrographs were taken to show the different modes fracture; dimple rupture and cleavage.[27] Figure 28 represents the fracture surface morphology of typical tensile failures. Figures 28a and b show the fracture surface of a typical HRAQ specimen. Figures 28c and d and Figure 28e and f illustrate the fracture surfaces of typical CRAQ and CRDQ specimens, respectively. Each of these conditions showed splitting phenomena in their fractured surfaces especially in CRDQ specimens.

Figure 29 is representative of the Charpy V-Notch (CVN) impact fractography. In Figures 29a and b, the typical CVN fracture surface at +70F is shown. Figure 29a shows the overall view of the fracture surface, whereas Figure 29b illustrates a mode of ductile fracture at 1000x magnification. In Figure 29c and d, the typical CVN fracture surface at -40F show a more brittle (cleavage) type mode of fracture. Due to the high level of mixed-mode phenomena (mixed shear/cleavage morphology), it was therefore difficult to assess the percentage of fiberous fracture present on the fracture surface of these Cu-Ni steels. The typical shear/cleavage mixture in the midthickness of the CVN specimen in these low-carbon high performance steels are shown in Figures 29e and f.

The scanning electron microscope can be easily converted into an instrument capable of chemically microanalyzing specimens. A representative chemical microanalysis of these 0.07C, Cu-Ni high-performance steels is shown in Figure 30.

4. Conclusions

4.1 Merits and Limitations of Optimized HPS

The main objective of this study was to develop a chemical composition and thermo-mechanical controlled processing (TMCP) that would produce an improved 100-ksi yield strength steel for high-performance steels (HPS) application. The following conclusions are drawn as the product of this investigation:

1. Low-carbon Cu-Ni steels relatively lean in other alloy additions offer combinations of yield strength and fracture toughness superior to present commercial structural steels.

2. Yield strengths exceeding 100-ksi with high Charpy V-Notch toughness down to -120F and lower are readily obtained by control of the carbon level and alloy additions for adequate hardenability when conventionally rolled and off-line quenched and tempered.

3. Cross-rolled plates containing 0.07C, 1.0Cu, 0.75Ni, and sufficient Mn, Cr, and Mo to ensure a critical-bar-diameter (D_I) hardenability of 3.0 can be expected to

exhibit the following properties when conventionally rolled and off-line quenched and tempered:

a. A minimum yield strength of 100-ksi through 2 inches and a minimum Charpy V-Notch energy at -40F of 100 ft-lb and 60 ft-lb for 1- and 2-inch-thick plate, respectively.

b. A minimum yield strength of 90 ksi at 4 inches and a Charpy V-Notch energy at -40F of 90 ft-lb.

4. When the foregoing steel is subjected to in-line interrupted accelerated cooling, a minimum yield strength of 90-ksi and a Charpy V-Notch energy at -40F of 90 ft-lb in 1-inch plate.

5. These high-perfomance steels at their respective carbon-levels (0.07) and carbon equivalents (0.68) should be weldable and safe under all conditions in the *zone one* region using the Graville diagram.

Table I - AASHTO Charpy Requirements for A514 Steel

Zone	Charpy Requirements *
1 (0F & above)	35 ft-lb at 0F
2 (-1F to -30F)	35 ft-lb at 0F
3 (-1F to -60F)	35 ft-lb at -30F

*Up to 4" thick mechanically fastened or up to 2.5" thick welded

Table II - ASTM Charpy Requirements for A710-A-1 Steel

Orientation	Charpy Requirements *
Longitudinal	20 ft-lb at -50F
Transverse	15 ft-lb at -50F

* In accordance with Test Frequency H of Specification A 673/A 673M (for average minimum values)

Table III: High-Performance Steels
Metallurgical Development

Application	Typical Component	Current Yield Strength ksi	HPS Yield Strength, ksi	Material Properties*			
				Fracture Toughness	Formability	Weldability	Corrosion Resistance
Navy Surface Ships	Carrier Flight Deck	100	100	1	3	1	4
	Double Hulls	50/80	50/80	2	3	1	3
Military Vehicles	Personnel Carriers	50/80	80/100	1	3	1	3
Commercial Ships	Double Hulls	36/50	50/80	2	3	1	2
	Deck	36/50	50/80	2	3	1	2
Offshore Structures	Welded Tubes	36/50	70/80	2	2	1	3
	Built-Up Sections	36/50	70/80	2	3	1	3
Pipelines	Welded Line Pipe	50/70	70/100	1	2	1	3
Tanks and Pressure Vessels	Light-Gage Shells	36/60	70	2	2	2	3
	Heavy-Gage Shells	36/50	70/100	1	2	1	3
	Heads	36/50	70/100	2	1	2	3
Transportation Equipment	Railroad Cars	36/60	80/100	1/2	2	1	3
	Trucks	36/50	80/100	1/2	2	1	3
Buildings	Built-Up Sections	36/50	50/100	2	3	2	3
	Welded Tubes	36/50	50/100	2	1	1	3
Bridges	Built-Up Sections	36/50	70/100	1	2	1	1
	Critical Members	36/50	70/100	1	2	1	1
Construction Equipment	Decks	36/50	70/80	3	3	2	1
	Crane Booms	80/100	80/100	1	2	1	3
	Buckets, Blades	100	100+	1	3	1	4

*1 - Critically Important 2 - Important 3 - Desirable 4 - Not Applicable

93-B054-2

Table IV - Compositions of A514-F, A710-A and A710 Type Steels

Elements	Steels			
	A514-F	***A710-A***	***U***	***V***
C	0.10-0.20	0.07*	0.075	0.073
Mn	0.60-1.00	0.40-0.70	1.50	1.49
P	0.035*	0.025*	0.012	0.015
S	0.035*	0.025*	0.0046	0.005
Si	0.15-0.35	0.40*	0.25	0.23
Cu	0.15-0.50	1.00-1.30	0.96	0.95
Ni	0.70-1.00	0.70-1.00	0.75	0.75
Cr	0.40-0.65	0.60-0.90	0.50	0.50
Mo	0.40-0.60	0.15-0.25	0.50	0.50
V	0.03-0.08	-	0.058	0.059
Al	NA	-	0.034	0.035
Cb	-	0.02min	0.025	0.022
B	0.0005-0.006	NA	NA	NA
CE**	0.615	0.552	0.688	0.685

**** Maximum Content***
***** Carbon Equivalent based on IIW formula,***
NA = Not Added

$$CE = C + Si/6 + Mn/6 + (Cu+Ni)/15 + (Cr+Mo)/5 + V/5$$

Table V - Compilation of Spray Quench Nozzle Characteristics

Nozzle I.D.	*Spray Angle (deg)*	*Water Pressure (psig)*	*Gal./min.*	*Nozzle Quantity*
Del SQ5	60	40	0.9	4
	60	70	1.1	4
Del SQ10	60	40	1.8	4
	60		2.4	4
Del SQ18	60	40	3.3	4
	60	70	4.1	4
Del SQ29	60	40	5	4
	60	70	6.3	4
Seinen 10.0		90	0.93	4
Hago 1900		90	0.31	4
Del CE 2-70deg	70	90	0.55	8
Del. 10.0	80	90	0.16	8
Monarch F-80	80	90		8

Table VI - Ae3 transformation temperatures for the re-heat treating study

Steel	U	V
*Ae3 (F)	1524	1523

*Ae3 = 1600 - (375x%C) - [(25x%Mn)-4.5] - (32x%Ni) + [(80x%Si)-10] - (3x%Cr) + %Mo

Table VII - Ae1 transformation temperatures for the Ae1 tempering study

Steel	U	V
*Ae1 (F)	1292	1291

*Ae1 = 1333 - (25x%Mn) - (26x%Ni) + (40x%Si) + (42x%Cr) + (20x%Mo)

Table VIII Plate Heat Treatment of Steels U and V

Designation	Thickness Inch	Rolling Practice	Simulation	Austenitizing Temp (F)	Cooling Medium	Cooling Rate (F/s)	Tempering Temp (F)
U-Steel (1-inch-thick cross rolled)							
Transverse Tests							
UAY	1	HRA	Production Q&T-1"	1650	IQ Water	50	1200
UAX	1	HRA	Production Q&T-1"	1650	IQ Water	50	1275
UAM	1	HRA	Production Q&T-4"	1650	Spray Q	9	1250
UAK	1	HRA	Production Q&T-4"	1650	Spray Q	9	1175
UBY	1	CRDQ	CR+Direct Quench-1"	CR-1600	USS Spray	50	1200
UBX	1	CRDQ	CR+Direct Quench-1"	CR-1600	USS Spray	50	1275
UCY	1	CRA	CR+Prod. Q&T-1"	1650	IQ Water	50	1200
UCX	1	CRA	CR+Prod. Q&T-1"	1650	IQ Water	50	1275
UCM	1	CRA	Production Q&T-4"	1650	Spray Q	5	1225
UCIT	1	CRA	CR + IAC-1"	1650	Spray-1050	15	None
UCIX	1	CRA	CR + IAC-1"	1650	Spray-1050	15	1250
Longitudinal Test							
UAW	1	HRA	Production Q&T-1"	1650	IQ Water	50	1250
UAP	1	HRA	Production Q&T-4"	1650	Spray Q	9	1250
UAN	1	HRA	Production Q&T-4"	1650	Spray Q	9	1175
UBW	1	CRDQ	CR+Direct Quench-1"	CR-1600	USS Spray	50	1250
UCW	1	CRA	CR+Prod. Q&T-1"	1650	IQ Water	50	1250
UCP	0.5	CRA	Production Q&T- 1/2"	1650	IQ Water	115	1250
UCN	0.5	CRA	Production Q&T-4"	1650	Air Cooled	2	1175
UCIL	1	CRA	CR+IAC-1"	1650	Spray-1050	15	None
UCIW	1	CRA	CR+IAC-1"	1650	Spray-1050	15	1250
V STEEL (2-inch-thick cross-rolled)							
Transverse Tests							
VAZ	2	HRA	Production Q&T-2"	1650	IQ Water	20	1175
VAY	2	HRA	Production Q&T-2"	1650	IQ Water	20	1200
VAX	2	HRA	Production Q&T-2"	1650	IQ Water	20	1275
VCZ	2	CRA	CR+Prod. Q&T-2"	1650	IQ Water	20	1175
VCY	2	CRA	CR+Prod. Q&T-2"	1650	IQ Water	20	1200
VCX	2	CRA	CR+Prod. Q&T-2"	1650	IQ Water	20	1275
VBZ	2	CRDQ	CR+Direct Quench-2"	CR-1600	USS Spray	20	1175
VBY	2	CRDQ	CR+Direct Quench-2"	CR-1600	USS Spray	20	1200
VBX	2	CRDQ	CR+Direct Quench-2"	CR-1600	USS Spray	20	1275
Longitudinal Tests							
VAW	2	HRA	Production Q&T-2"	1650	IQ Water	20	1250
VCW	2	CRA	CR+Prod. Q&T-2"	1650	IQ Water	20	1250
VBW	2	CRDQ	CR+Direct Quench-2"	1600	USS Spray	20	1250

Table IX - Mechanical Properties of Steel U (1" Plate Gauge)

U-STEEL Processing Condition Temperature, deg. F	*Codes*	*Tensile Properties* Y.S. ksi	T.S. ksi	EL. %	R.A. %	Y.S./T.S.	*Charpy V-Notch* Transition Temperature, deg. F 20 ft-lb	35 ft-lb	60 ft-lb	15 mils	*Charpy V-Notch Energy* 70 F	0 F	-40 F	-80 F	-120 F
TRANSVERSE TESTS															
HRA (1650)+IQ+T1275	UAX	99	106	25	71	0.93	<-200	-170	-120	-200	-	110	110	90	60
HRA (1650)+IQ+T1200	UAY	114	121	22	67	0.94	-160	-125	-55	-130	-	85	65	50	35
HRA-4" Simulation 1650F+SQ(9F/s)															
Tempered at 1250F	UAM	96	107	26	72.5	0.90	-130	-100	-80	-120	-	90	75	55	25
HRA-4" Simulation 1650F+SQ(9F/s)															
Tempered at 1175F	UAK	112	123	24	64	0.90	-100	-70	0	-90	70	60	48	30	10
CRDQ+1275T	UBX	127	130	20	60	0.98	-185	-120	-60	-160	-	70	68	50	35
CRDQ+1200T	UBY	146	146	19	60	1.00	-100	-40	80	-80	-	50	35	25	15
CRA (1650)+IQ+T1275	UCX	99	108	24	70	0.92	<-200	-170	-120	-200	-	110	110	90	75
CRA (1650)+IQ+T1200	UCY	122	127	22	66	0.96	-160	-125	-55	-130	-	85	65	50	35
CRA-4" Simulation 1650F+SQ(5F/s)															
Tempered at 1225F	UCM	104	118	22	64	0.88	-115	-75	-30	-100	80	70	55	40	10
CRA (1650) CR+IAC (SQ, 1050F) (15F/s)	UCIT	120	140	17	61	0.84	-65	-40	-	-60	50	40	35	8	-
CRA (1650) CR+IAC (SQ, 1050F) (15F/s)															
Tempered at 1250F	UCIX	89	110	24	62.5	0.81	-80	-65	-50	-75	-	90	90	20	10
LONGITUDINAL TESTS															
HRA (1650)+IQ+T1250 (IQ)	UAW	105	112	26	71	0.94	-190	-180	-160	-200	-	135	140	110	70
HRA-4" Simulation 1650F+SQ(9F/s)															
Tempered at 1250F	UAP	93	107	26	70	0.87	-170	-110	-100	-140	-	115	100	85	35
HRA-4" Simulation 1650F+SQ(9F/s)															
Tempered at 1175F	UAN	108	122	24	65	0.88	-120	-95	-50	-100	120	85	65	45	20
CRDQ+1250T	UBW	129	131	23	68	0.98	-160	-140	-90	-140	-	90	85	60	55
CRA (1650)+IQ+T1250	UCW	110	116	26	73	0.95	<-200	<-200	-180	<-200	-	135	140	130	75
CRA (1650)+IQ+T1250 (1/2")	UCP	122	128	22	72	0.95	<-200	-200	-140	-200	130	120	115	100	75
CRA (1650)+AC(2F/s)+T1175 (1/2")	UCN	98	122	26	71	0.80	-90	-60	-30	-80	120	80	55	20	-
CRA (1650) CR+IAC (SQ, 1050F) (15F/s)	UCIL	77	123	21	65	0.63	0	+5	+10	0	90	20	15	10	-
CRA (1650) CR+IAC (SQ, 1050F) (15F/s)															
Tempered at 1250F	UCIW	88	110	25	66	0.80	-85	-75	-70	-80	-	125	120	25	15

Table X. Mechanical Properties of Steel V (2" Plate Gauge)

V-STEEL	*Codes*	*Tensile Properties*					*Charpy V-Notch* Transition Temperature, deg. F				*Charpy V-Notch Energy*				
Processing Condition Temperature, deg. F		Y.S. ksi	T.S. ksi	EL. %	R.A. %	Y.S./T.S.	20 ft-lb	35 ft-lb	60 ft-lb	15 mils	70 F	0 F	-40 F	-80 F	-120 F
TRANSVERSE TESTS															
HRA (1650)+IQ+T1275	VAX	91	101	26	70	0.9	-155	-150	-110	-150	-	110	108	80	45
HRA (1650)+IQ+T1200	VAY	100	110	25	70	0.9	-100	-80	-60	-85	-	100	80	35	10
HRA (1650)+IQ+T1175	VAZ	110	119	22	67	0.92	-90	-70	-40	-80	-	80	60	30	2
CRDQ+T1275	VBX	113	118	22	67	0.96	-120	-90	-60	-80	-	72	60	15	5
CRDQ+T1200	VBY	124	128	21	62	0.96	-75	-60	-35	-65	-	70	55	17	7
CRDQ+T1175	VBZ	134	137	20	61	0.97	-45	-20	-	-40	-	45	25	15	5
CRA (1650)+IQ+T1275	VCX	89	101	26	71	0.88	-140	-100	-70	-120	-	118	82	30	20
CRA (1650)+IQ+T1200	VCY	102	111	24	67	0.92	-100	-80	-50	-80	-	90	70	35	15
CRA (1650)+IQ+T1175	VCZ	111	120	22	67	0.92	-80	-55	0	-60	-	60	45	20	5
LONGITUDINAL TESTS															
HRA (1650)+IQ+T1250	VAW	114	122	24	69	0.94	-120	-115	-90	-110	-	85	80	60	20
CRDQ+T1250	VBW	128	133	23	67	0.96	-60	-20	35	-40	-	35	25	10	5
CRA (1650)+IQ+T1250	VCW	112	120	23	67	0.94	-75	-60	-45	-70	-	80	60	15	5

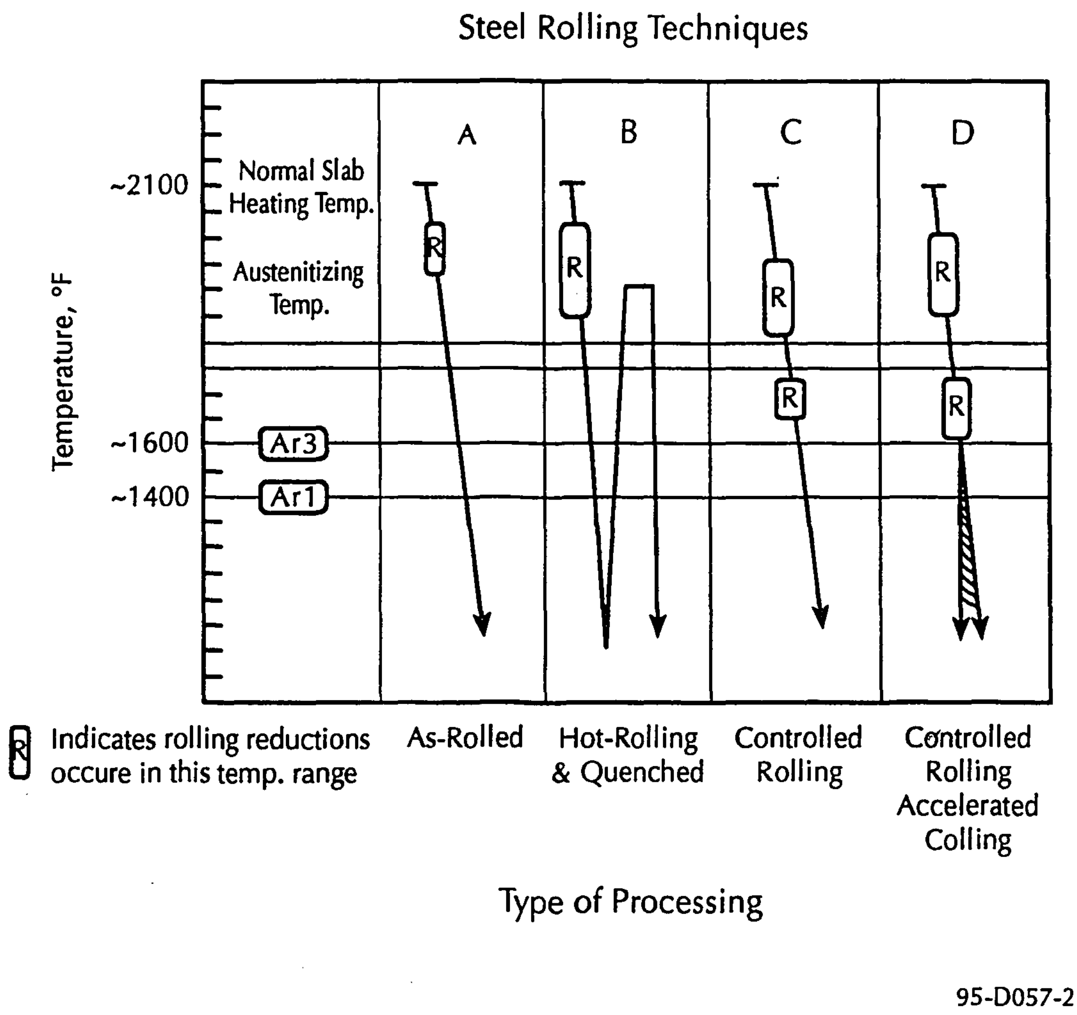

Figure 1 Schematic Representation of TMCP Treatments

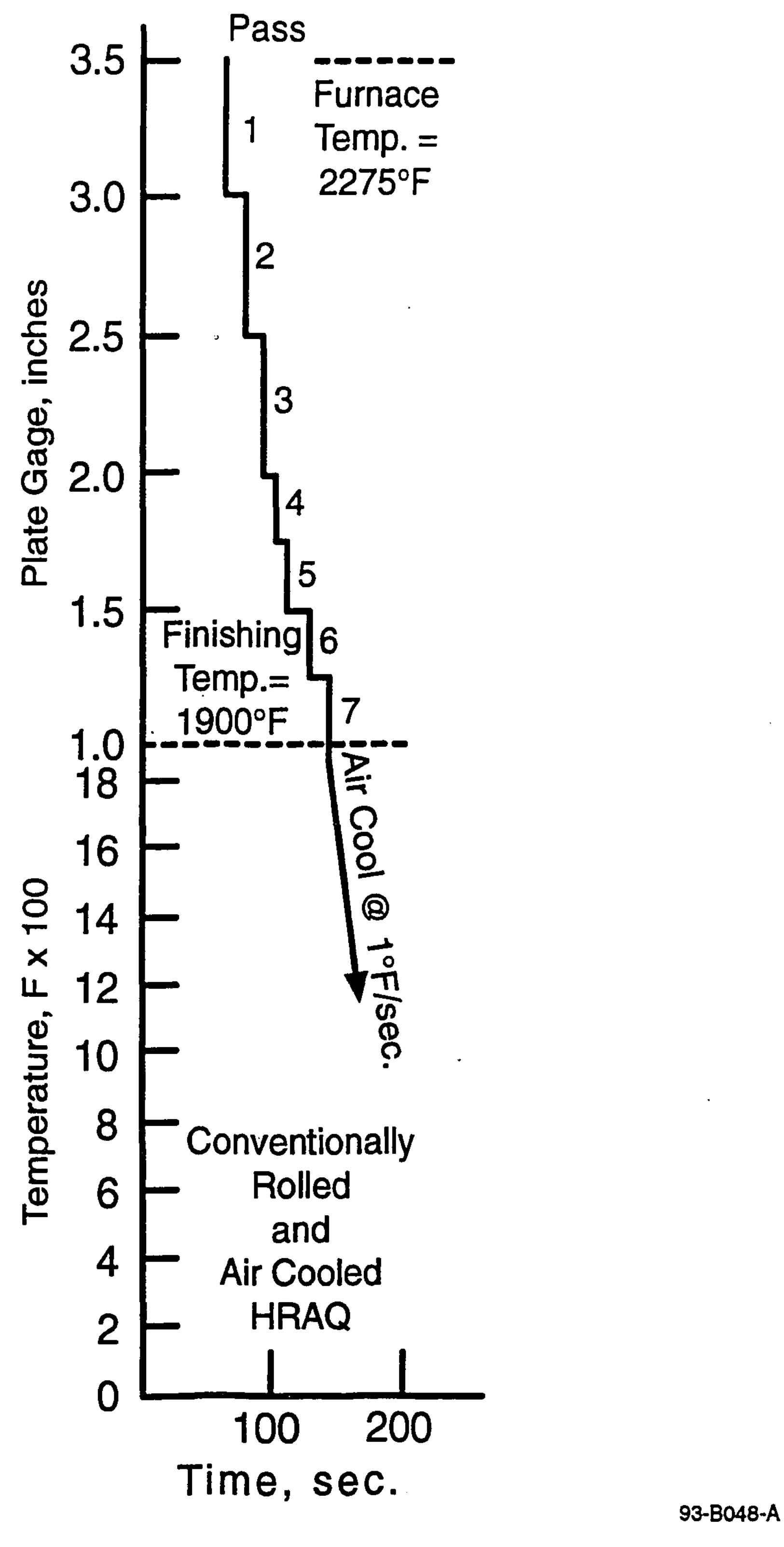

Figure 2 Rolling Schedule for Steel Plates Conventionally Hot-Rolled and Offline Air-Cooled

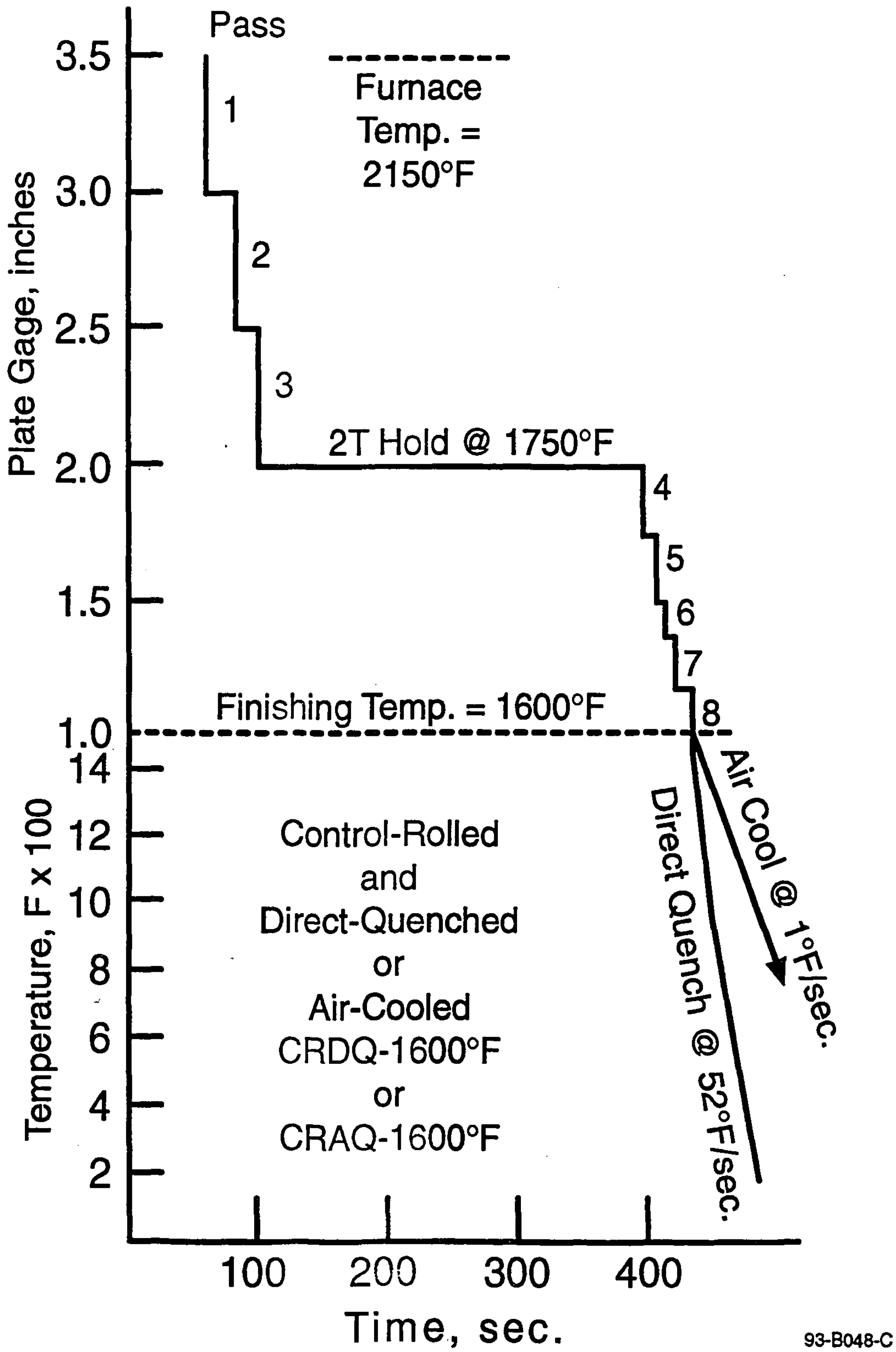

Figure 3 Rolling Schedule for Plates Control-Rolled to 1600°F and Direct-Quenched or Offline Air-Cooled

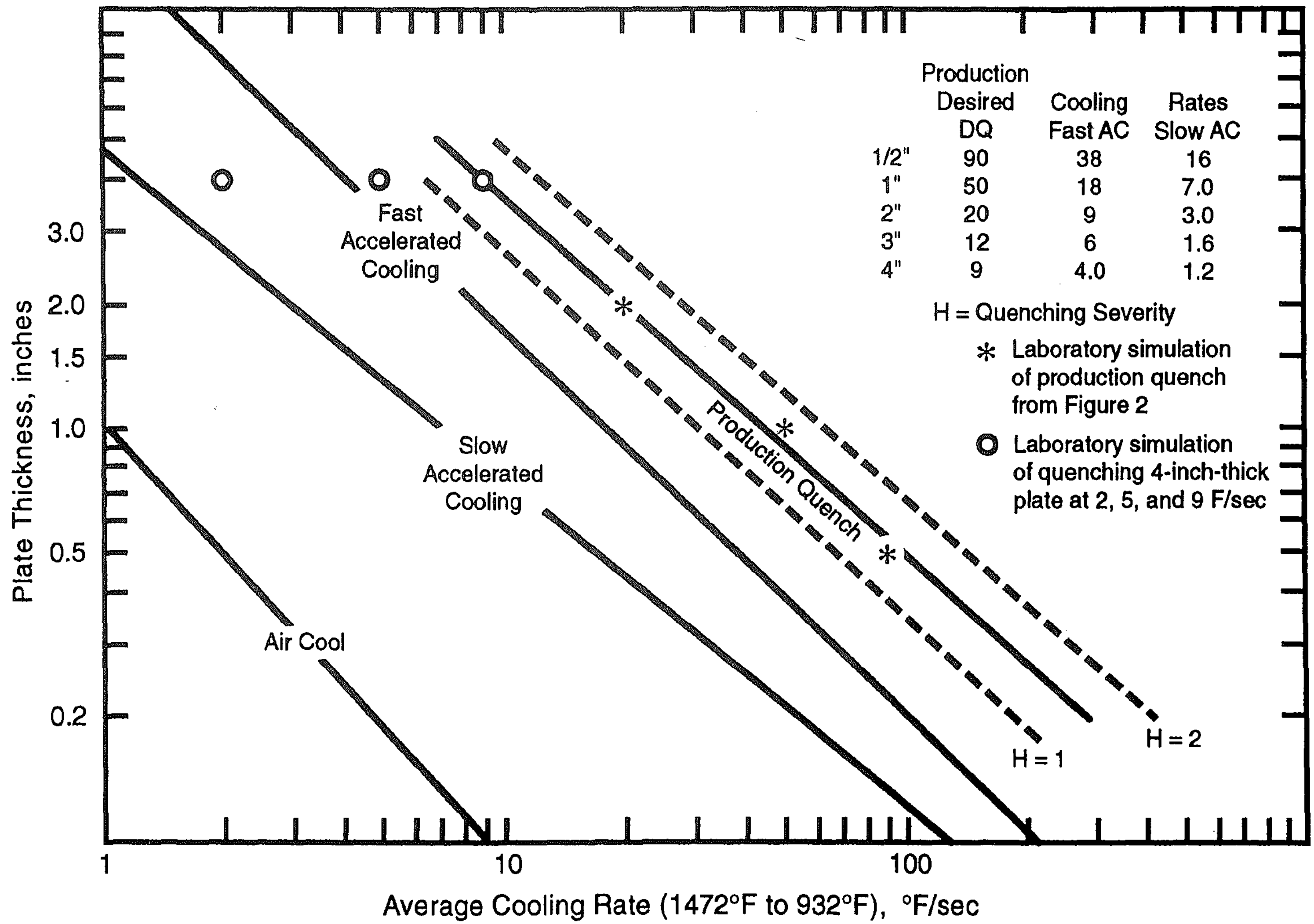

Figure 4 Illustration of Various Cooling Practices

96-E016

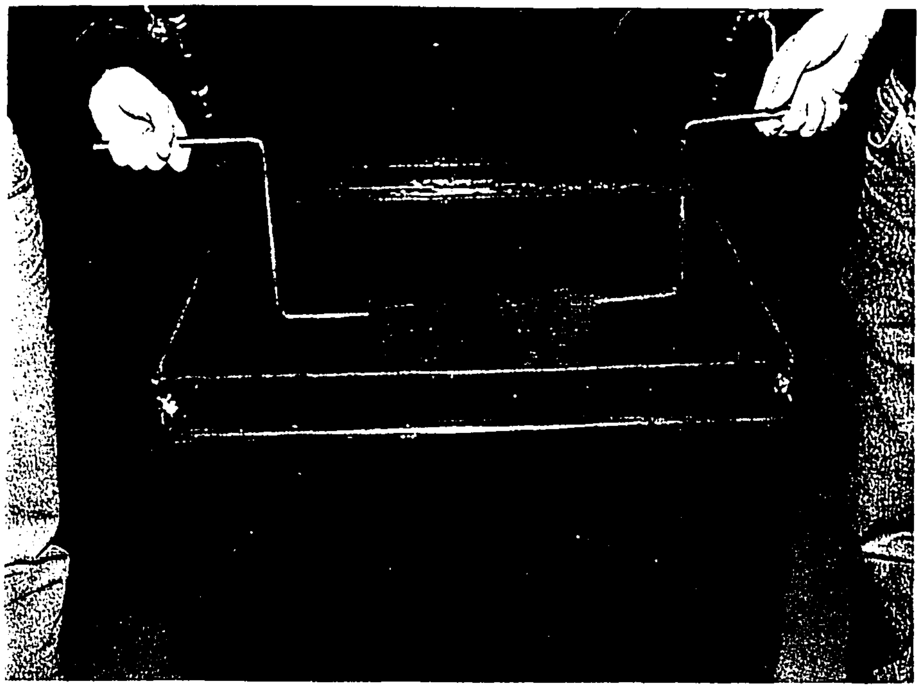

Figure 5 - Plate being immersion quenched.

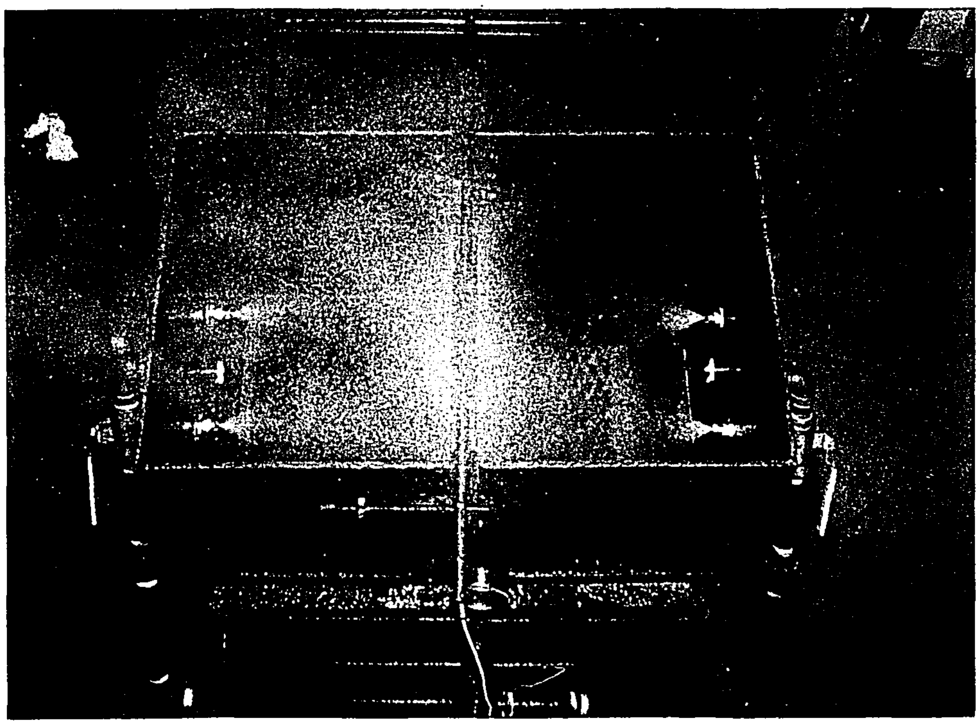

Figure 6 - Plate being spray quenched.

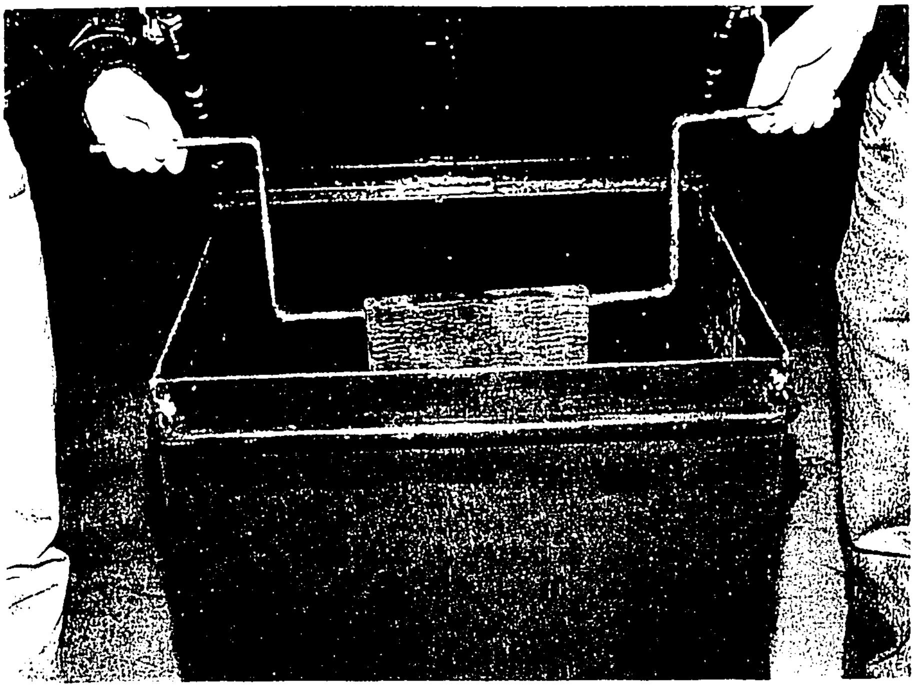

Figure 5 - Plate being immersion quenched.

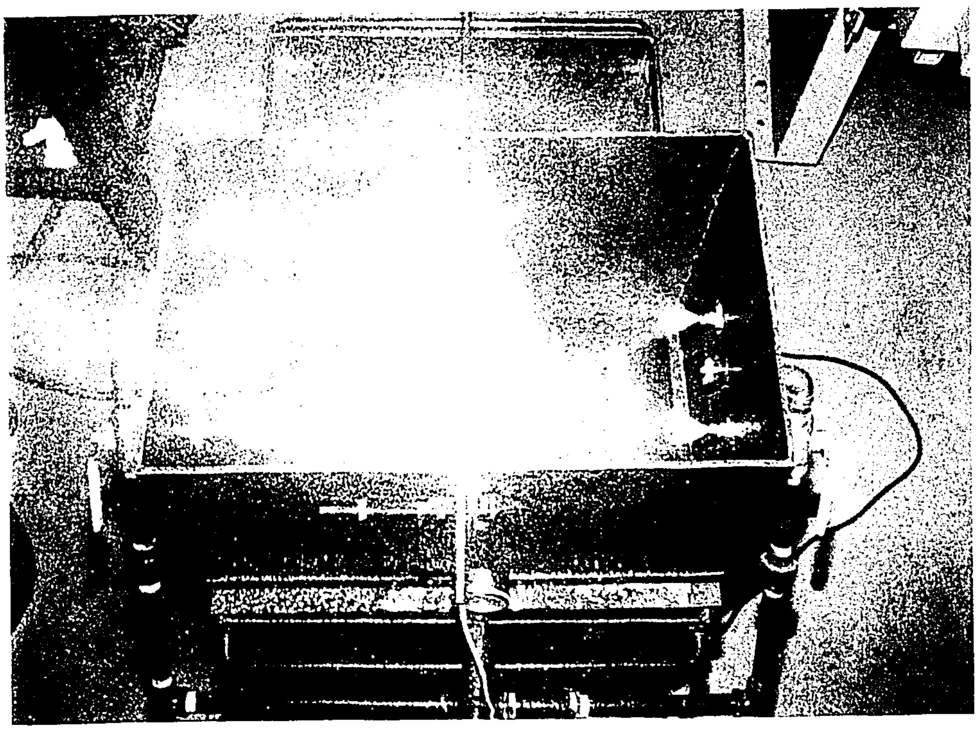

Figure 6 - Plate being spray quenched.

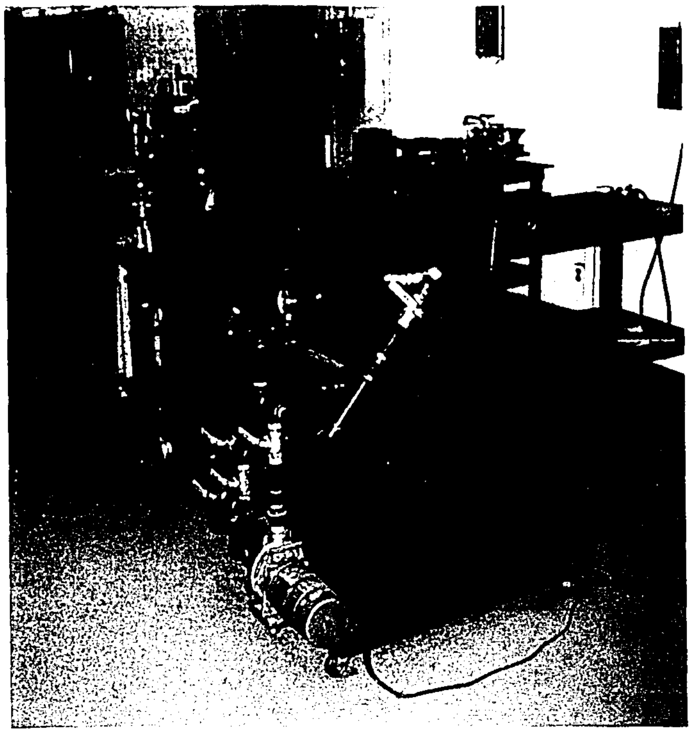

a.

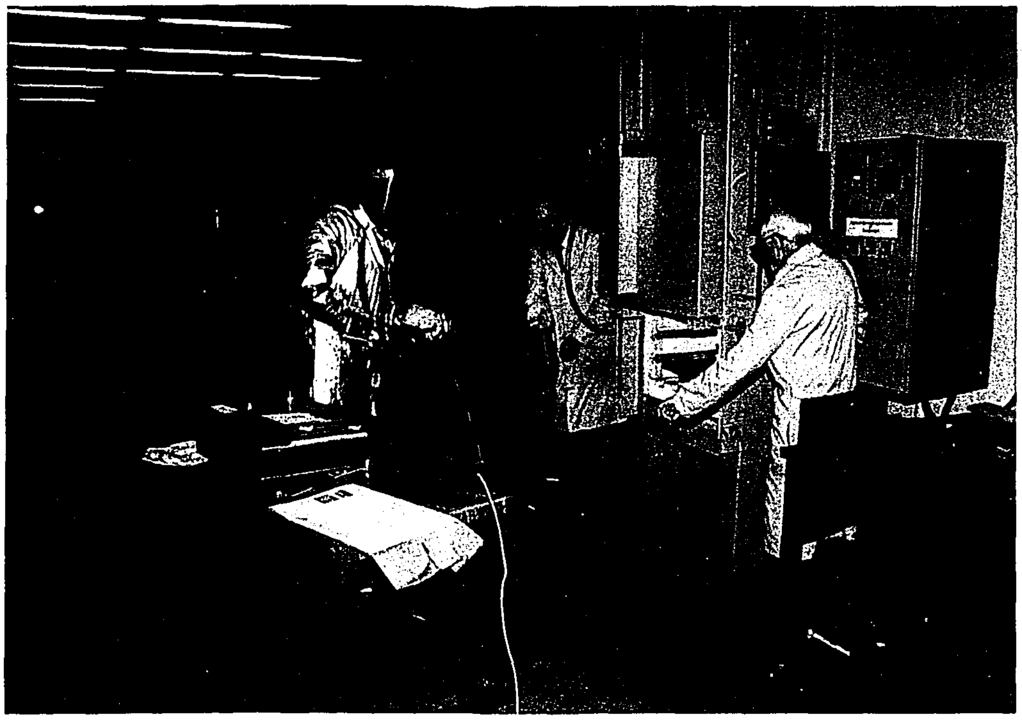

b.

Figure 7 - ATLSS Water Quenching and Heat Treating Facility.

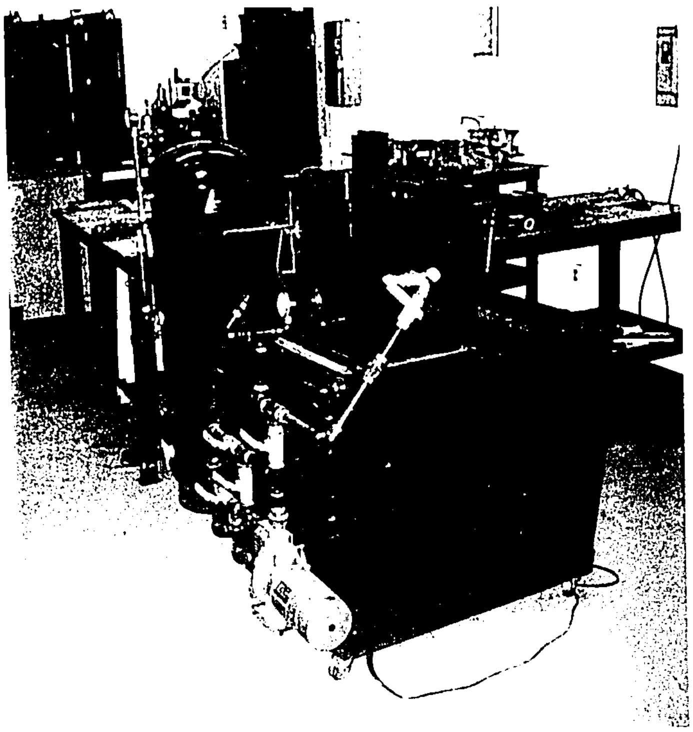

a.

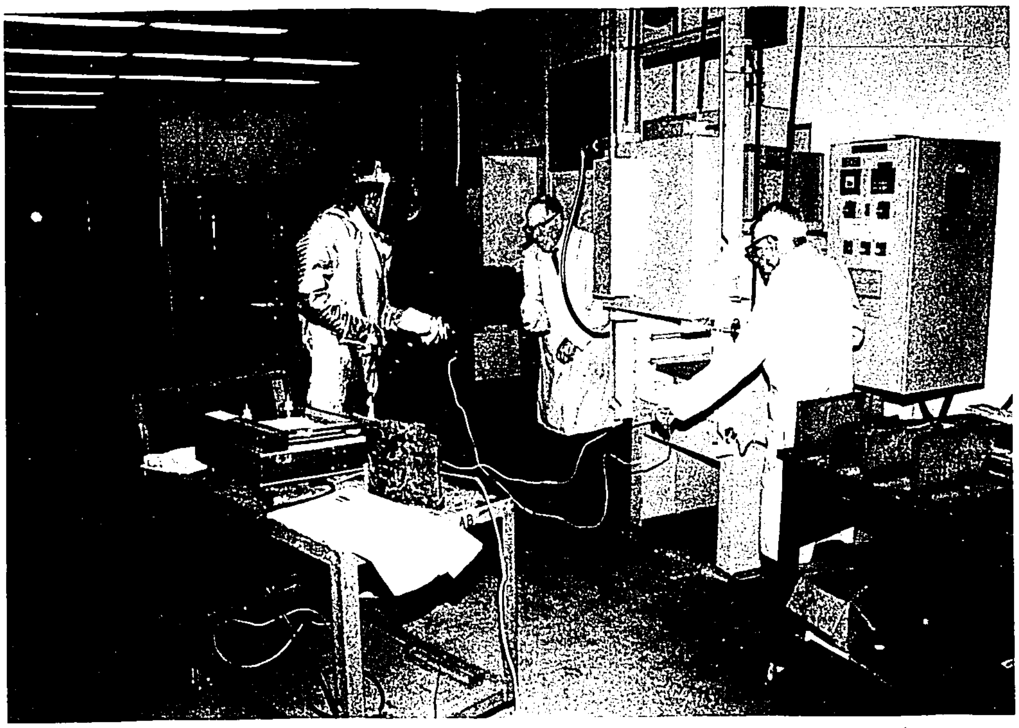

b.

Figure 7 - ATLSS Water Quenching and Heat Treating Facility.

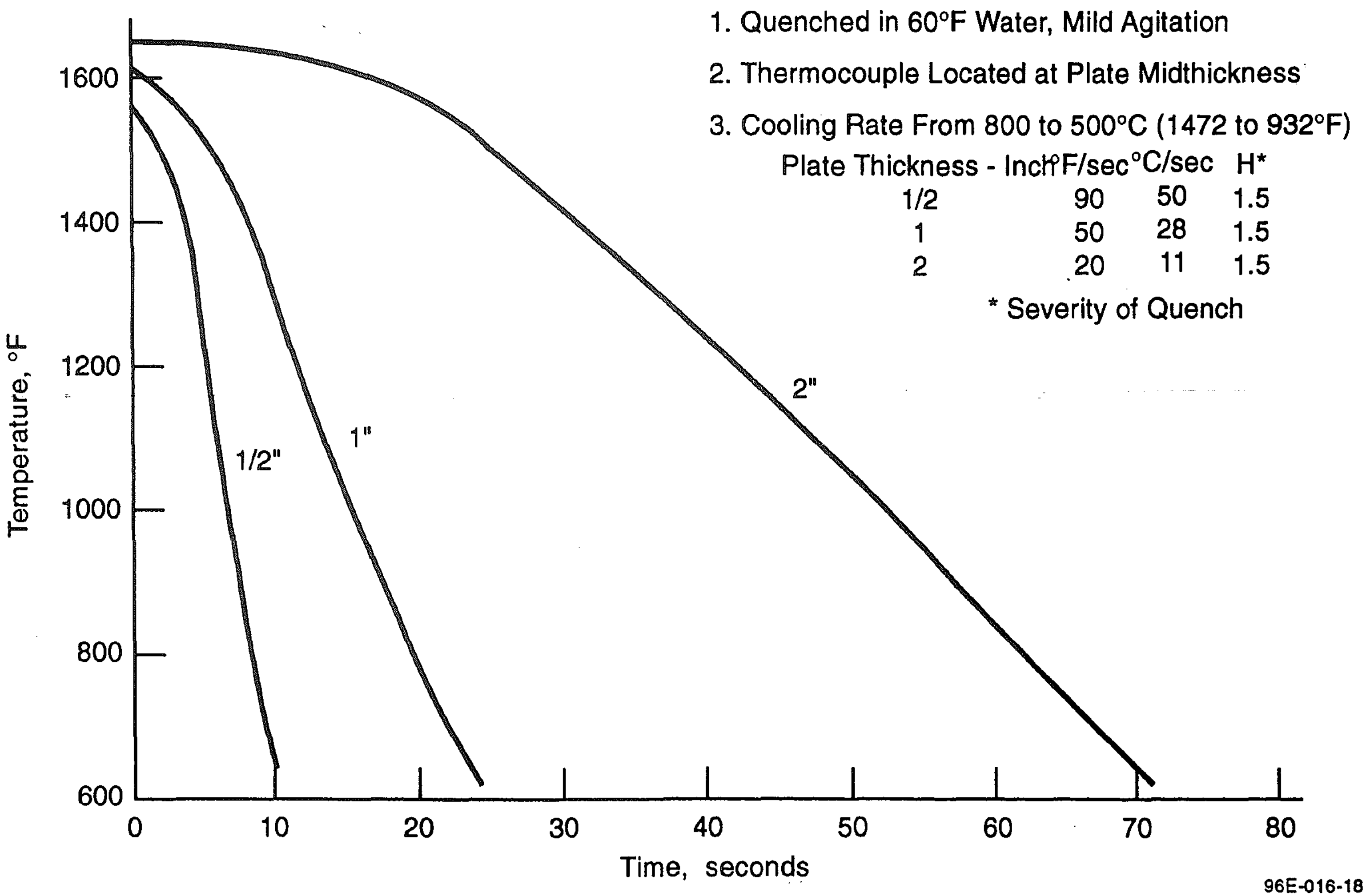

Figure 8 Cooling Curves for Laboratory Water-Quenched Plates

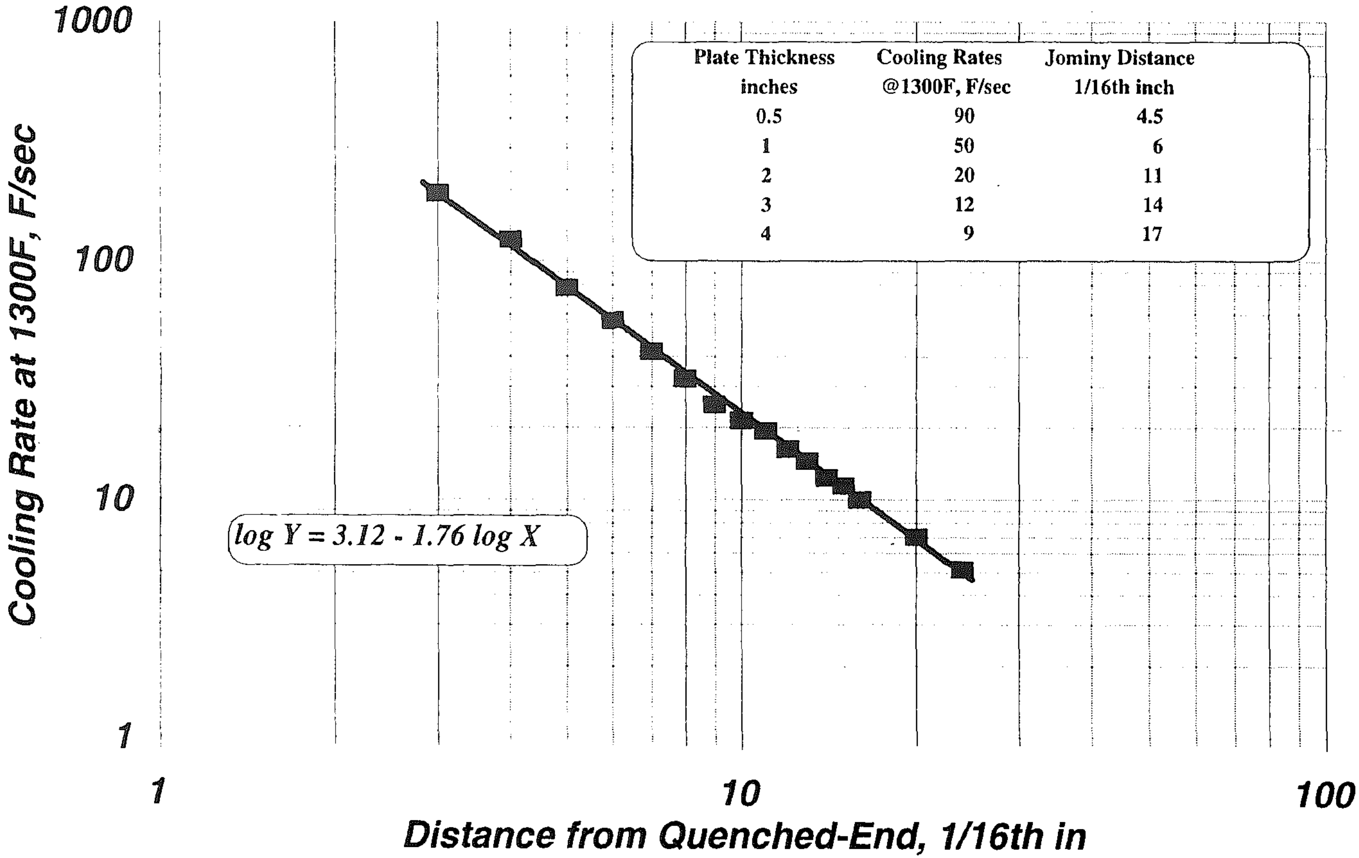

Figure 9 Jominy Test Cooling Rates and Corresponding Distances from Quenched End for Cooling Rates of Typical Production Spray Quenched and ATLSS Laboratory Immersion Quenched Steel Plates

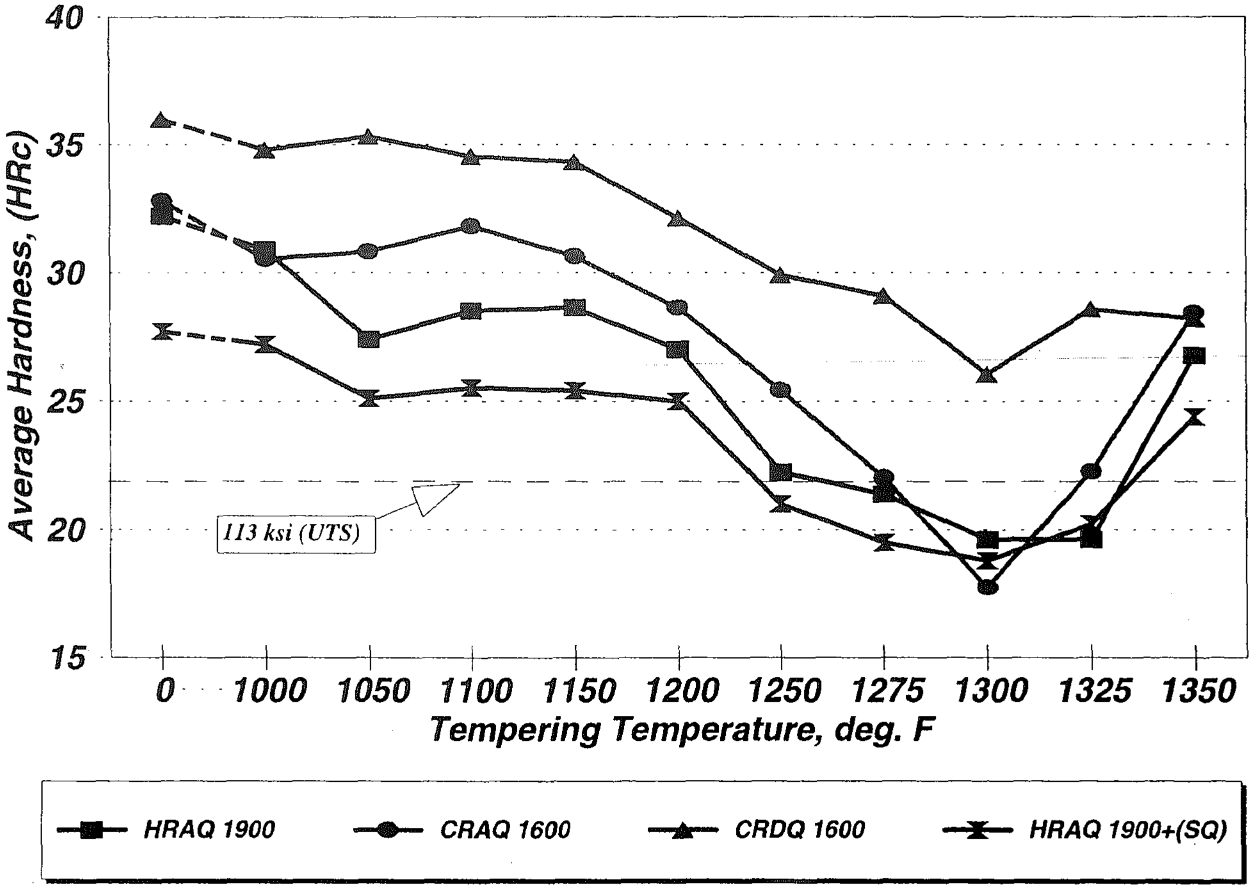

Figure 10a. Effect of Tempering on Hardness for Various Treatments of Steel U

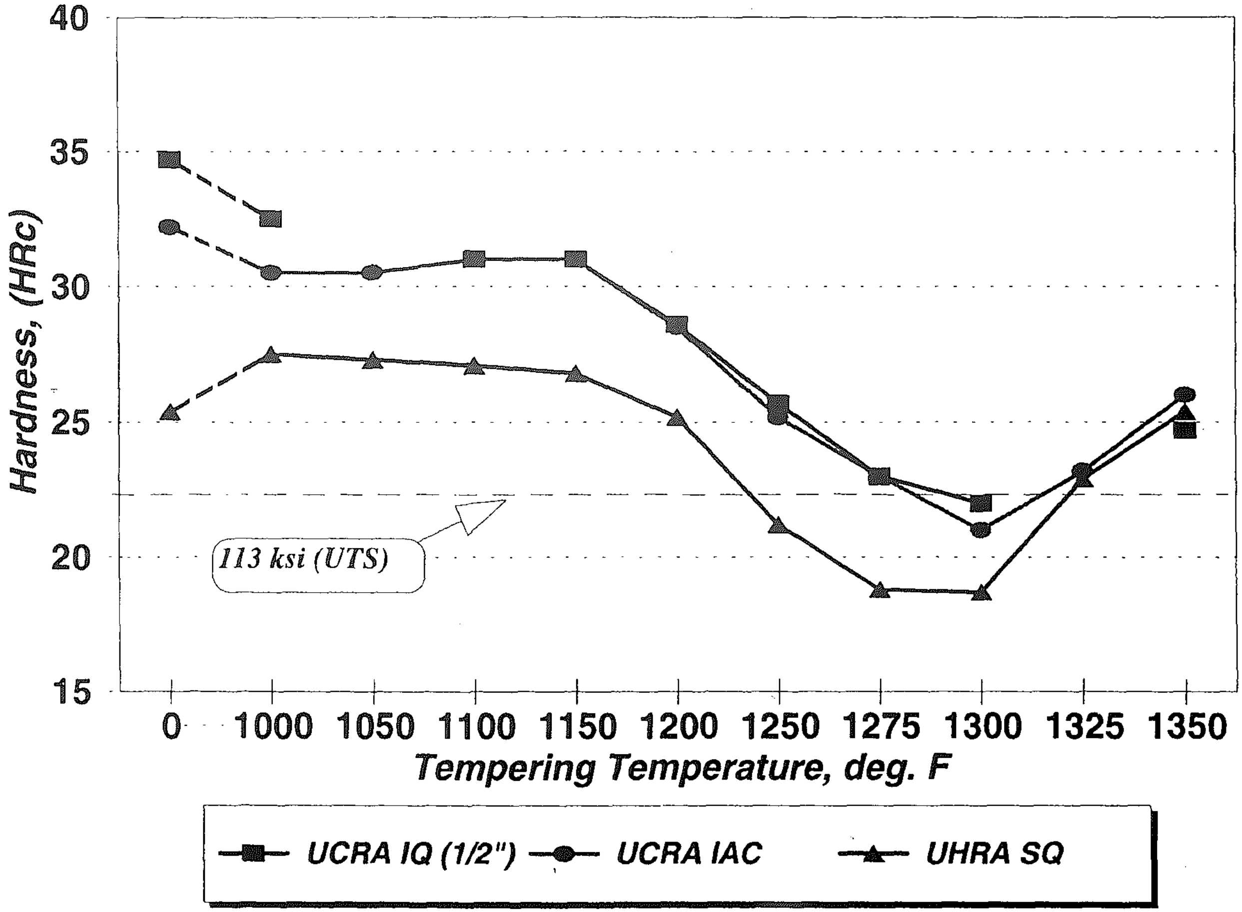

Figure 10b. Effect of Tempering on Hardness for Other Treatments of Steel U

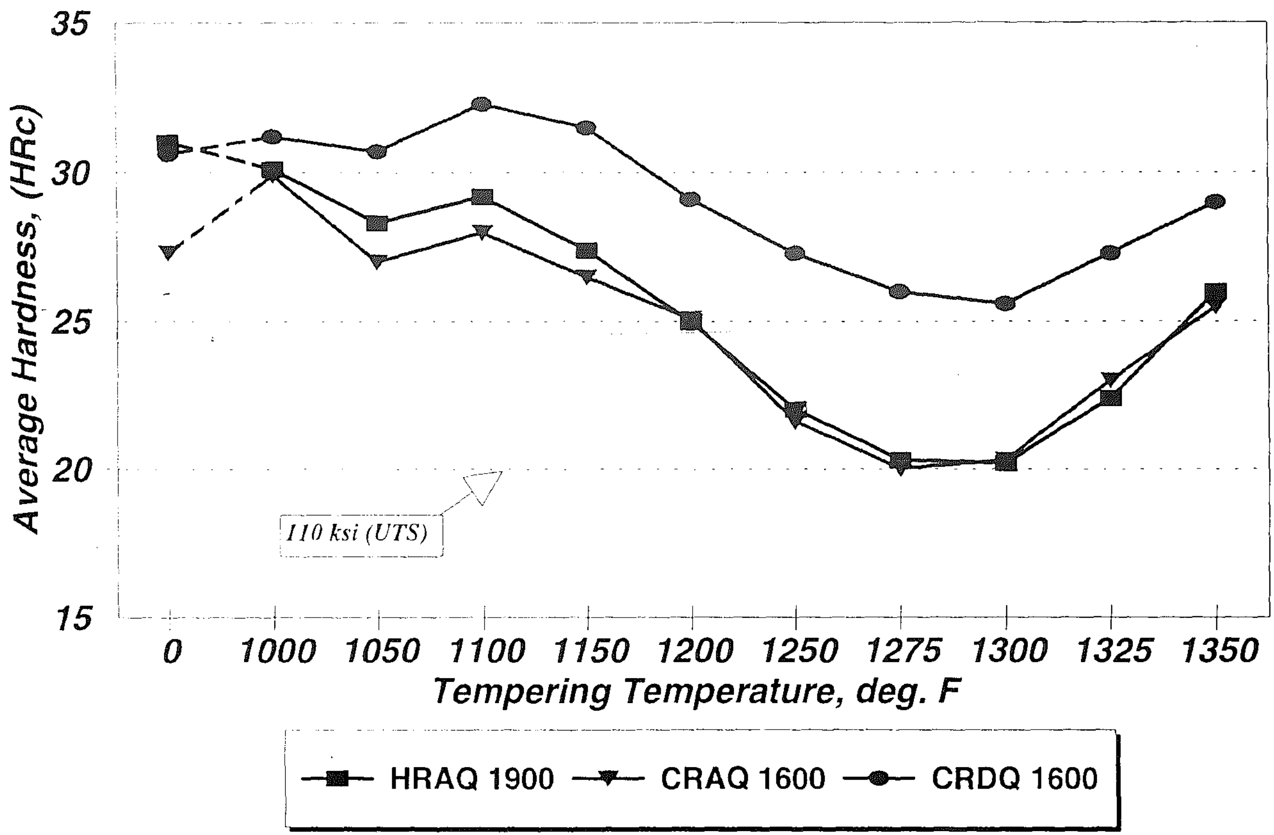

Figure 11. Effect of Tempering on Hardness for Various Treatments of Steel V

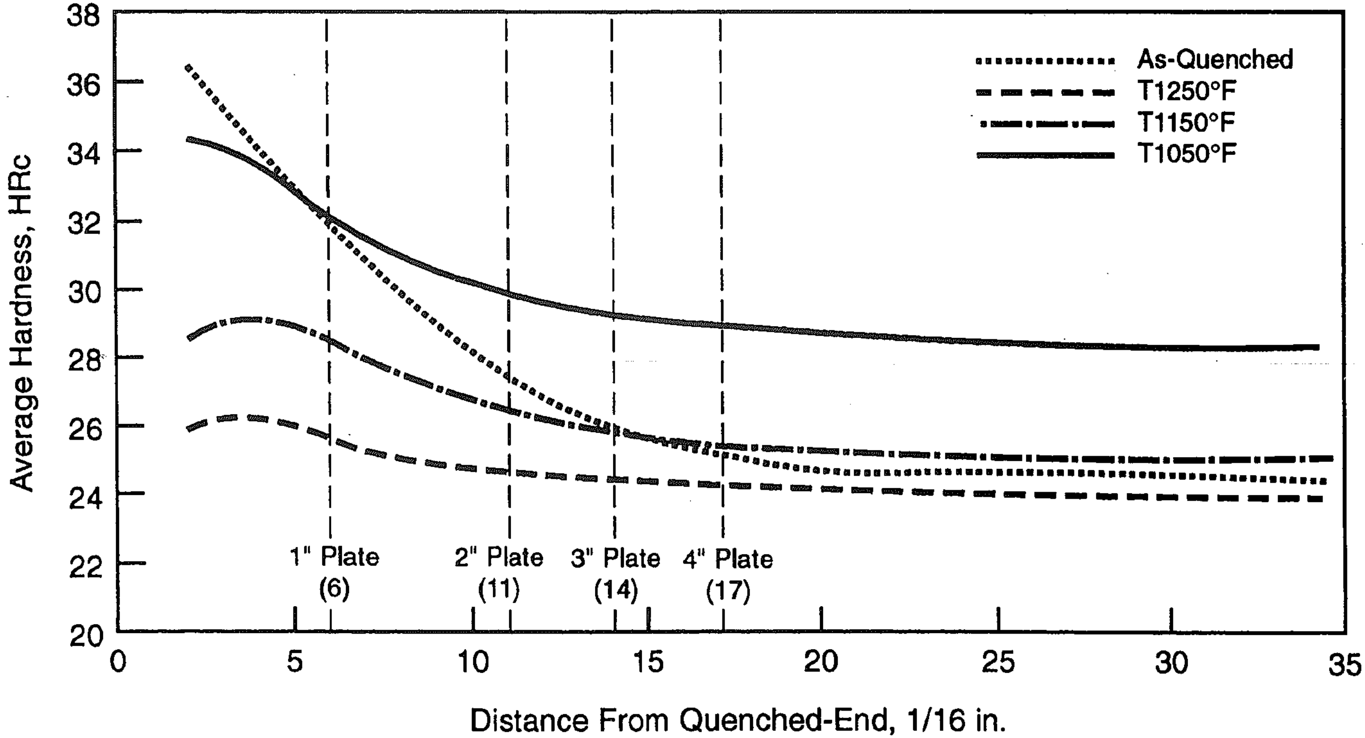

Figure 12 Jominy End-Quench High-Side Hardenability Results at Various Tempering Temperatures: U&V Steels

96-E016-3

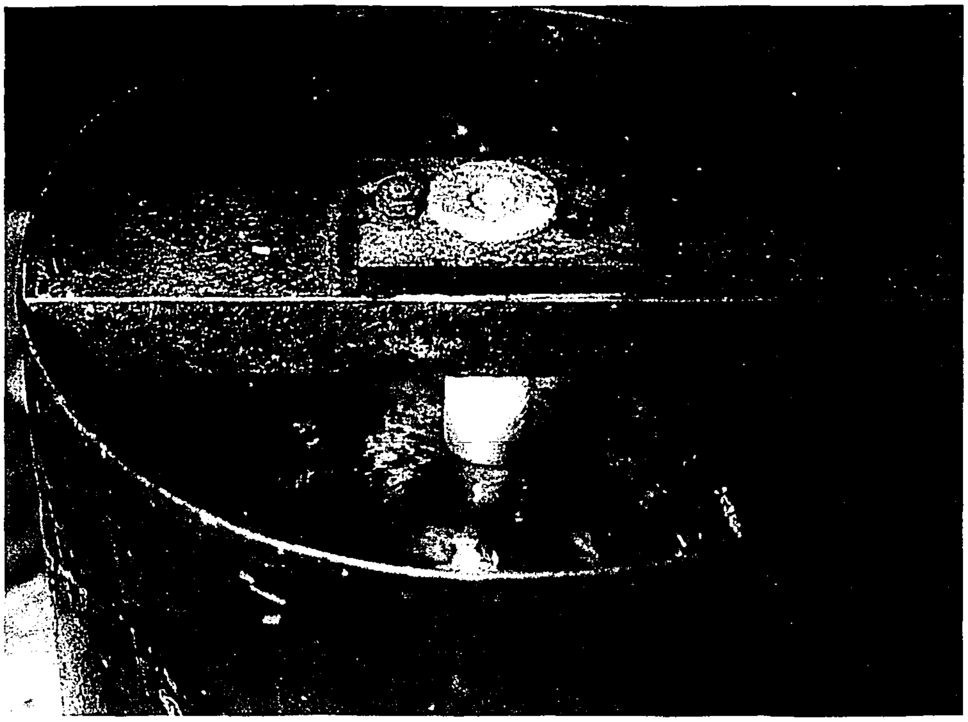

Figure 13 - ATLSS' Jominy End-Quench Hardenability Apparatus

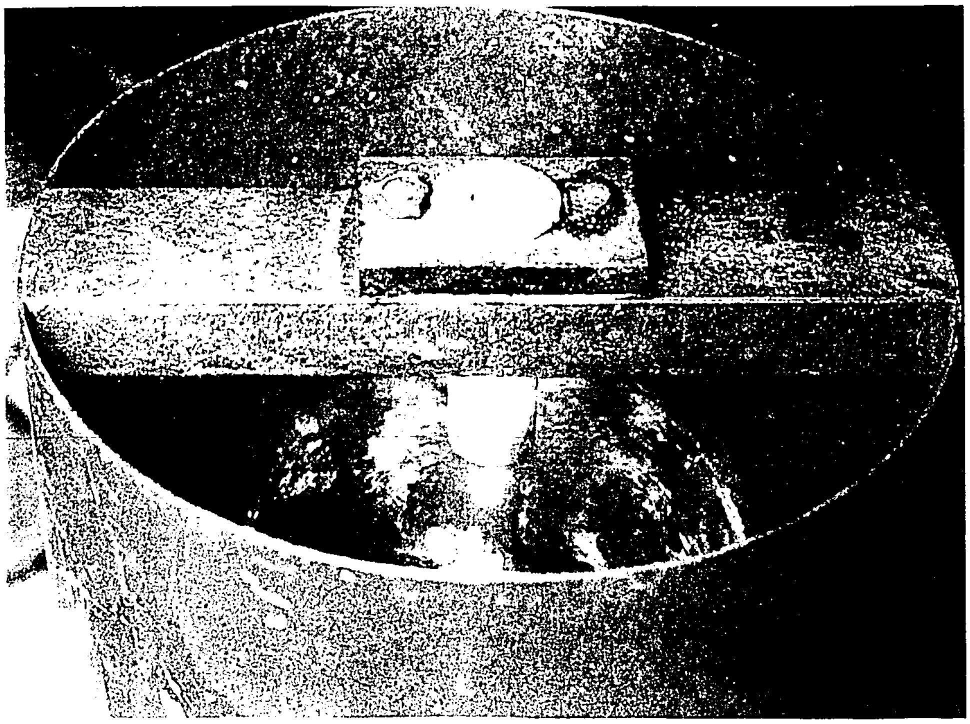

Figure 13 - ATLSS' Jominy End-Quench Hardenability Apparatus

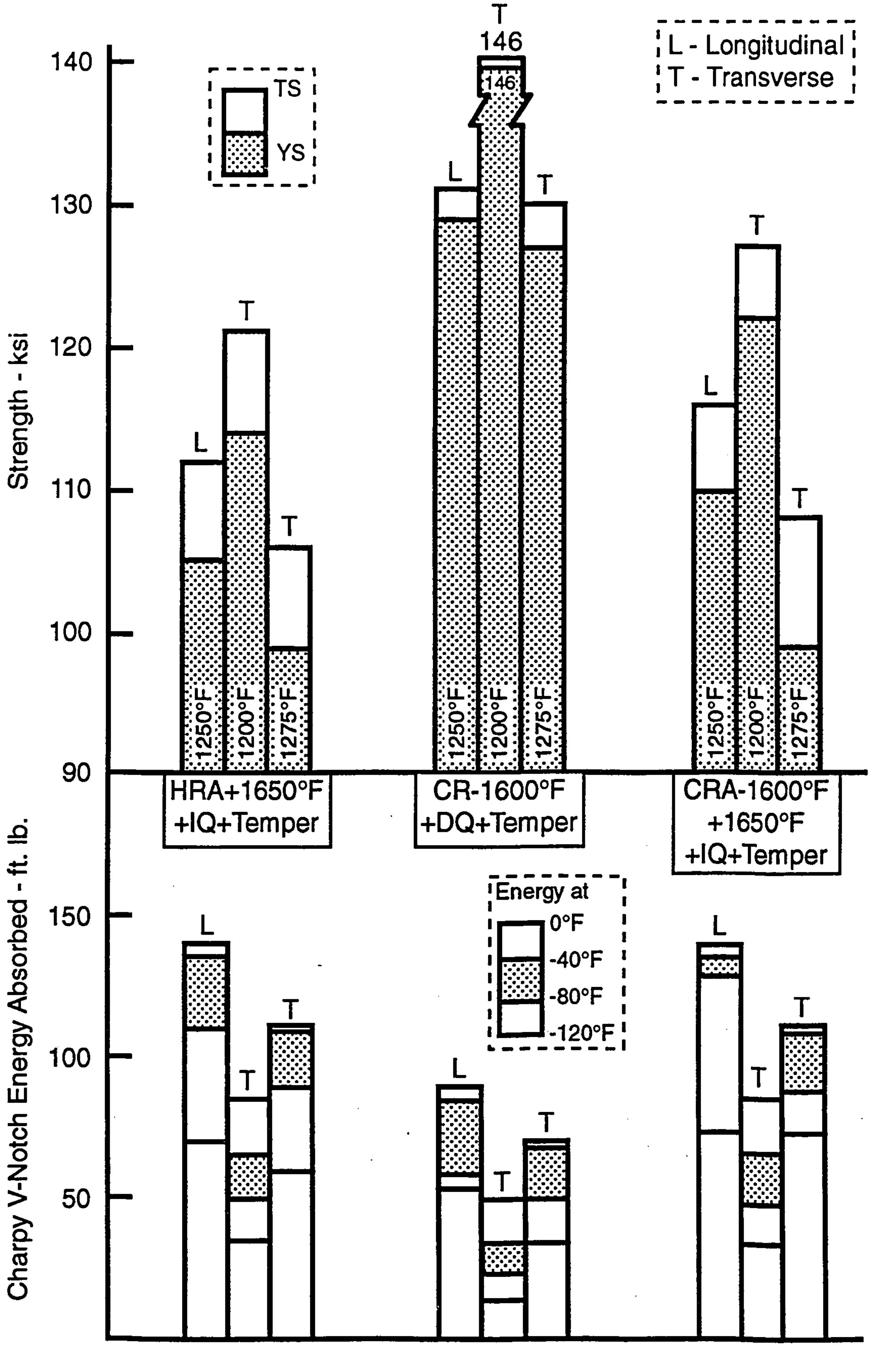

Figure 14 Strength and Toughness Properties of Cross-Rolled 1-inch-thick Steel U Plate

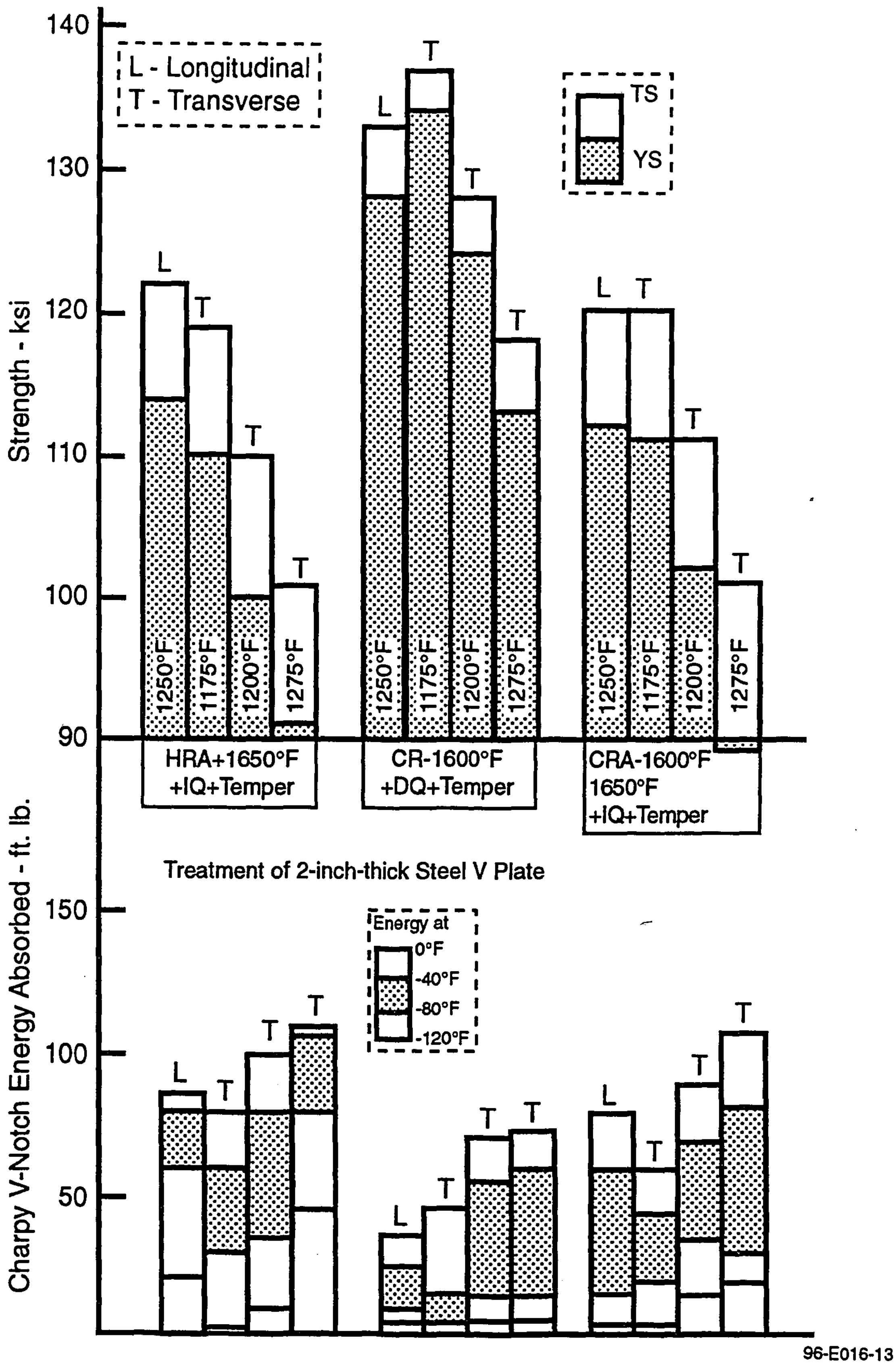

Figure 15 Strength and Toughness Properties of Cross-Rolled 2-inch-thick Steel V Plate

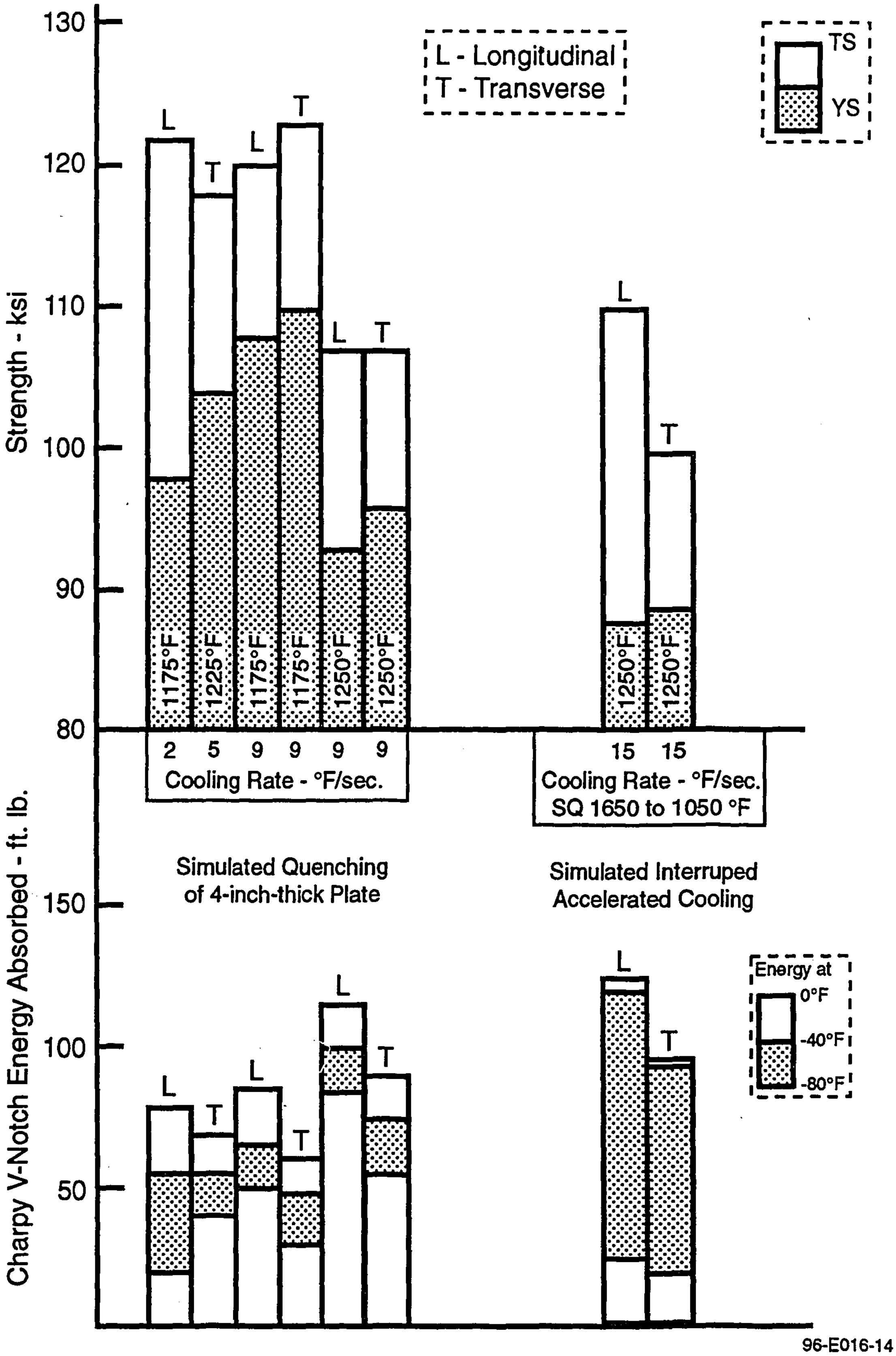

Figure 16 Strength and Toughness Properties for Special Processing Simulations of Steel U

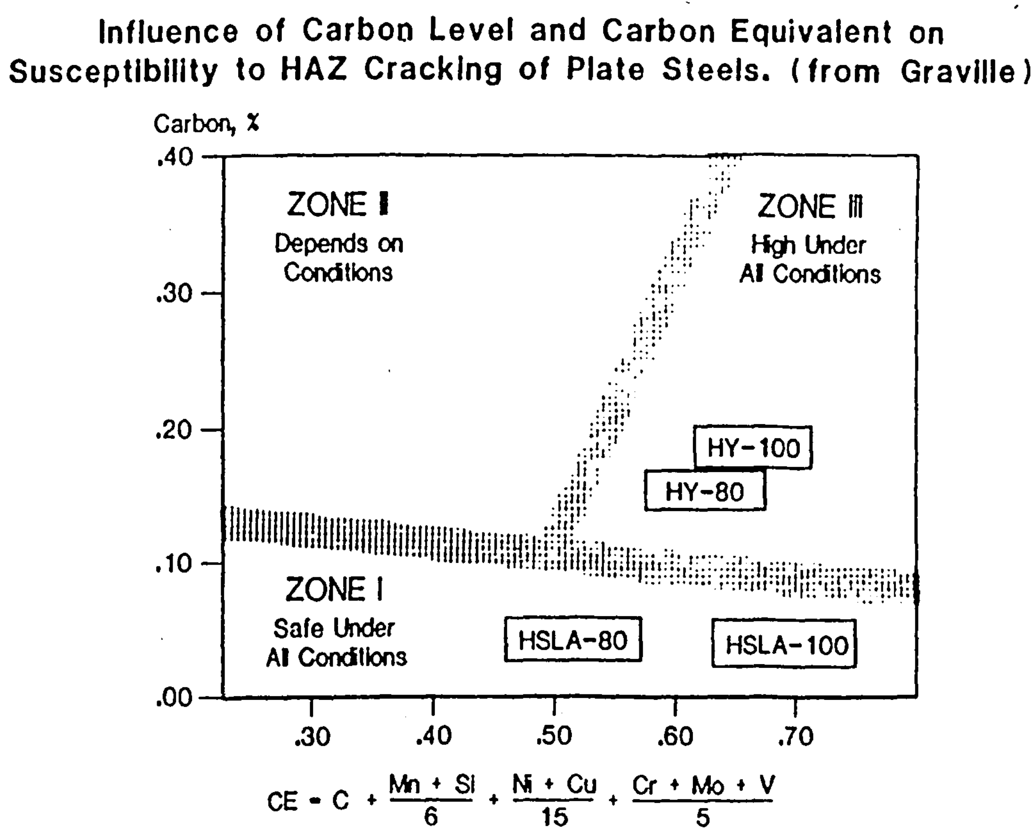

Figure 17 - Influence of Carbon Level and Carbon Equivalent on Susceptibility to HAZ Cracking of Plate Steels (from Graville)[17]

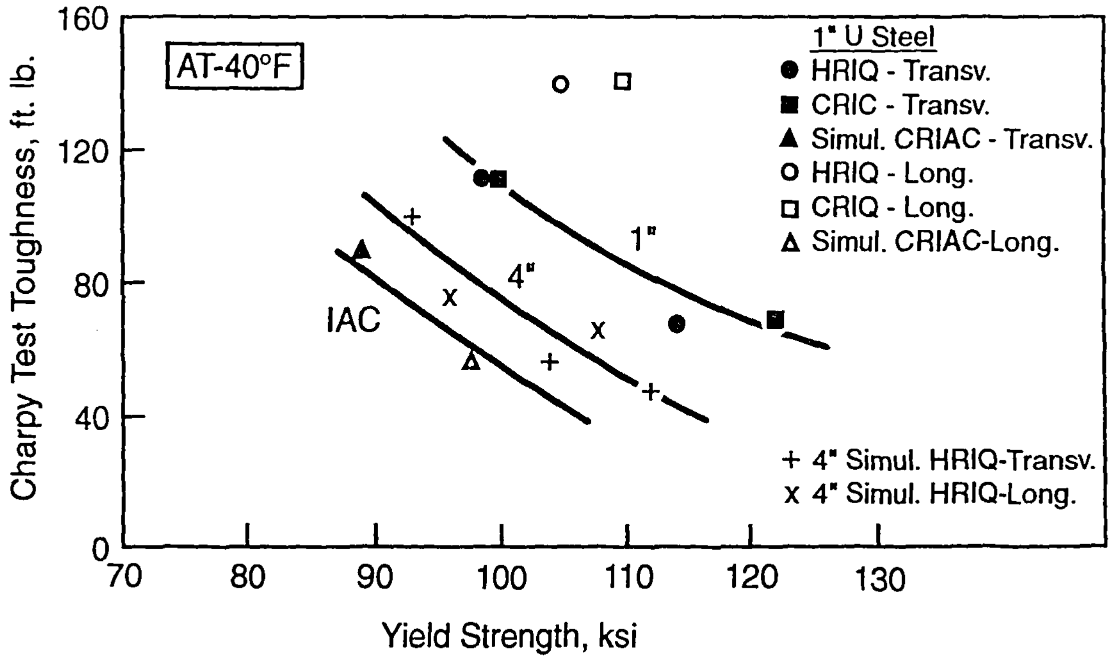

Figure 18a Yield Strength vs Notch Toughness of Steel U

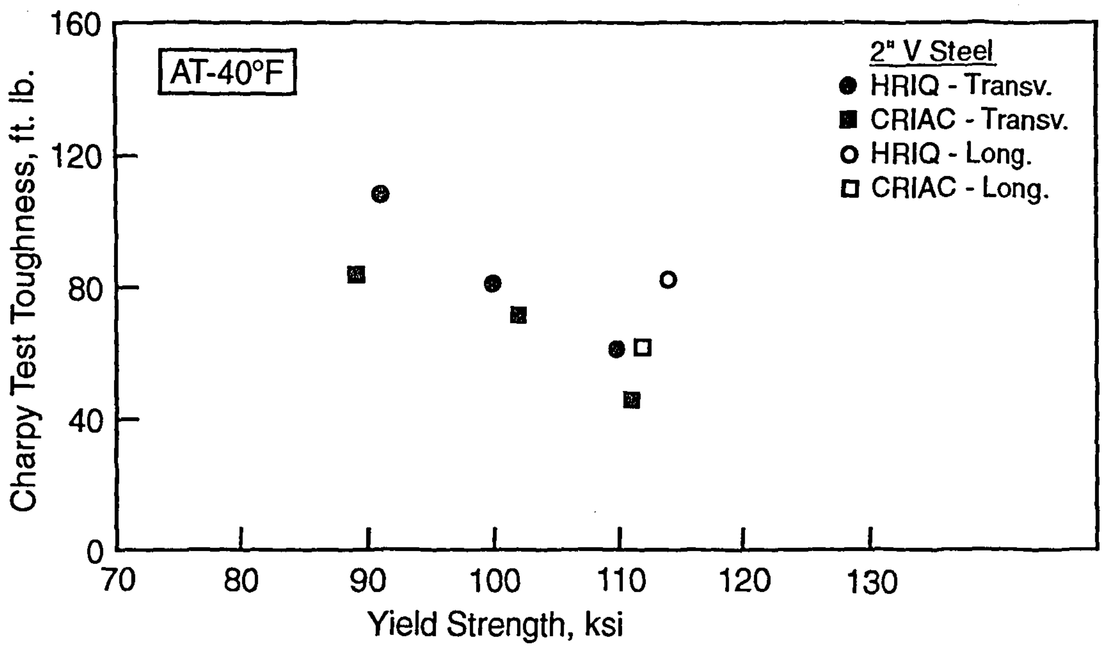

Figure 18b Yield Strength vs Notch Toughness of Steel V

96-E016-9

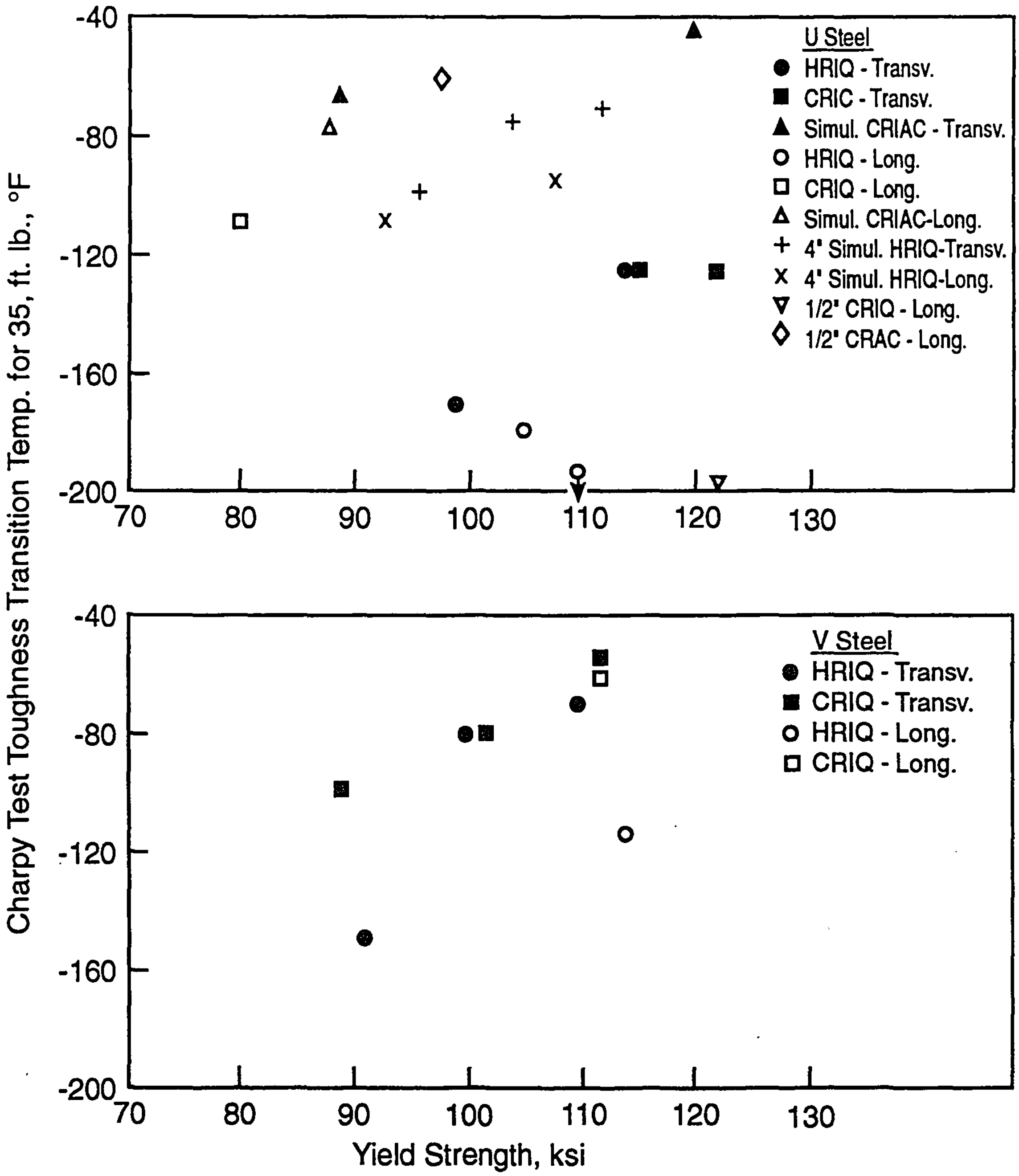

Figure 19 Charpy Transition (35ft.-lb.) Temperature for Various Treatments of U and V Steels

96-E016-10

Steel U

C	Mn	P	S	Si	Cu	Ni	Cr	Mo	V	Cb	Al	N
0.075	1.50	0.012	0.25	0.25	0.96	0.75	0.50	0.50	0.058	0.025	0.035	0.0065

U-HRAQ (As Q)

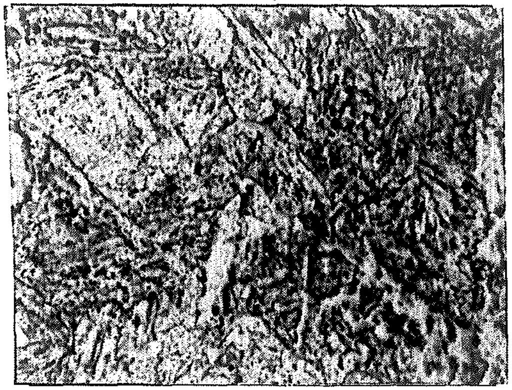

U-HRAQ+T1200F

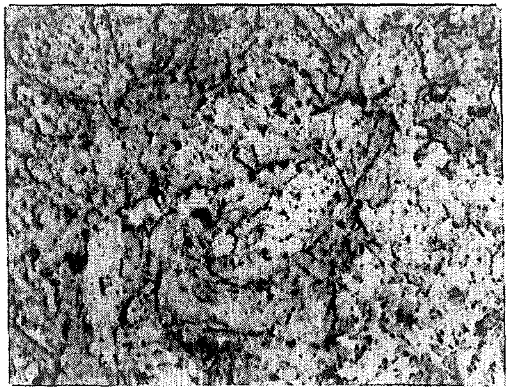

U-HRAQ+T1250F

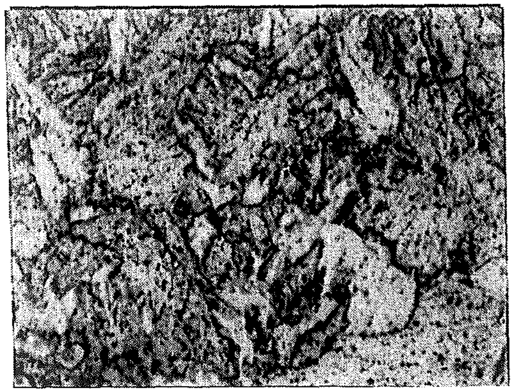

U-HRAQ+T1275F

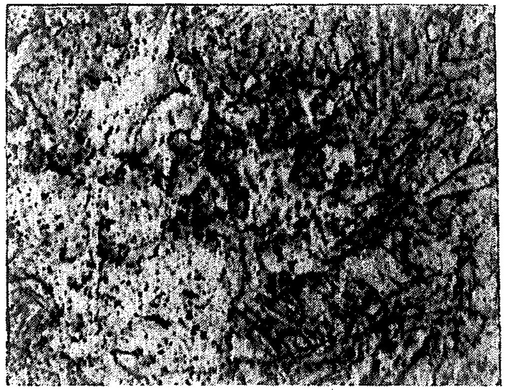

U-HRAQ+T1300F

U-HRAQ+T1350F

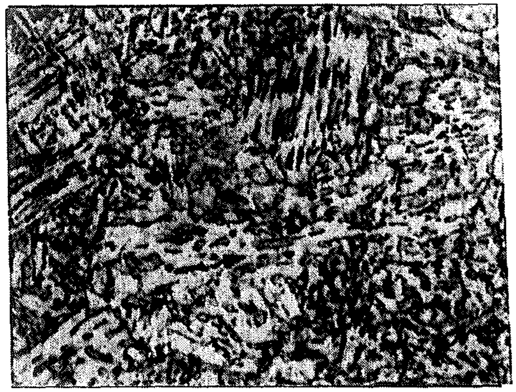

X1000 Nital-Picral

95-D057-12

Figure 20a - Steel U Tempered Series Microstructures (HRAQ 1900)

Steel U

C	Mn	P	S	Si	Cu	Ni	Cr	Mo	V	Cb	Al	N
0.075	1.50	0.012	0.25	0.25	0.96	0.75	0.50	0.50	0.058	0.025	0.035	0.0065

U-CRDQ (As Q)

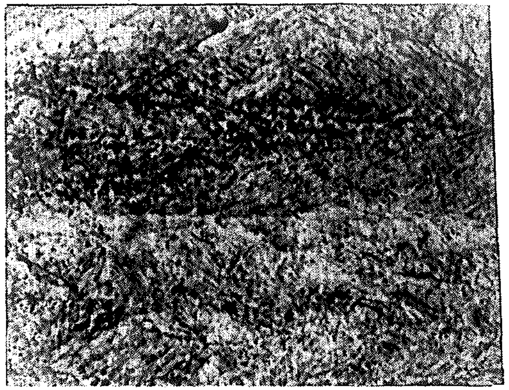

U-CRDQ +T1200F

U-CRDQ +T1250F

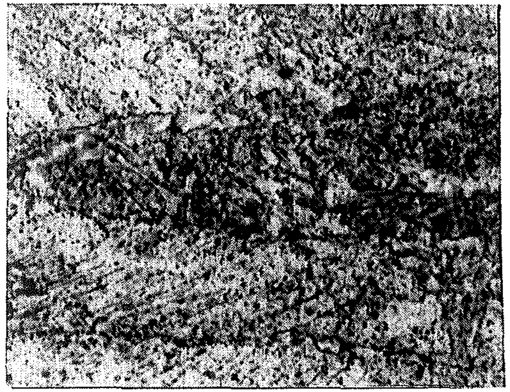

U-CRDQ +T1275F

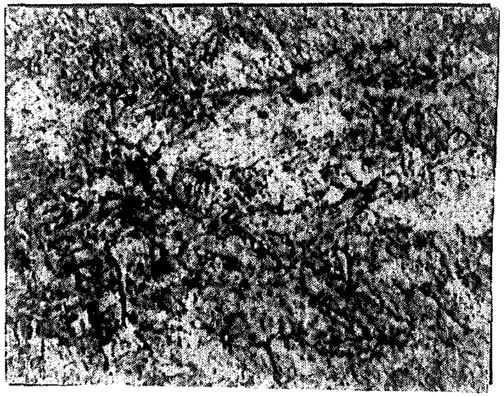

U-CRDQ +T1300F

U-CRDQ +T1350F

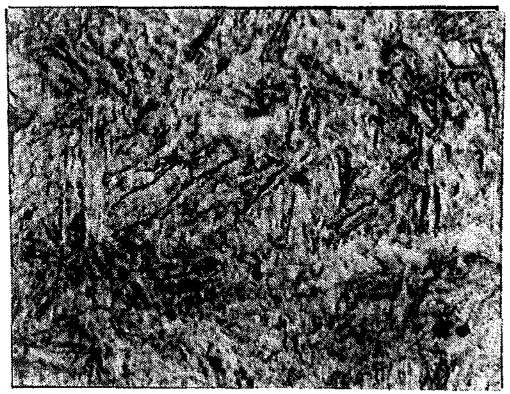

X1000 Nital-Picral

95-D057-13

Figure 20b - Steel U Tempered Series Microstructures (CRDQ 1600)

Steel U

C	Mn	P	S	Si	Cu	Ni	Cr	Mo	V	Cb	Al	N
0.075	1.50	0.012	0.25	0.25	0.96	0.75	0.50	0.50	0.058	0.025	0.035	0.0065

U-CRAQ (As Q)

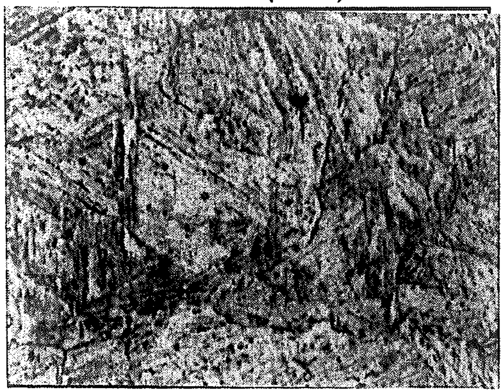

U-CRAQ +T1200F

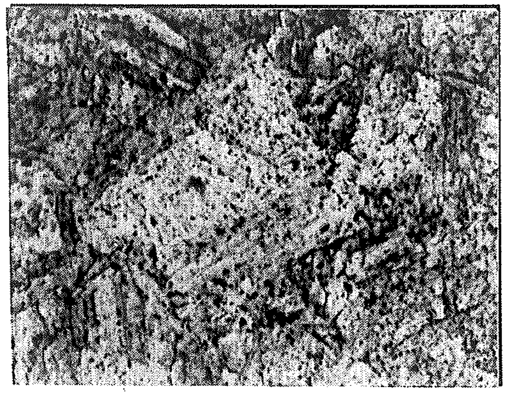

U-CRAQ +T1250F

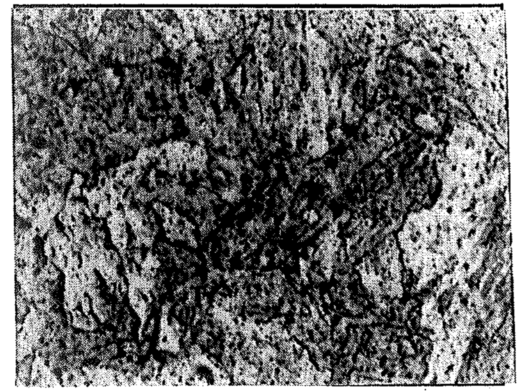

U-CRAQ +T1275F

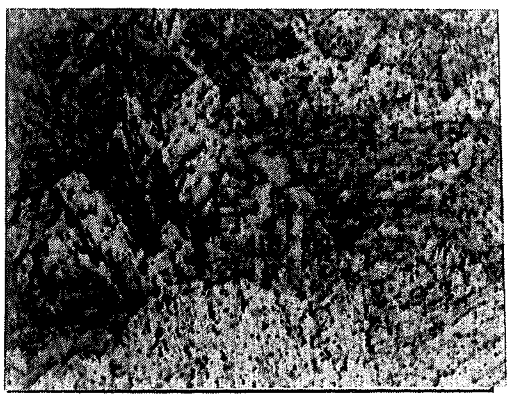

U-CRAQ +T1300F

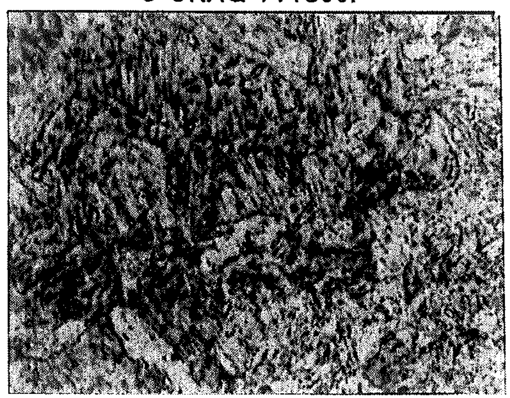

U-CRAQ +T1350F

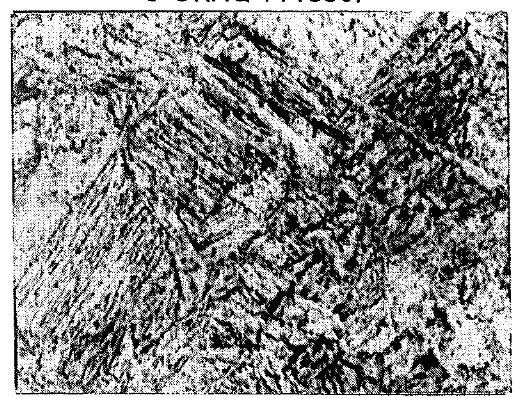

X1000 Nital-Picral

95-D057-14

Figure 20c - Steel U Tempered Series Microstructures (CRAQ 1600)

Steel U

C	Mn	P	S	Si	Cu	Ni	Cr	Mo	V	Cb	Al	N
0.075	1.50	0.012	0.25	0.25	0.96	0.75	0.50	0.50	0.058	0.025	0.035	0.0065

HRAQ-1900

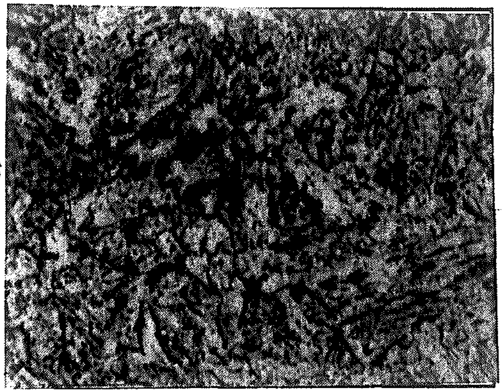

CRDQ-1600

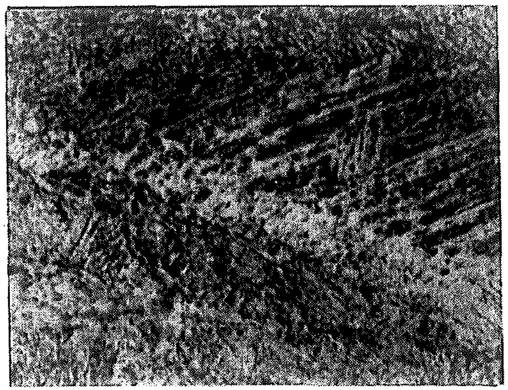

CRAQ-1600

X1000 Nital-Picral

95-D057-18

Figure 20d - Micrographs of Steel U in the As-Quenched Condition

Steel V

C	Mn	P	S	Si	Cu	Ni	Cr	Mo	V	Cb	Al	N
0.073	1.49	0.015	0.005	0.23	0.95	0.75	0.50	0.50	0.059	0.022	0.034	0.0064

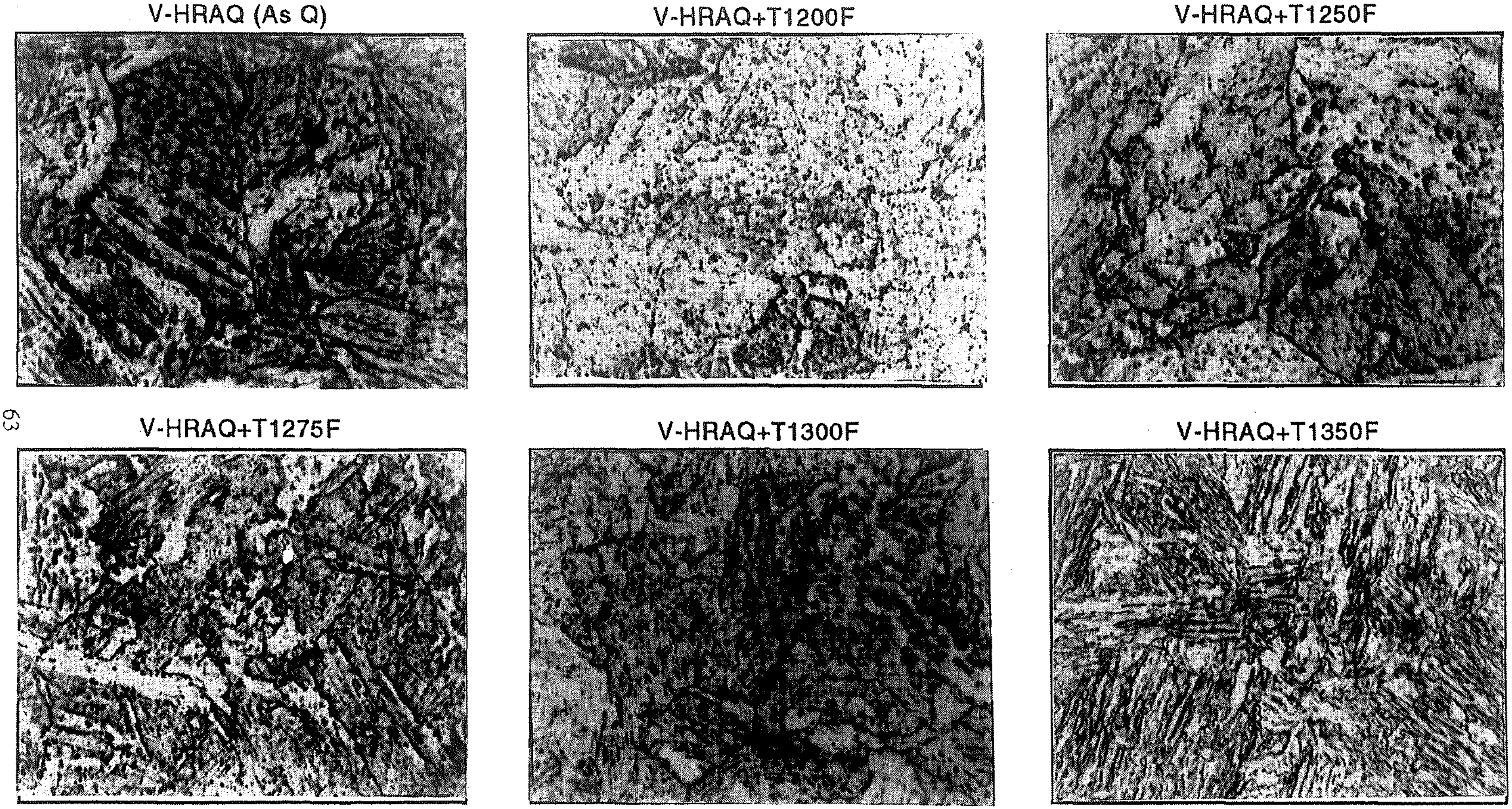

X1000 Nital-Picral

95-D057-15

Figure 21a - Steel V Tempered Series Microstructures (HRAQ 1900)

Steel V

C	Mn	P	S	Si	Cu	Ni	Cr	Mo	V	Cb	Al	N
0.073	1.49	0.015	0.005	0.23	0.95	0.75	0.50	0.50	0.059	0.022	0.034	0.0064

V-CRDQ (As Q)

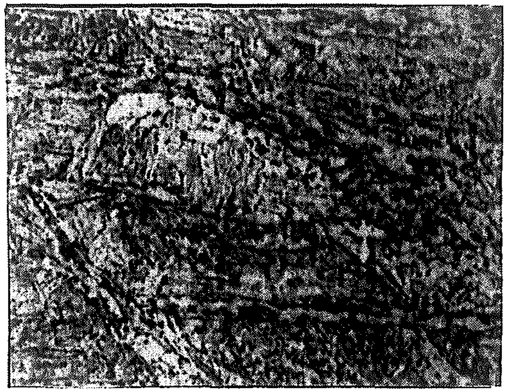

V-CRDQ +T1200F

V-CRDQ +T1250F

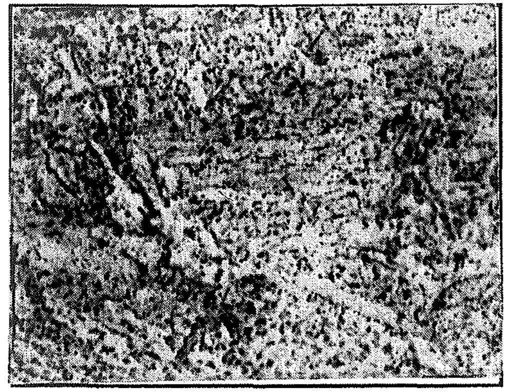

V-CRDQ +T1275F

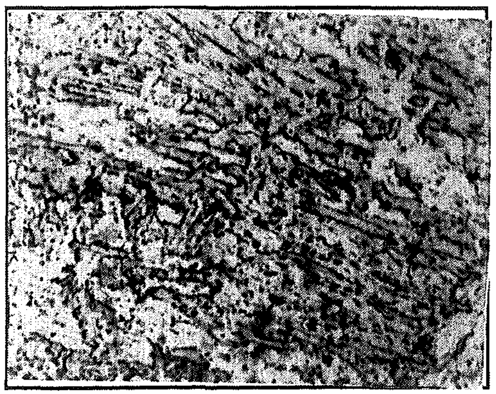

V-CRDQ +T1300F

V-CRDQ +T1350F

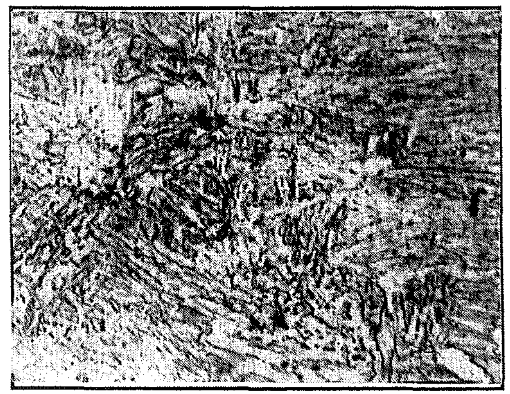

X1000 Nital-Picral

Figure 21b - Steel V Tempered Series Microstructures (CRDQ 1600)

95-D057-16

Steel V

C	Mn	P	S	Si	Cu	Ni	Cr	Mo	V	Cb	Al	N
0.073	1.49	0.015	0.005	0.23	0.95	0.75	0.50	0.50	0.059	0.022	0.034	0.0064

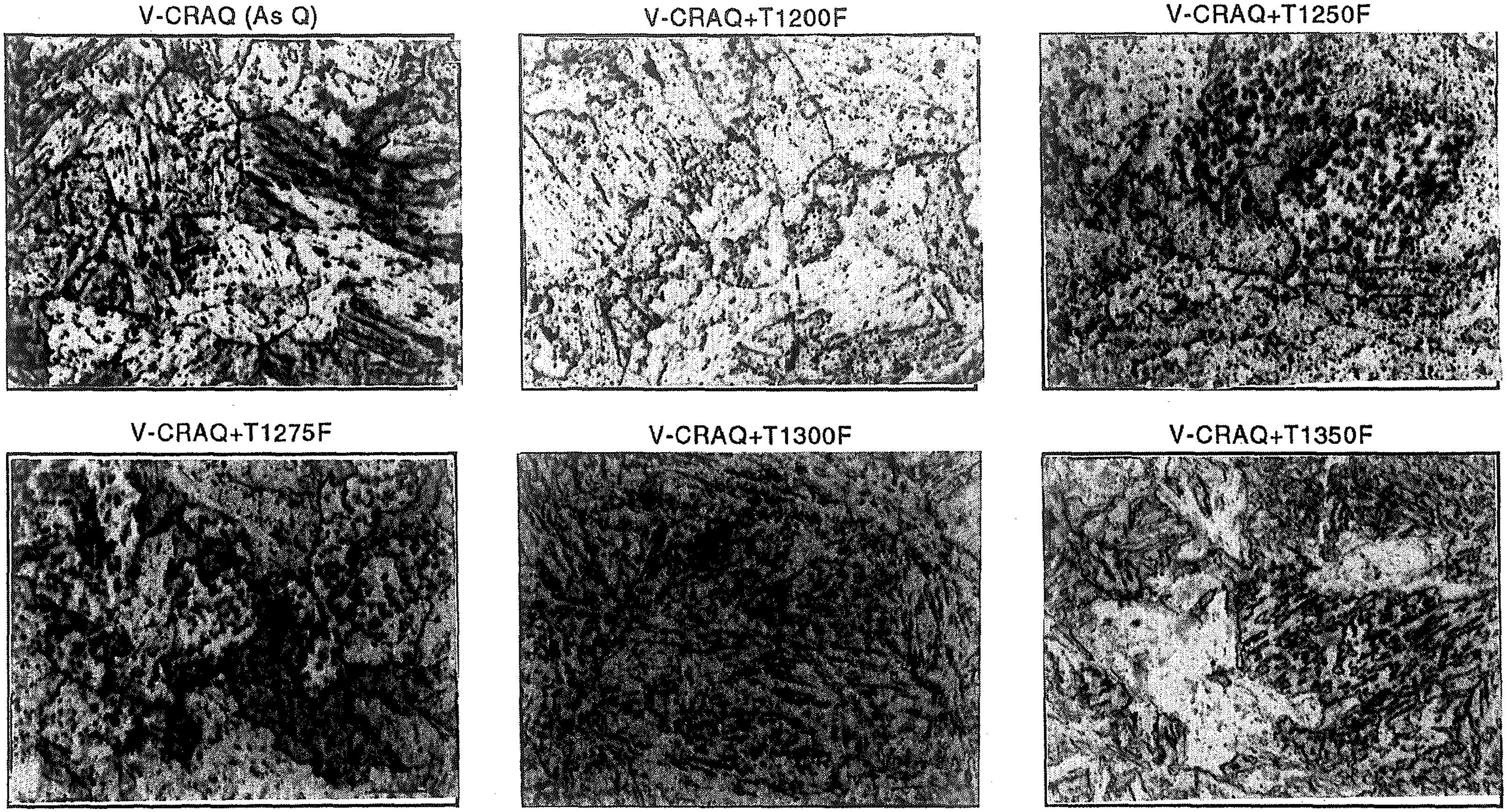

X1000 Nital-Picral

Figure 21c - Steel V Tempered Series Microstructures (CRAQ 1900)

95-D057-17

Steel V

C	Mn	P	S	Si	Cu	Ni	Cr	Mo	V	Cb	Al	N
0.073	1.49	0.015	0.005	0.23	0.95	0.75	0.50	0.50	0.059	0.022	0.034	0.0064

HRAQ-1900

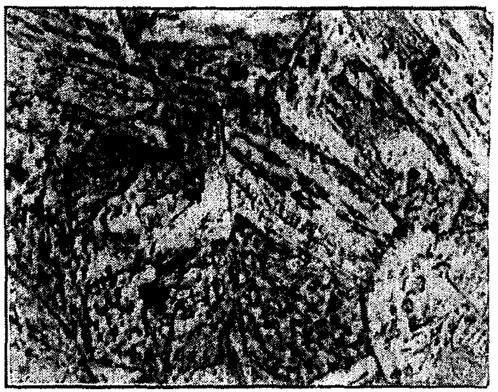

CRDQ-1600

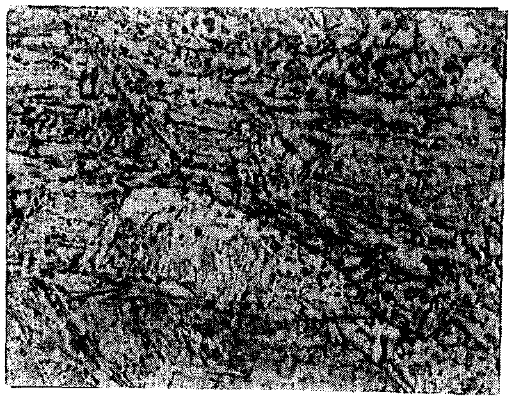

CRAQ-1600

X1000 Nital-Picral

95-D057-19

Figure 21d - Micrographs of Steel V in the As-Quenched Condition

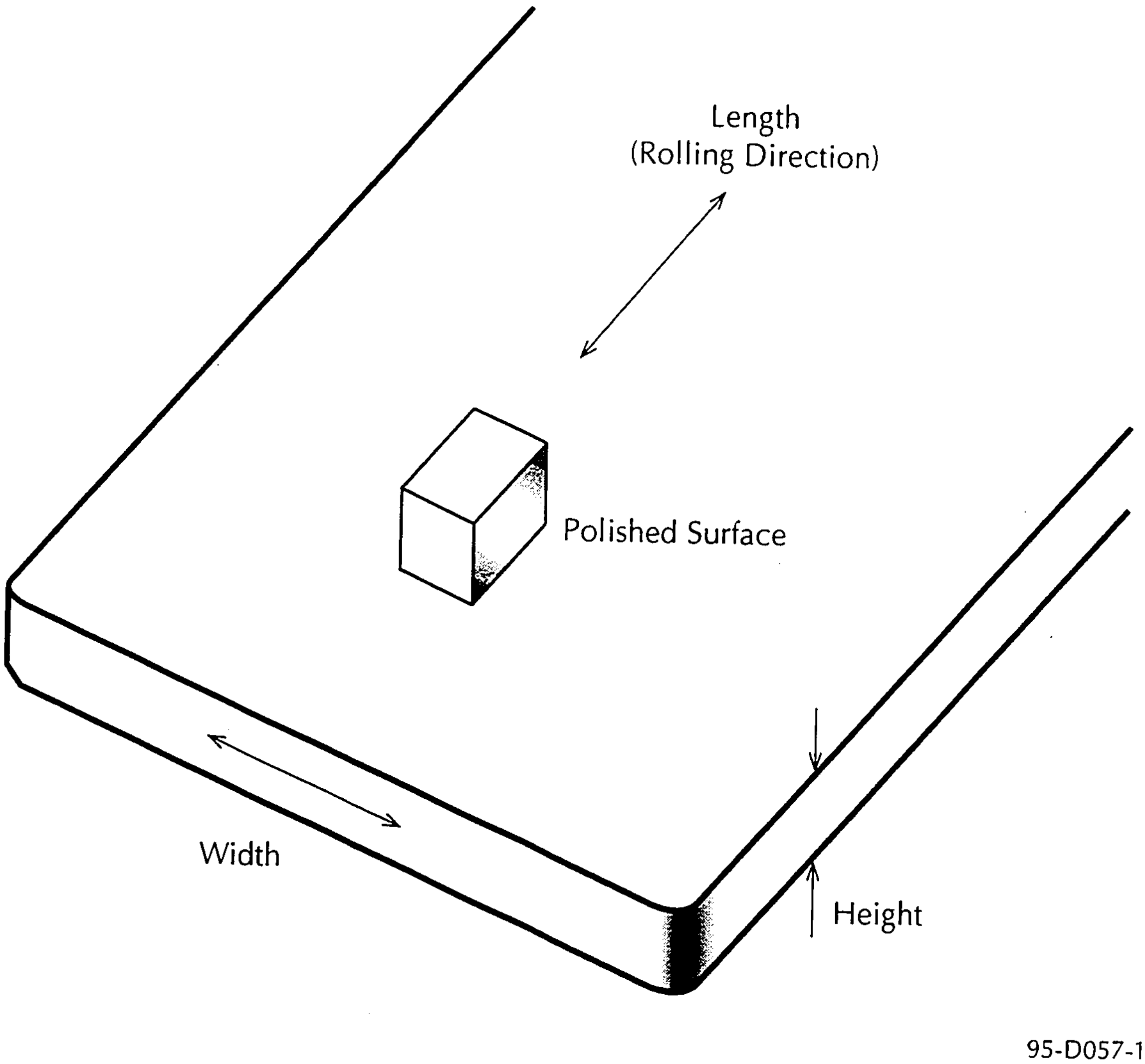

Figure 22 Appropriation of Metallographic Specimens

Steel U

C	Mn	P	S	Si	Cu	Ni	Cr	Mo	V	Cb	Al	N
0.075	1.50	0.012	0.25	0.25	0.96	0.75	0.50	0.50	0.058	0.025	0.035	0.0065

1/16" From Quenched-End

2/16" From Quenched-End

3/16" From Quenched-End

4/16" From Quenched-End

5/16" From Quenched-End

6/16" From Quenched-End

X1000 Nital-Picral

95-D057-5

Figure 23a - Steel U Jominy End Quenched Hardenability Microstructures

Steel U

C	Mn	P	S	Si	Cu	Ni	Cr	Mo	V	Cb	Al	N
0.075	1.50	0.012	0.25	0.25	0.96	0.75	0.50	0.50	0.058	0.025	0.035	0.0065

7/16" From Quenched-End

8/16" From Quenched-End

9/16" From Quenched-End

10/16" From Quenched-End

11/16" From Quenched-End

12/16" From Quenched-End

X1000 Nital-Picral

95-D057-6

Figure 23b - Steel U Jominy End Quenched Hardenability Microstructures

Steel U

C	Mn	P	S	Si	Cu	Ni	Cr	Mo	V	Cb	Al	N
0.075	1.50	0.012	0.25	0.25	0.96	0.75	0.50	0.50	0.058	0.025	0.035	0.0065

13/16" From Quenched-End

14/16" From Quenched-End

15/16" From Quenched-End

16/16" From Quenched-End

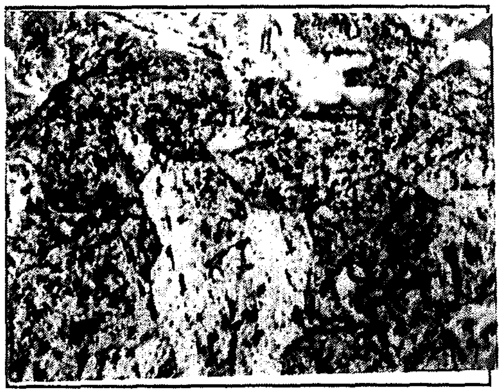

18/16" From Quenched-End

20/16" From Quenched-End

X1000 Nital-Picral

95-D057-7

Figure 23c - Steel U Jominy End Quenched Hardenability Microstructures

Steel U

C	Mn	P	S	Si	Cu	Ni	Cr	Mo	V	Cb	Al	N
0.075	1.50	0.012	0.25	0.25	0.96	0.75	0.50	0.50	0.058	0.025	0.035	0.0065

22/16" From Quenched-End

24/16" From Quenched-End

26/16" From Quenched-End

28/16" From Quenched-End

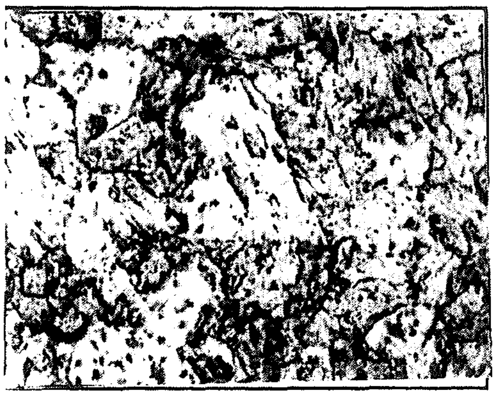

30/16" From Quenched-End

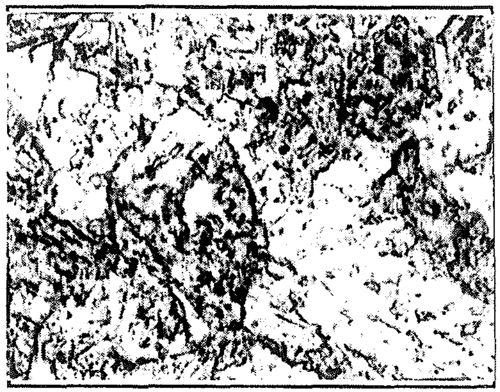

32/16" From Quenched-End

X1000 Nital-Picral

95-D057-8

Figure 23d - Steel U Jominy End Quenched Hardenability Microstructures

Steel U

C	Mn	P	S	Si	Cu	Ni	Cr	Mo	V	Cb	Al	N
0.075	1.50	0.012	0.25	0.25	0.96	0.75	0.50	0.50	0.058	0.025	0.035	0.0065

1/16" From Quenched-End

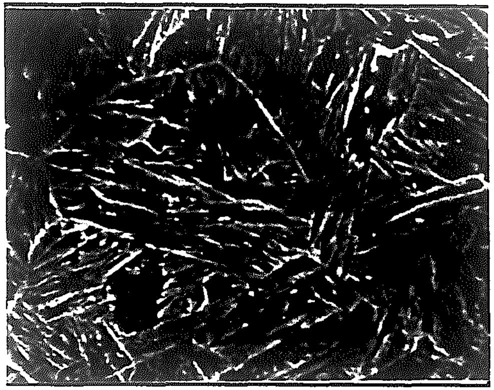

2/16" From Quenched-End

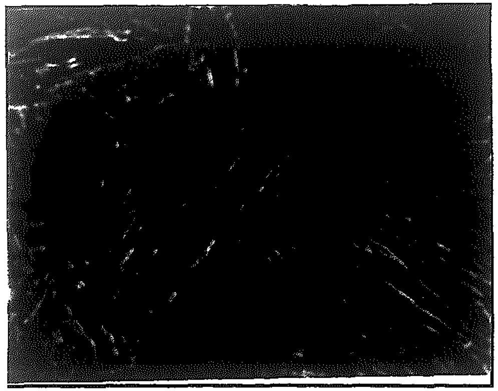

3/16" From Quenched-End

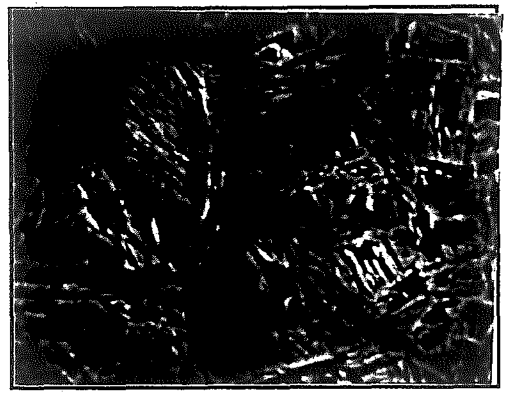

4/16" From Quenched-End

5/16" From Quenched-End

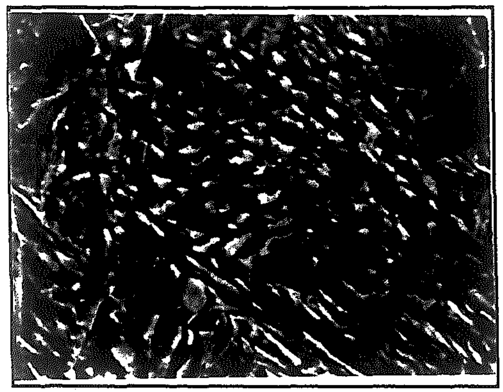

X2500Nital-Picral

95-D057-9

Figure 24a - Steel U Jominy Bar Hardenability SEM Microstructures

Steel U

C	Mn	P	S	Si	Cu	Ni	Cr	Mo	V	Cb	Al	N
0.075	1.50	0.012	0.25	0.25	0.96	0.75	0.50	0.50	0.058	0.025	0.035	0.0065

6/16" From Quenched-End

7/16" From Quenched-End

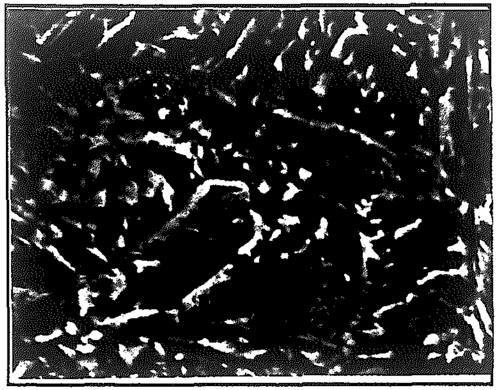

8/16" From Quenched-End

12/16" From Quenched-End

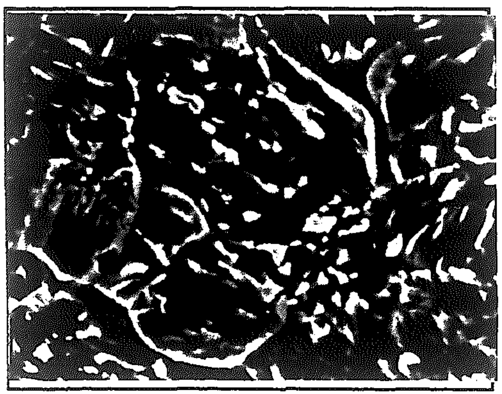

16/16" From Quenched-End

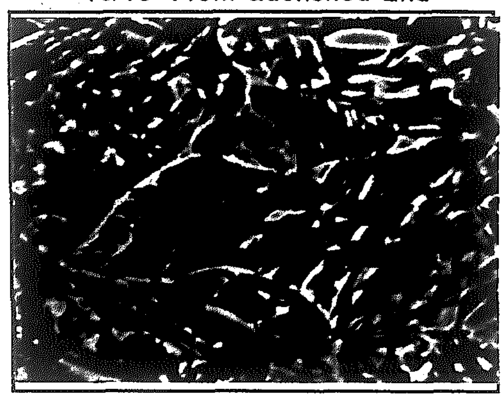

X2500Nital-Picral

95-D057-10

Figure 24b - Steel U Jominy Bar Hardenability SEM Microstructures

Steel U

C	Mn	P	S	Si	Cu	Ni	Cr	Mo	V	Cb	Al	N
0.075	1.50	0.012	0.25	0.25	0.96	0.75	0.50	0.50	0.058	0.025	0.035	0.0065

20/16" From Quenched-End

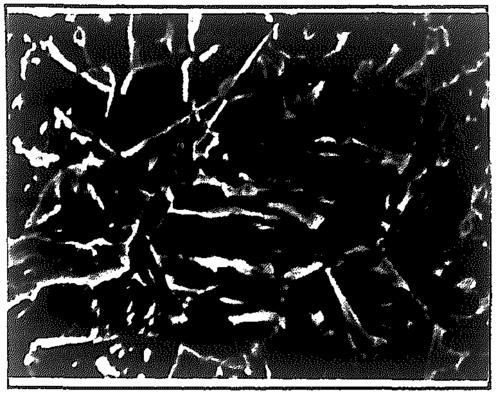

24/16" From Quenched-End

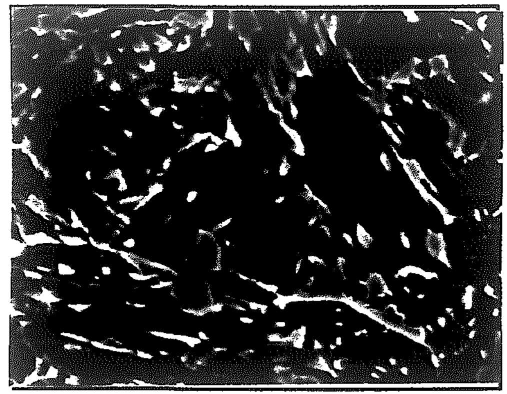

28/16" From Quenched-End

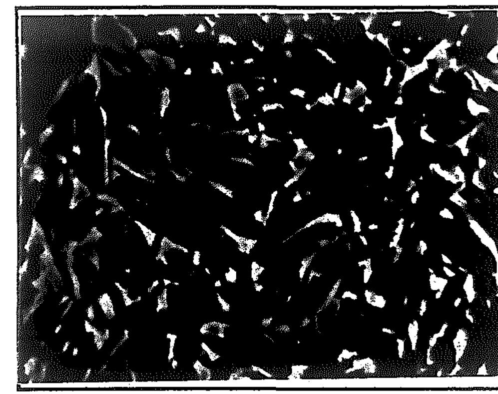

32/16" From Quenched-End

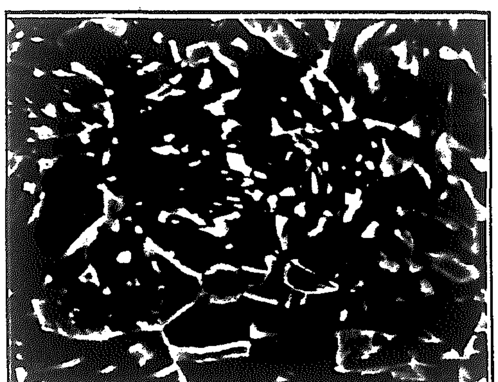

34/16" From Quenched-End

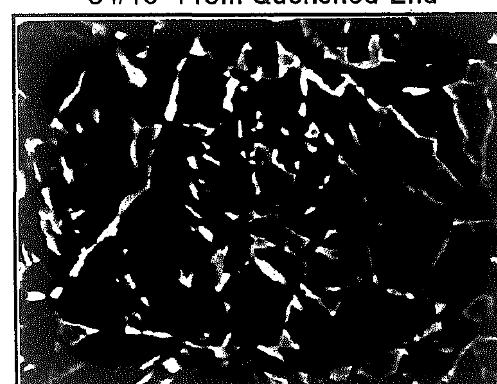

X2500Nital-Picral

Figure 24c - Steel U Jominy Bar Hardenability SEM Microstructures

95-D057-11

Steel V

C	Mn	P	S	Si	Cu	Ni	Cr	Mo	V	Cb	Al	N
0.073	1.49	0.015	0.005	0.23	0.95	0.75	0.50	0.50	0.059	0.022	0.034	0.0064

1/16" From Quenched-End

2/16" From Quenched-End

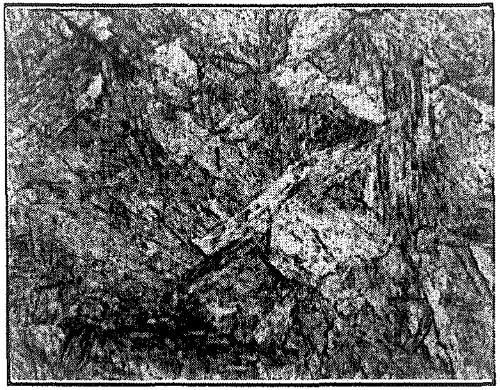

3/16" From Quenched-End

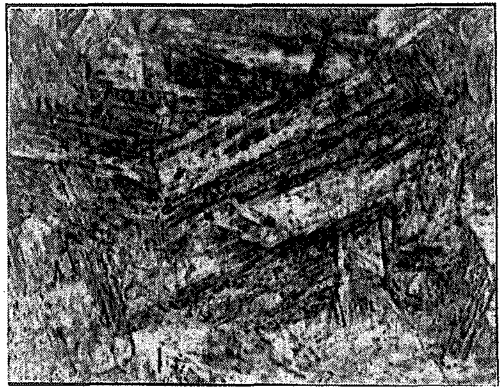

4/16" From Quenched-End

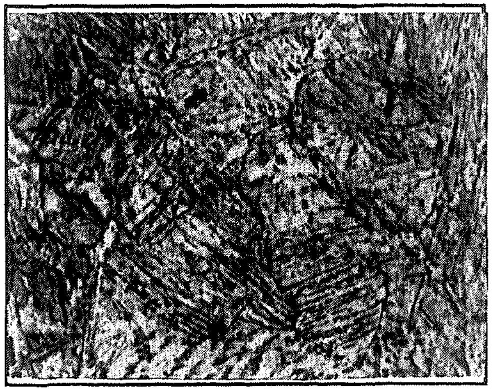

5/16" From Quenched-End

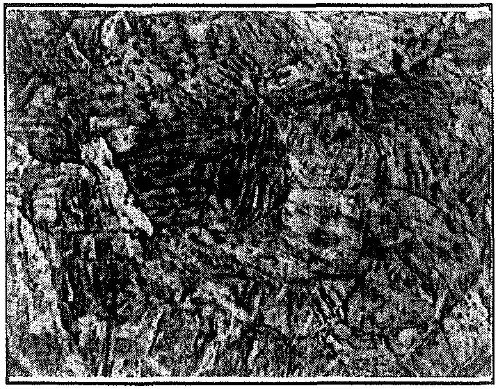

6/16" From Quenched-End

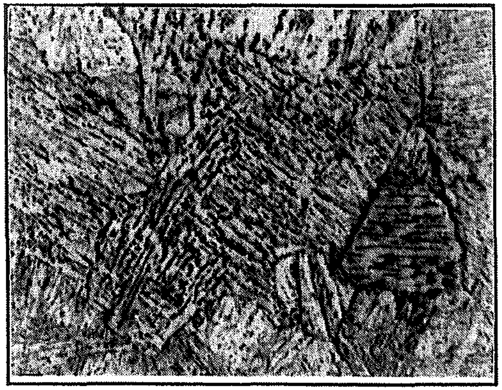

X1000 Nital-Picral

95-D057-1

Figure 25a - Steel V Jominy End Quenched Hardenability Microstructures

Steel V

C	Mn	P	S	Si	Cu	Ni	Cr	Mo	V	Cb	Al	N
0.073	1.49	0.015	0.005	0.23	0.95	0.75	0.50	0.50	0.059	0.022	0.034	0.0064

7/16" From Quenched-End

8/16" From Quenched-End

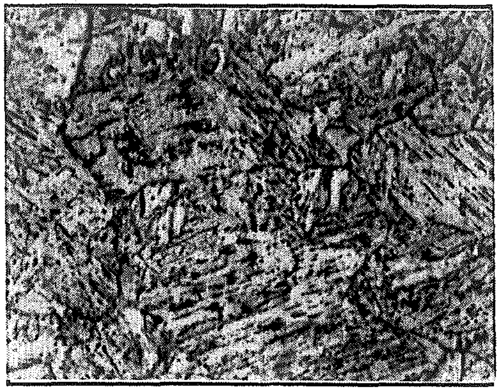

9/16" From Quenched-End

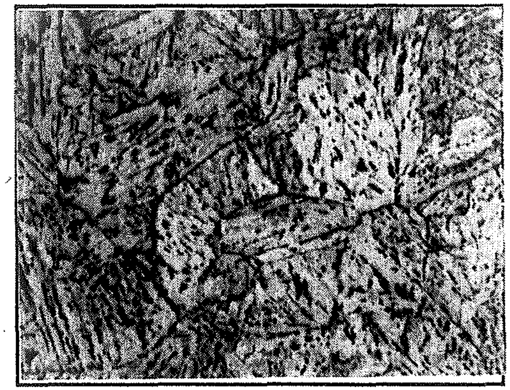

10/16" From Quenched-End

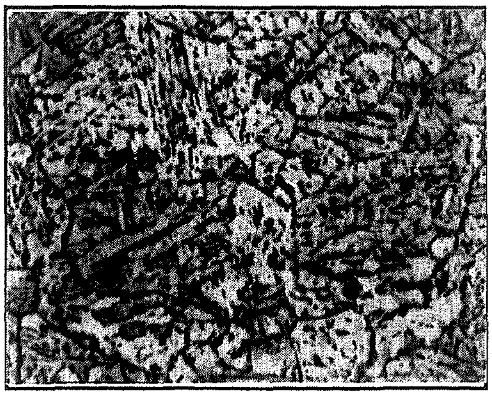

11/16" From Quenched-End

12/16" From Quenched-End

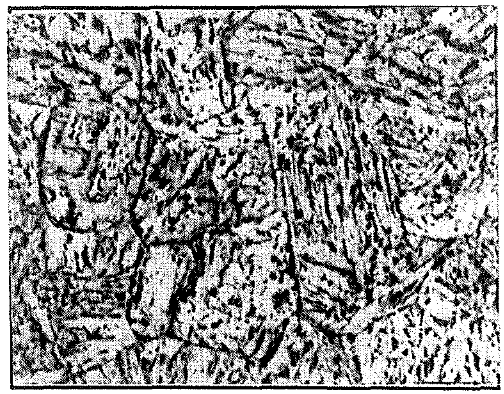

X1000 Nital-Picral

95-D057-2

Figure 25b - Steel V Jominy End Quenched Hardenability Microstructures

Steel V

C	Mn	P	S	Si	Cu	Ni	Cr	Mo	V	Cb	Al	N
0.073	1.49	0.015	0.005	0.23	0.95	0.75	0.50	0.50	0.059	0.022	0.034	0.0064

13/16" From Quenched-End

14/16" From Quenched-End

15/16" From Quenched-End

16/16" From Quenched-End

18/16" From Quenched-End

20/16" From Quenched-End

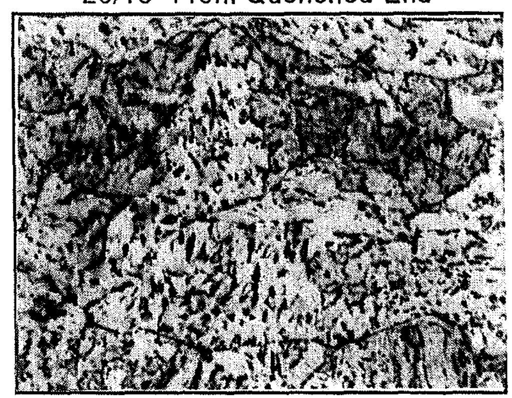

X1000 Nital-Picral

95-D057-3

Figure 25c - Steel V Jominy End Quenched Hardenability Microstructures

Steel V

C	Mn	P	S	Si	Cu	Ni	Cr	Mo	V	Cb	Al	N
0.073	1.49	0.015	0.005	0.23	0.95	0.75	0.50	0.50	0.059	0.022	0.034	0.0064

22/16" From Quenched-End

24/16" From Quenched-End

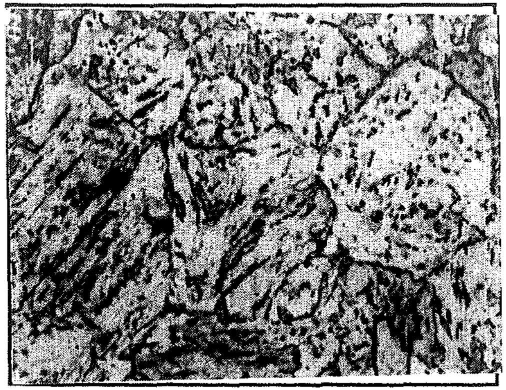

26/16" From Quenched-End

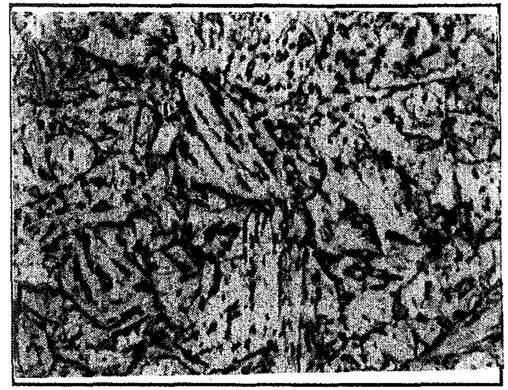

28/16" From Quenched-End

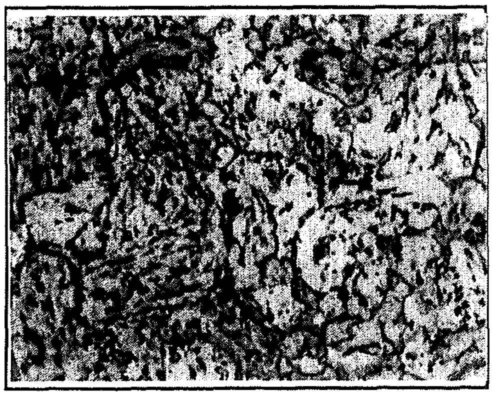

30/16" From Quenched-End

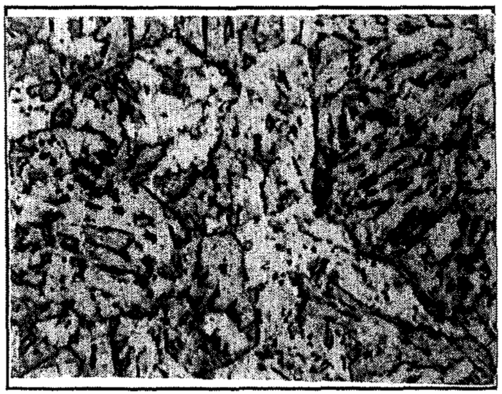

32/16" From Quenched-End

X1000 Nital-Picral

95-D057-4

Figure 25d - Steel V Jominy End Quenched Hardenability Microstructures

Steel U

C	Mn	P	S	Si	Cu	Ni	Cr	Mo	V	Cb	Al	N
0.075	1.50	0.012	0.25	0.25	0.96	0.75	0.50	0.50	0.058	0.025	0.035	0.0065

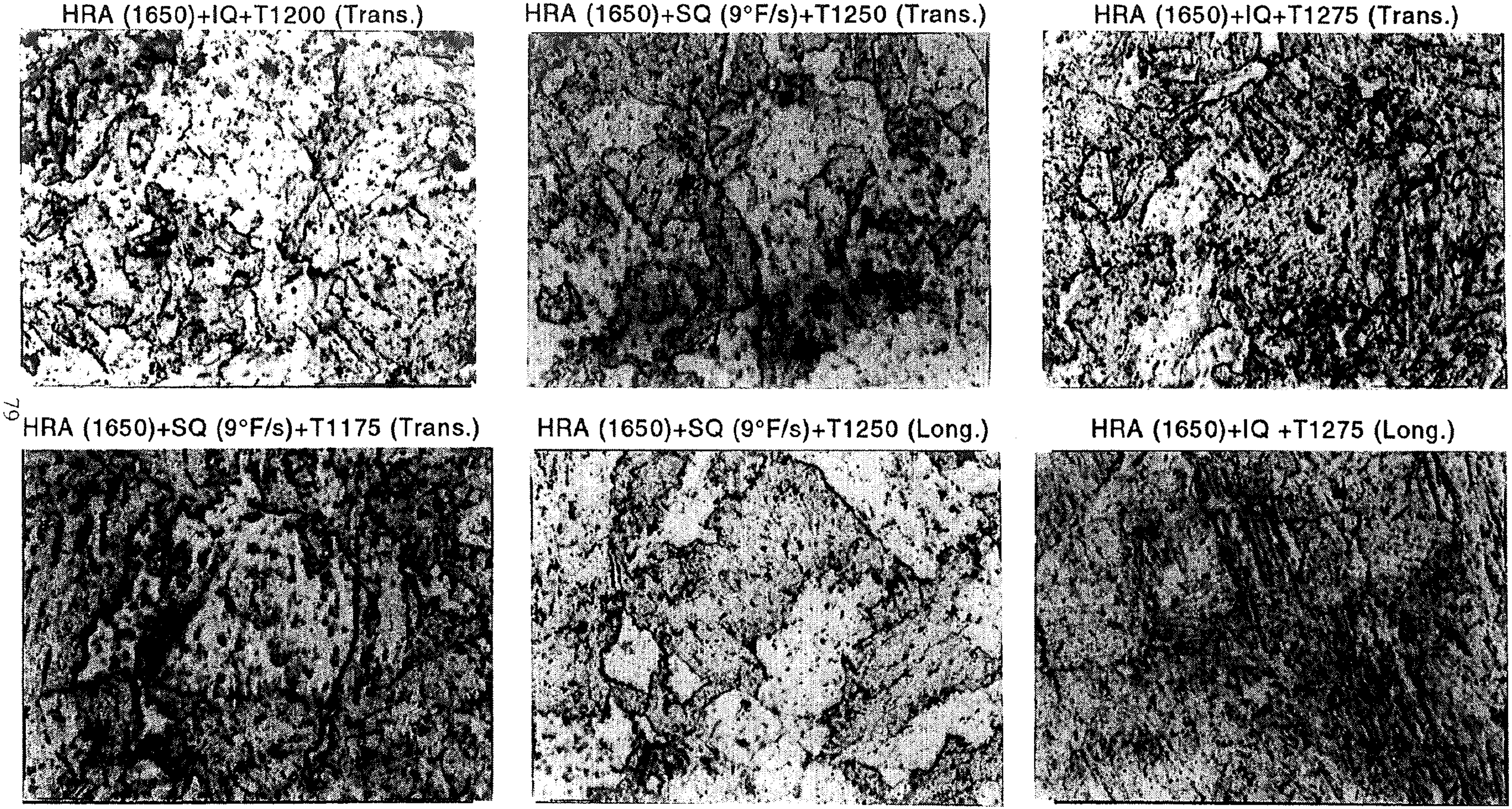

X1000Nital-Picral

95-D057-36

Figure 26a Microstructures of Steel U Mechanically Tested Specimens (HRA 1900)

Steel U

C	Mn	P	S	Si	Cu	Ni	Cr	Mo	V	Cb	Al	N
0.075	1.50	0.012	0.25	0.25	0.96	0.75	0.50	0.50	0.058	0.025	0.035	0.0065

CRDQ+T1200 (Trans.)

CRDQ+T1275 (Trans.)

CRDQ+T1250 (Trans.)

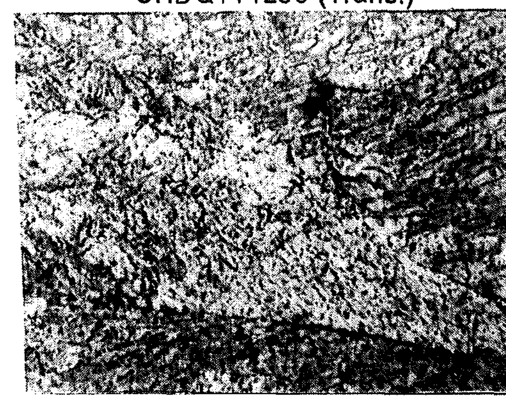

X1000Nital-Picral

95-D057-37

Figure 26b Microstructures of Steel U Mechanically Tested Specimens (CRDQ 1600)

Steel U

C	Mn	P	S	Si	Cu	Ni	Cr	Mo	V	Cb	Al	N
0.075	1.50	0.012	0.25	0.25	0.96	0.75	0.50	0.50	0.058	0.025	0.035	0.0065

CRA (1650)+IQ+T1200 (Trans.)

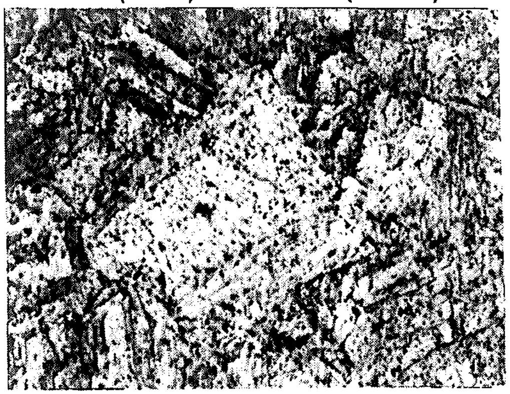

CRA (1650)+SQ (5°F/s)+T1250 (Trans.)

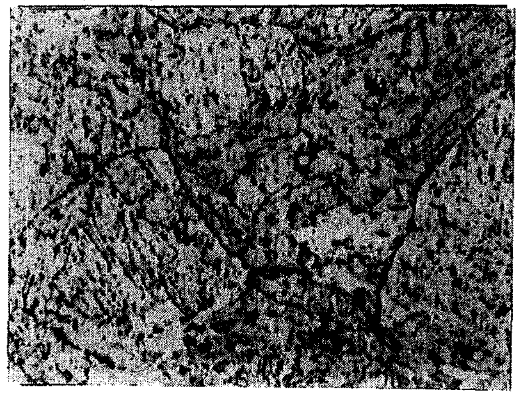

CRA (1650)+IQ+T1275 (Trans.)

CRA (1650)+IQ+T1250 (Long.)

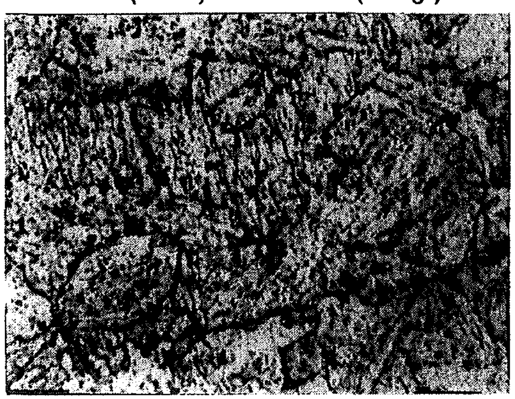

CRA (1650)+IQ+T1250 (Long.)

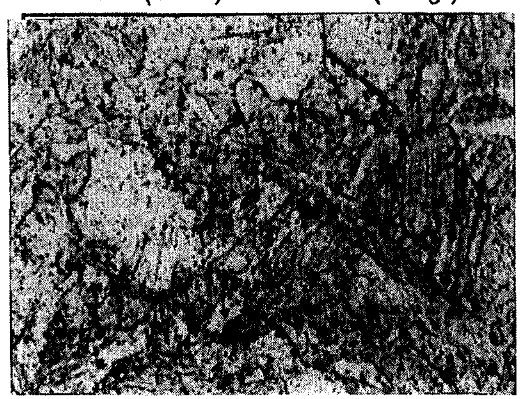

CRA (1650)+AC +T1175 (Long.)

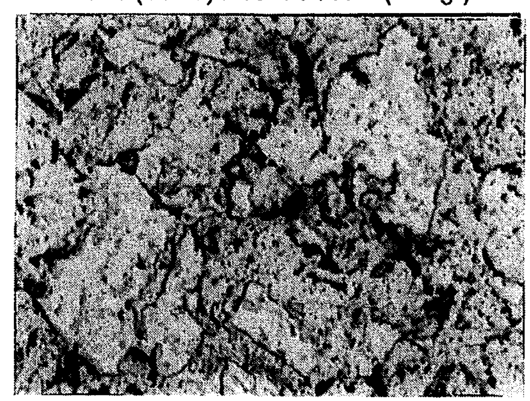

X1000Nital-Picral

95-D057-38

Figure 26c Microstructures of Steel U Mechanically Tested Specimens (CRA 1600)

Steel U

C	Mn	P	S	Si	Cu	Ni	Cr	Mo	V	Cb	Al	N
0.075	1.50	0.012	0.25	0.25	0.96	0.75	0.50	0.50	0.058	0.025	0.035	0.0065

CRA 1600 + 1650F + AC

CRA 1600 + 1650F + AC + T1200F

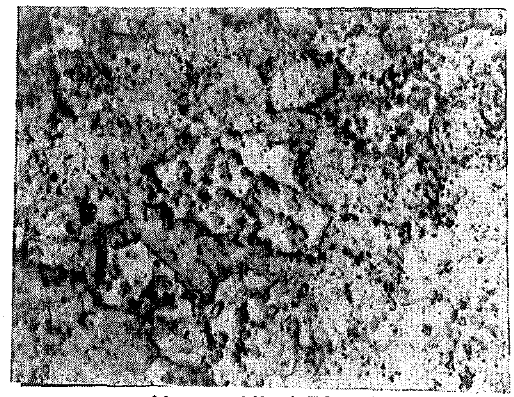

X1000 Nital-Picral

Figure26d Micrographs of Steel U with 1/2" Plate Gauge (CRA 1600)

Steel U

C	Mn	P	S	Si	Cu	Ni	Cr	Mo	V	Cb	Al	N
0.075	1.50	0.012	0.25	0.25	0.96	0.75	0.50	0.50	0.058	0.025	0.035	0.0065

CRA (1650)+CR+IAC (SQ 1050) (Trans.)

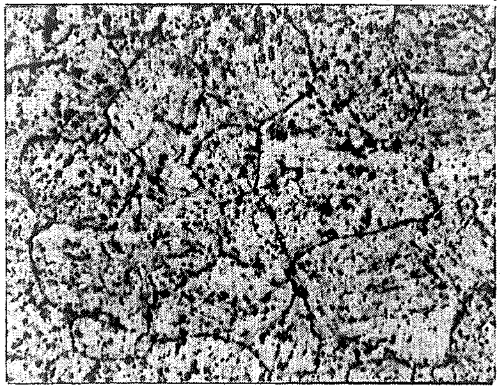

CRA (1650)+CR+IAC+T1250 (Trans.)

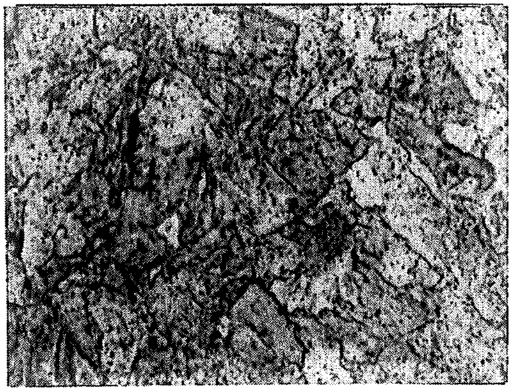

CRA (1650)+CR+IAC (SQ, 1050) (Long.)

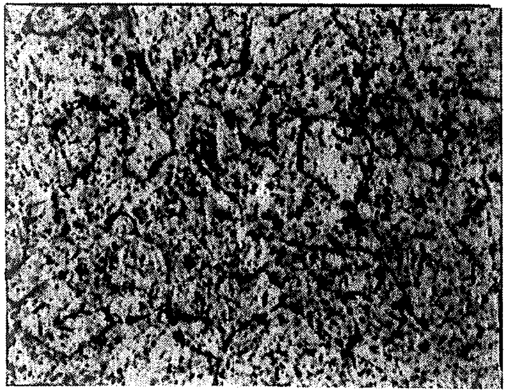

CRA (1650)+CR+IAC+T1250 (Long.)

X1000Nital-Picral

95-D057-39

Figure 26e Microstructures of Steel U Mechanically Tested Specimens (Sim. IAC 1650/1050)

Steel V

C	Mn	P	S	Si	Cu	Ni	Cr	Mo	V	Cb	Al	N
0.073	1.49	0.015	0.005	0.23	0.95	0.75	0.50	0.50	0.059	0.022	0.034	0.0064

HRA (1650)+IQ+T1175 (Trans.)

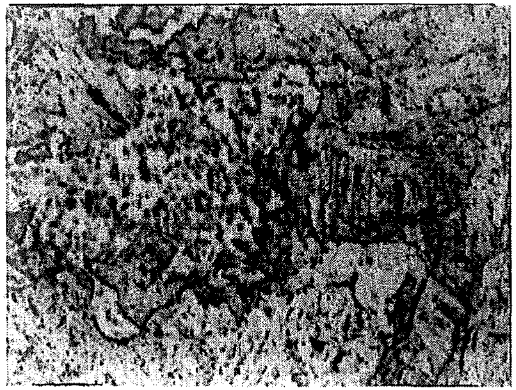

HRA (1650)+IQ+T1200 (Trans.)

HRA (1650)+IQ+T1275 (Trans.)

HRA (1650)+IQ+T1250 (Long.)

X1000Nital-Picral

95-D057-40

Figure 26f Microstructures of Steel V Mechanically Tested Specimens (HRA 1900)

Steel V

C	Mn	P	S	Si	Cu	Ni	Cr	Mo	V	Cb	Al	N
0.073	1.49	0.015	0.005	0.23	0.95	0.75	0.50	0.50	0.059	0.022	0.034	0.0064

CRDQ+T1175 (Trans.)

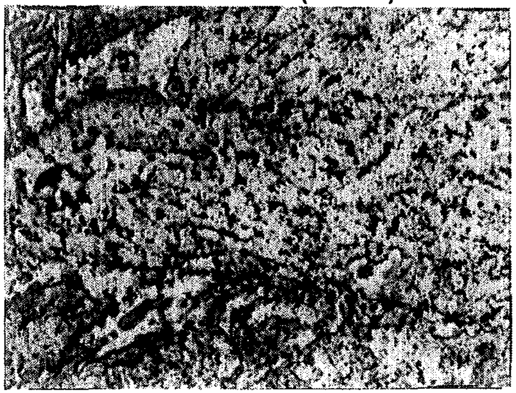

CRDQ+T1200 (Trans.)

CRDQ+T1275 (Trans.)

CRDQ+T1250 (Long.)

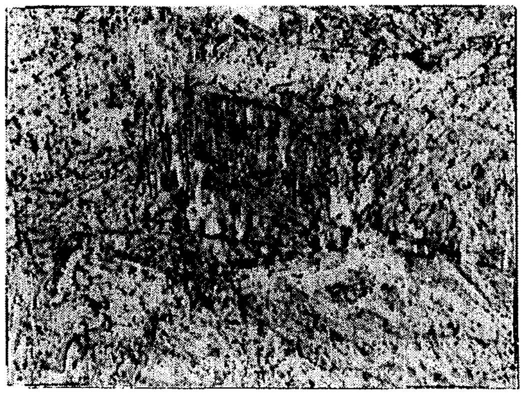

X1000Nital-Picral

95-D057-41

Figure 26g Microstructures of Steel V Mechanically Tested Specimens (CRDQ 1600)

Steel V

C	Mn	P	S	Si	Cu	Ni	Cr	Mo	V	Cb	Al	N
0.073	1.49	0.015	0.005	0.23	0.95	0.75	0.50	0.50	0.059	0.022	0.034	0.0064

CRA (1650)+IQ+T1175 (Trans.)

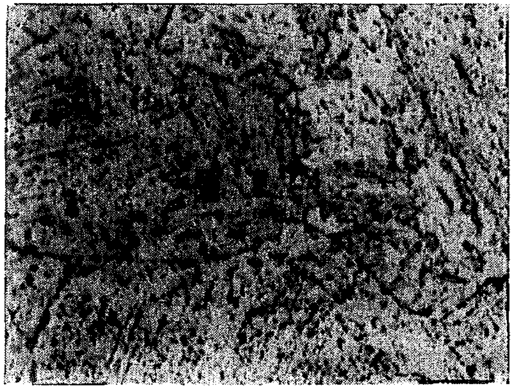

CRA (1650)+IQ+T1200 (Trans.)

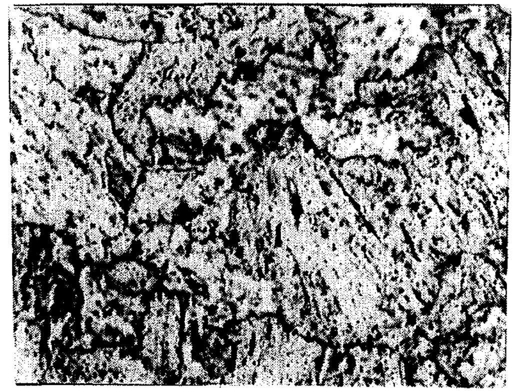

CRA (1650)+IQ+T1275 (Trans.)

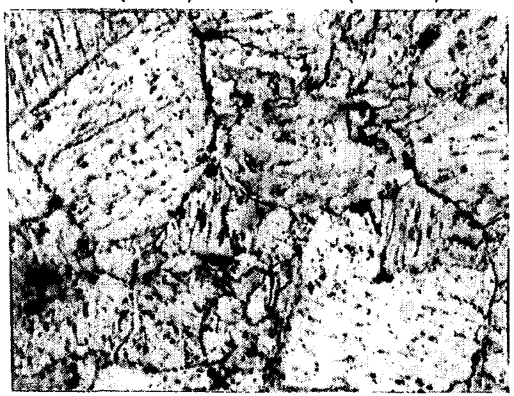

CRA (1650)+IQ+T1250 (Long.)

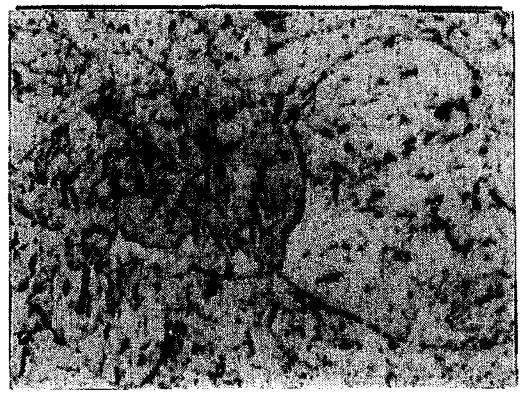

X1000Nital-Picral

95-D057-42

Figure 26h Microstructures of Steel V Mechanically Tested Specimens (CRA 1600)

a.

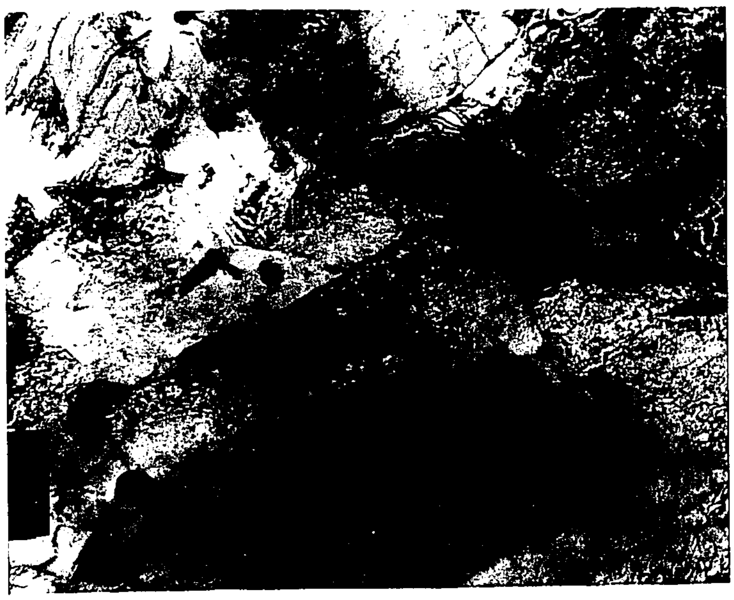

b.

Figure 27 a and b - Typical Cu-Ni HPS TEM Micrographs at (a) 46,000x and (b) 28,000x with dislocation within the grains and Cu-precipitates present in grain boundary.

c.

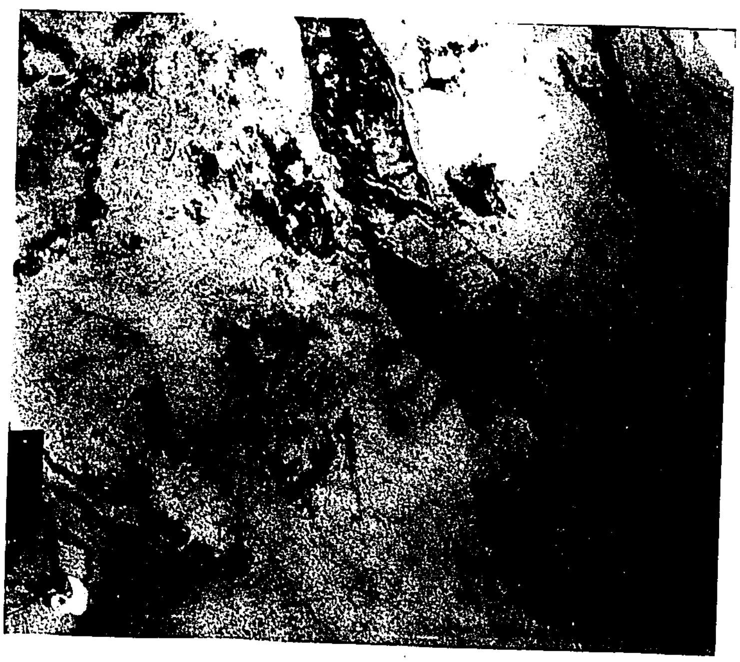

d.

Figure 27 c and d - Typical Cu-Ni HPS TEM Micrographs at (c) 46,000x and (d) 36,000x with dislocation present throughout the grains

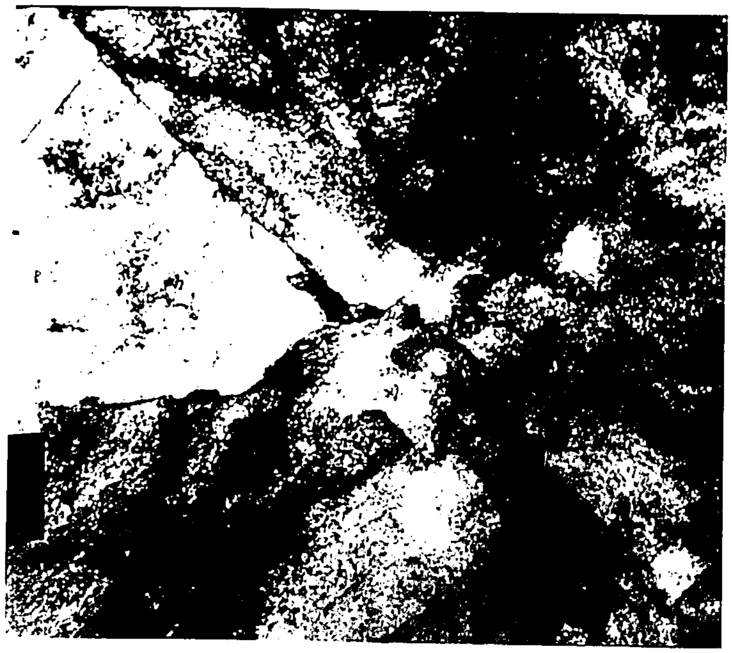

e.

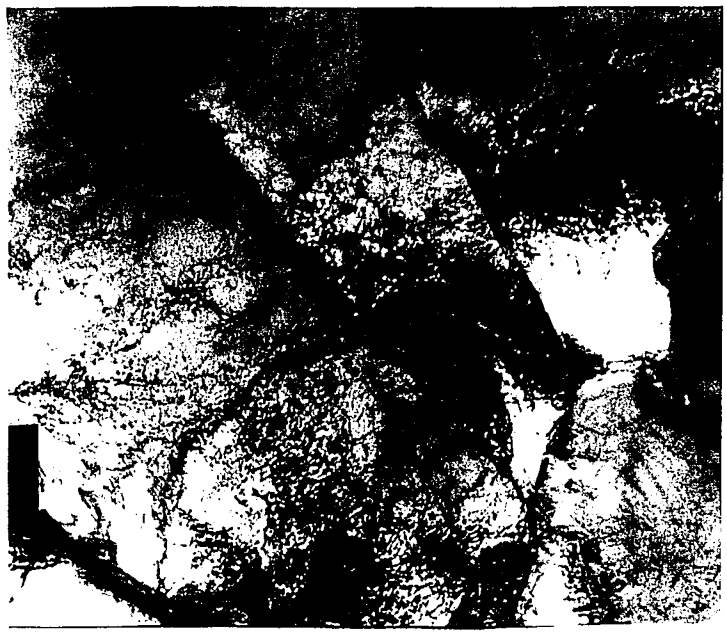

f.

Figure 27 e and f - Typical Cu-Ni HPS TEM Micrographs at (e) 17,000x and (f) 36,000x with dislocation present throughout the grains with some Cu-precipitates

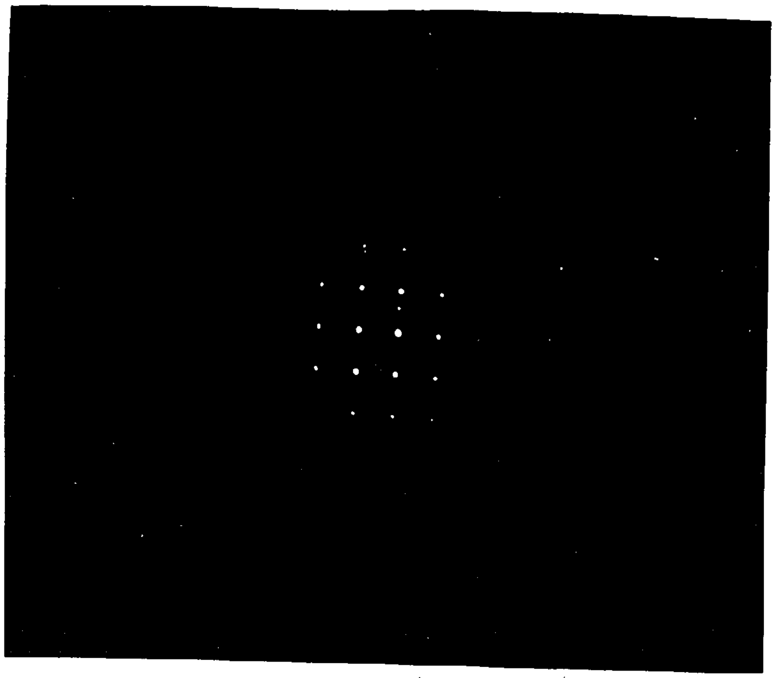

Figure 27 g - TEM Crystallographic representation of a typical Cu-precipitate with an FCC lattice structure

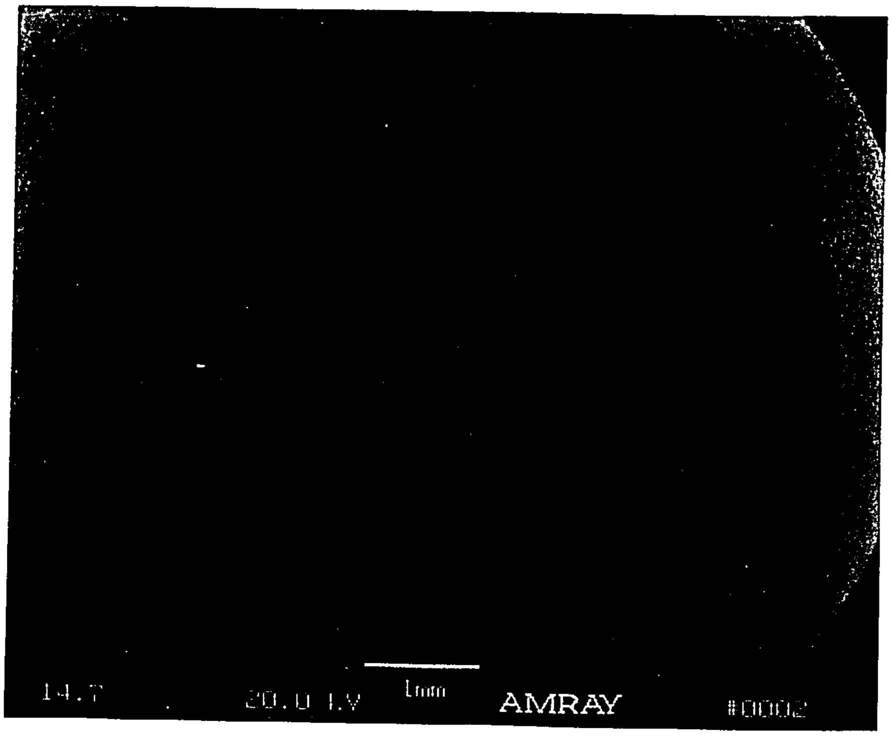

a.

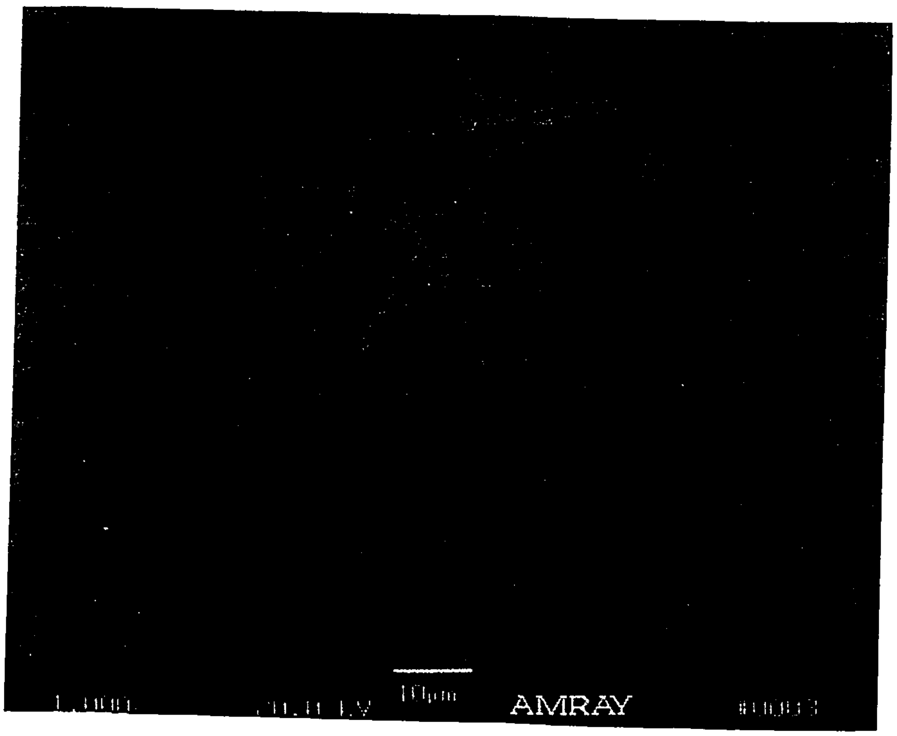

b.

Figure 28 a and b - Typical HPS tensile fracture surfaces of HRAQ specimens

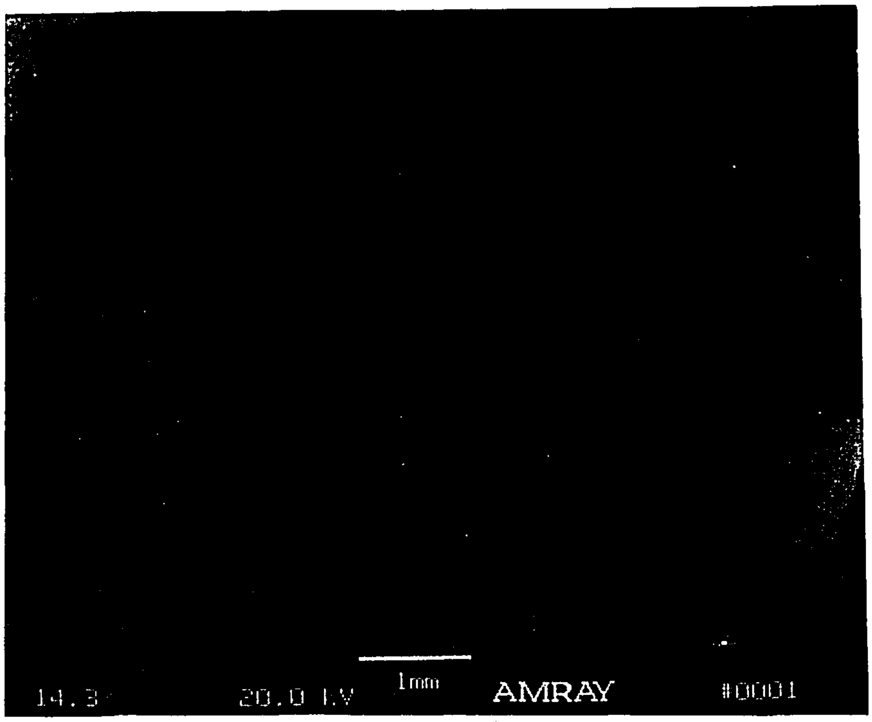

c.

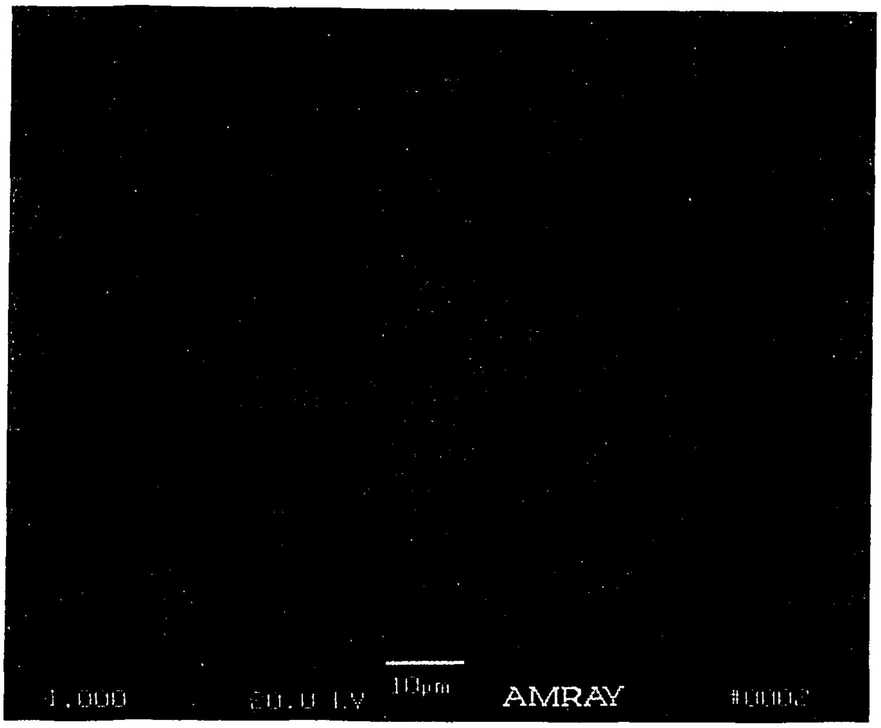

d.

Figure 28 c and d - Typical HPS tensile fracture surfaces of CRAQ specimens

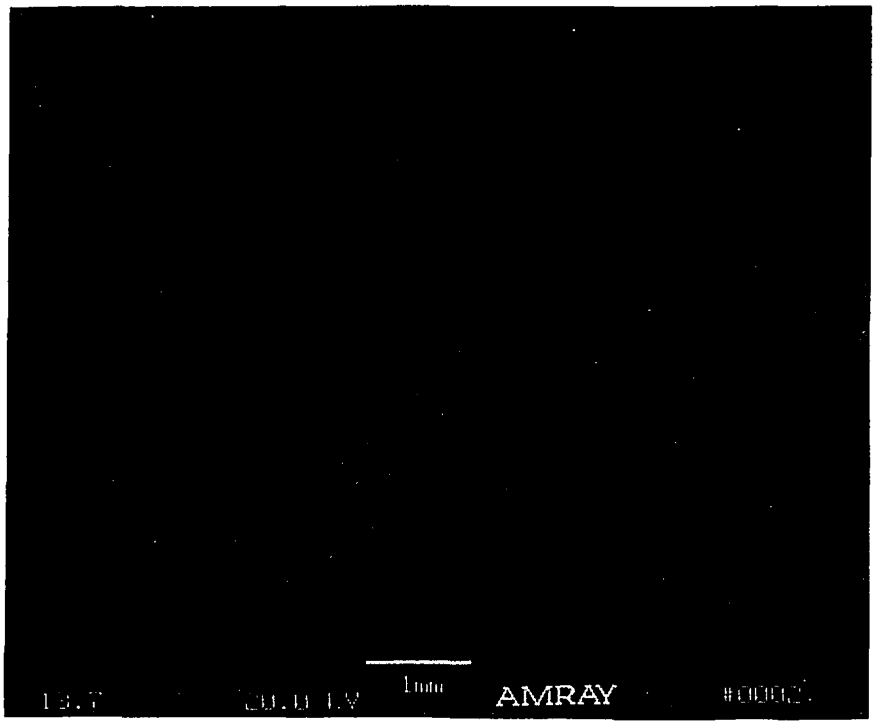

e.

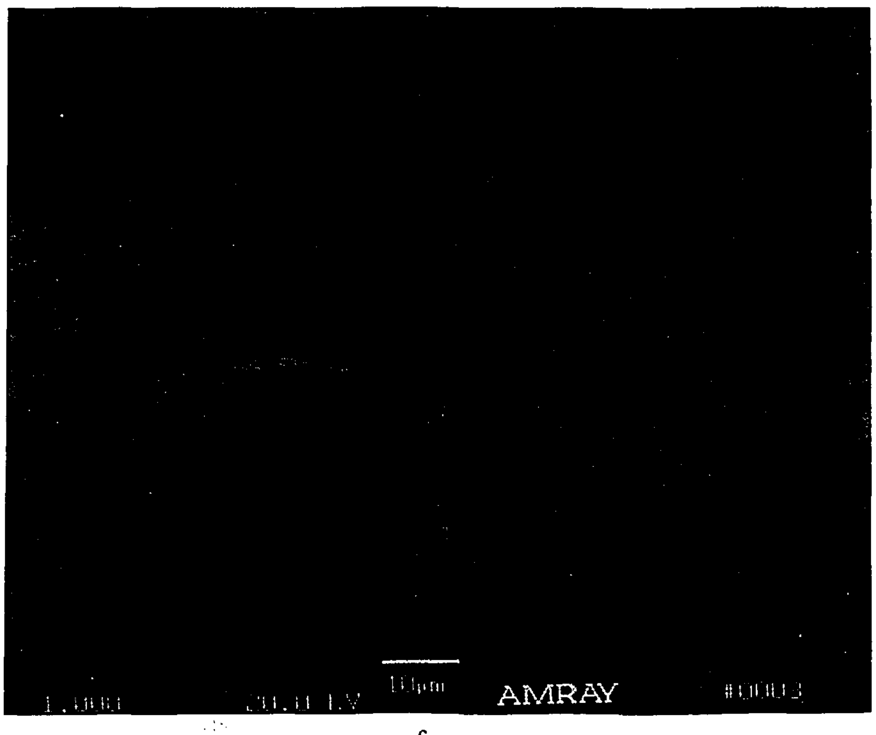

f.

Figure 28 e and f - Typical HPS tensile fracture surfaces of CRDQ specimens

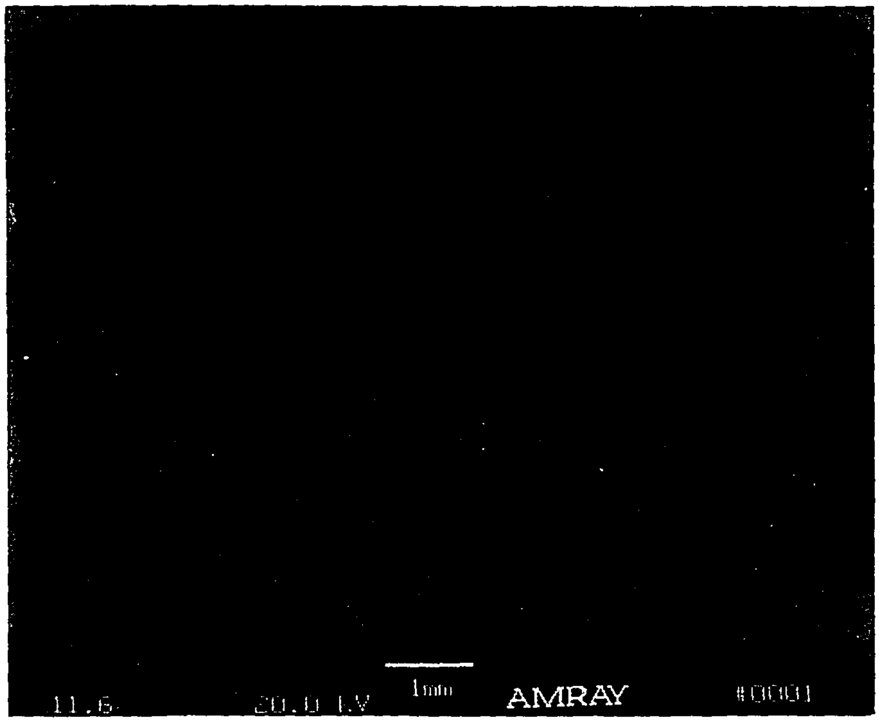

a.

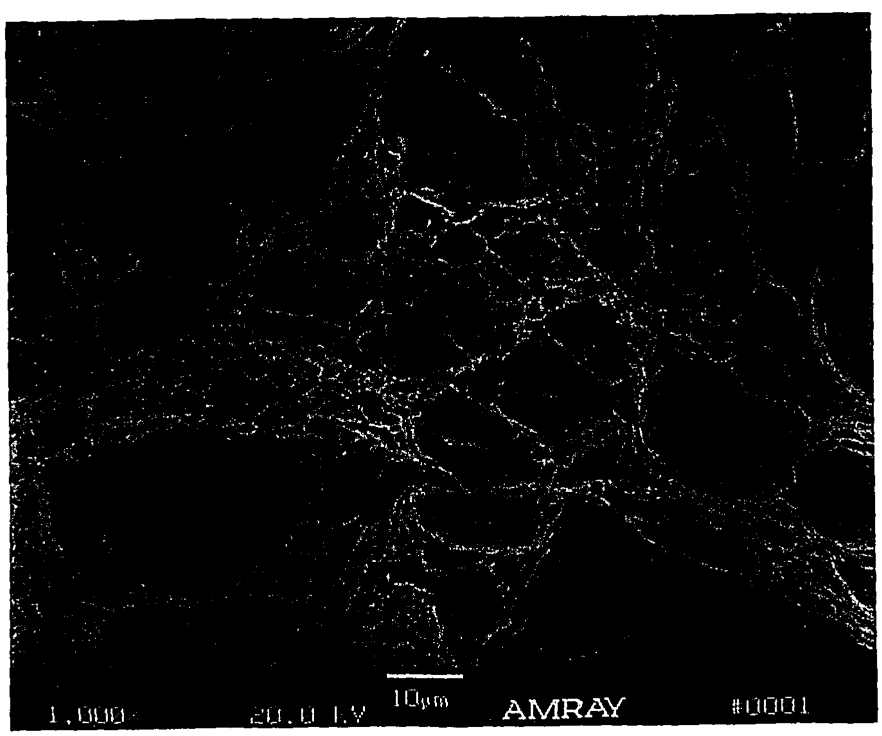

b.

Figure 29 a and b - Typical HPS CVN fracture surface at +70F

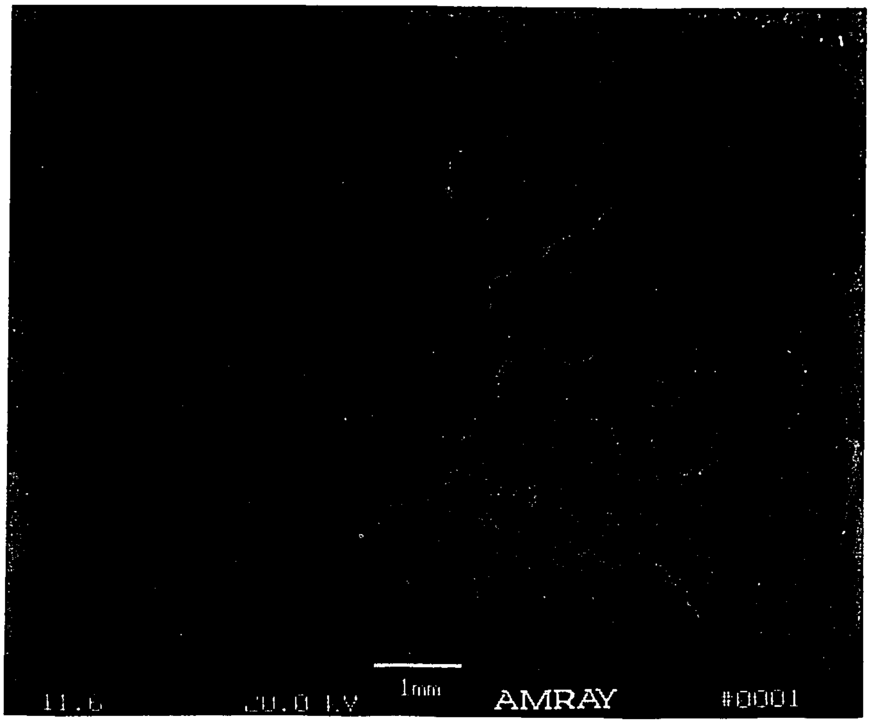

c.

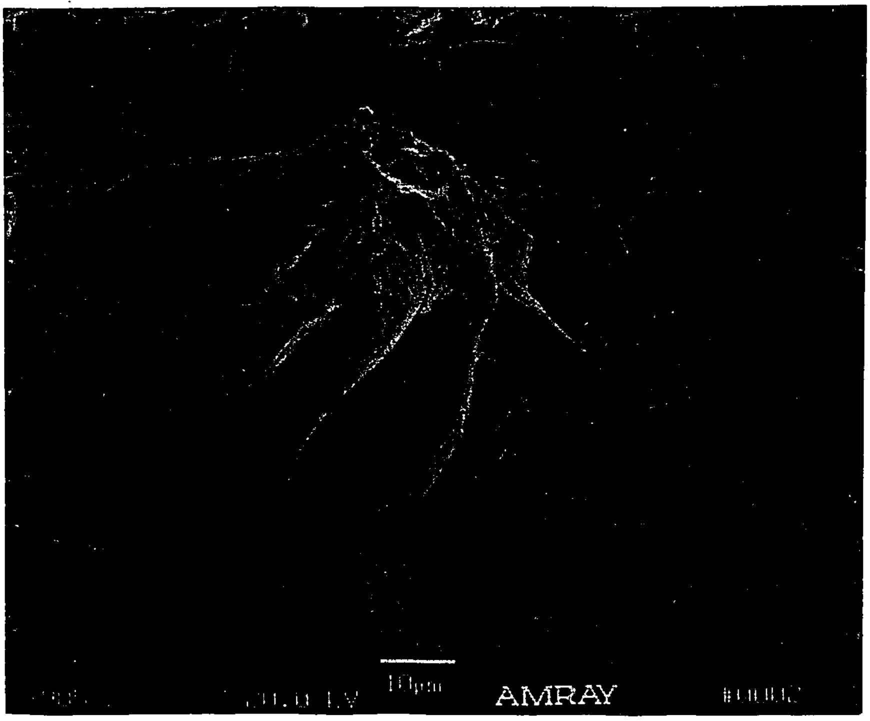

d.

Figure 29 c and d - Typical HPS CVN fracture surface at -40F

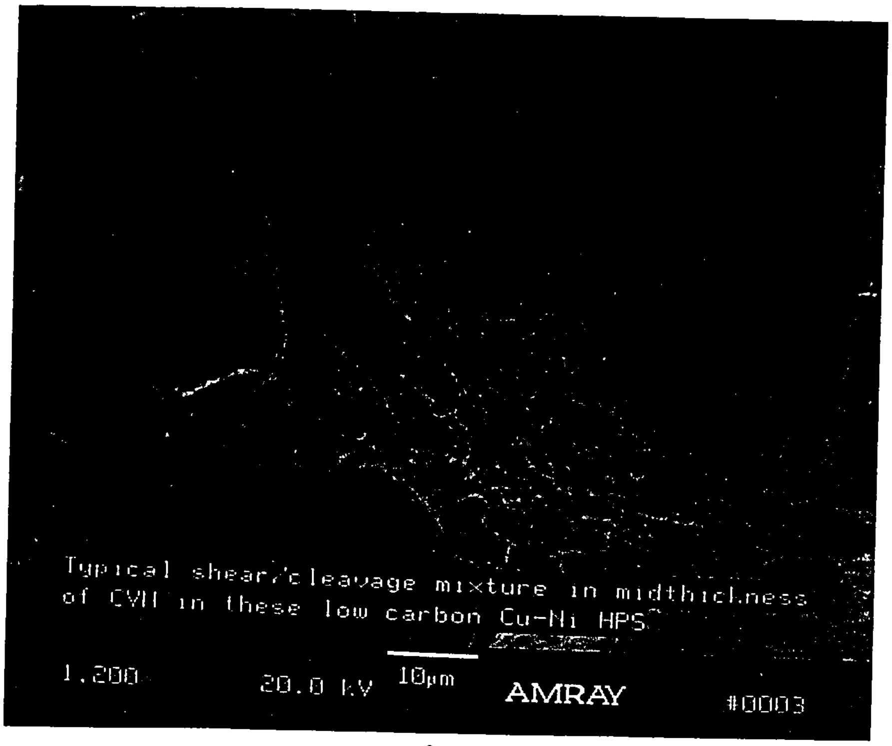

e.

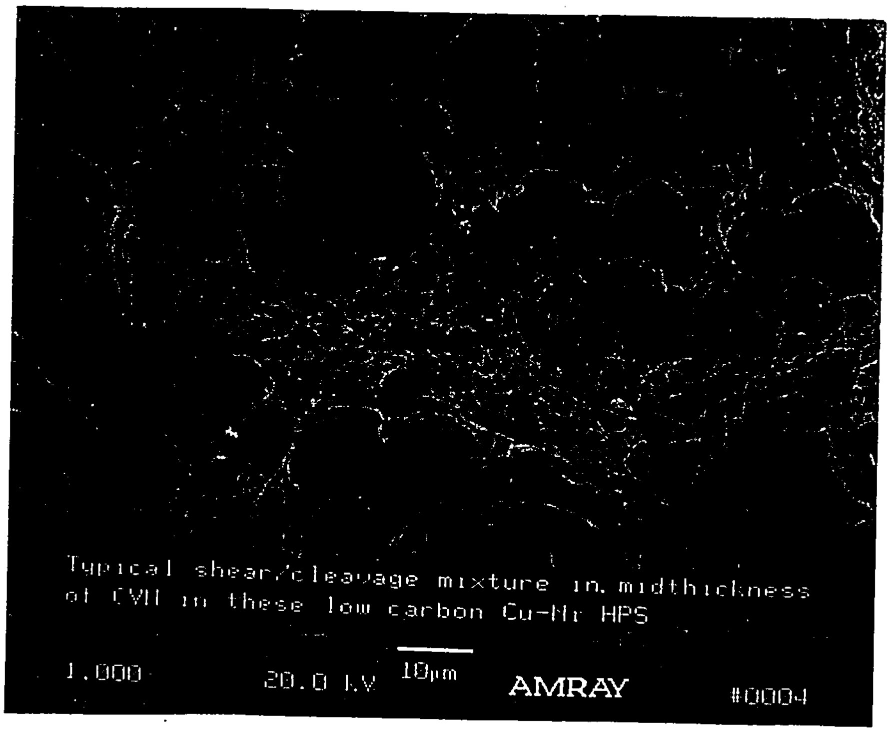

f.

Figure 29 e and f - Typical HPS CVN fracture surface with shear/cleavage mixed mode in midthickness.

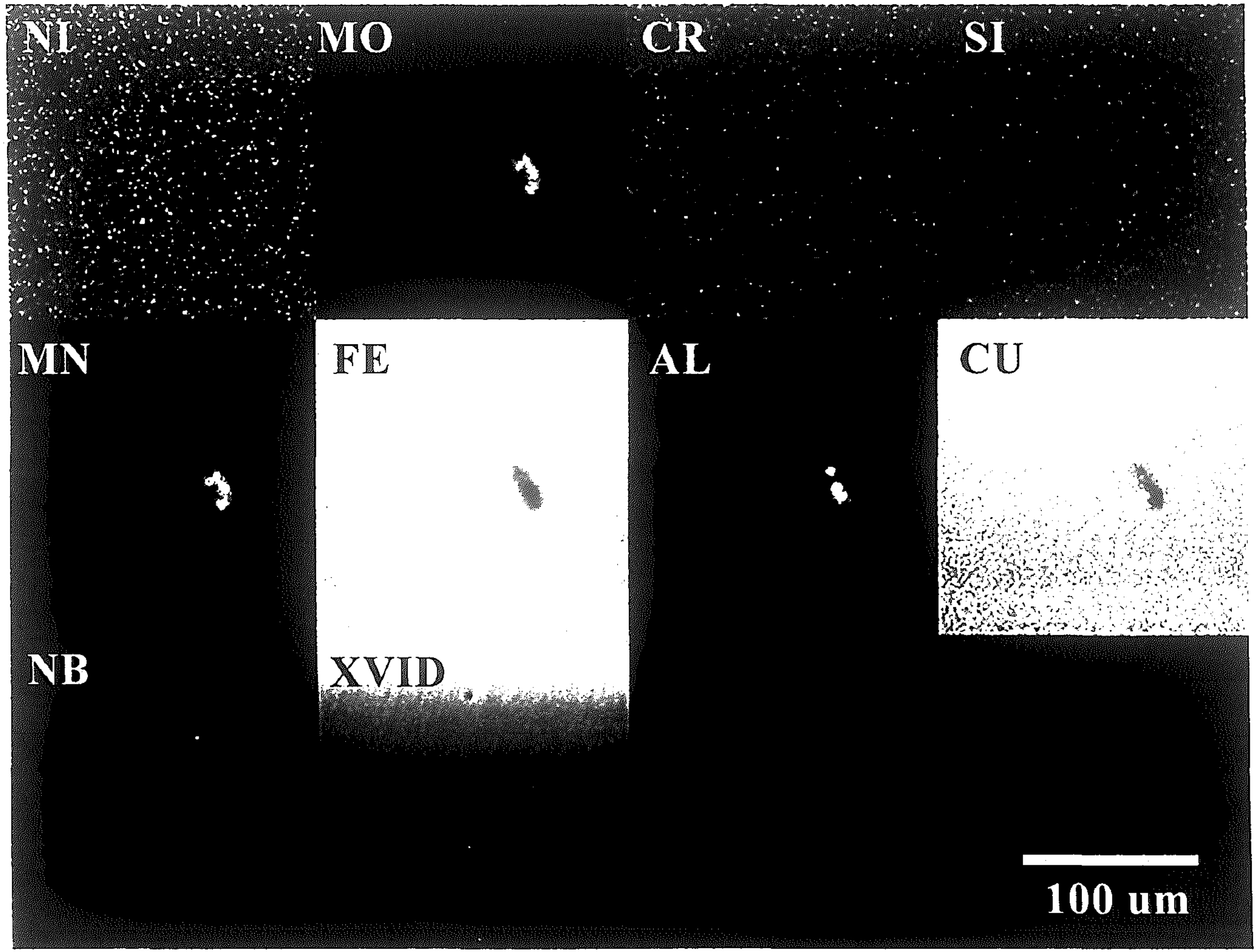

Figure 30 EDS Map of 0.07C, Cu-Ni HPS

Bibliography

1. Basham, K. D., Infrastructure: New Materials and Methods of Repair; Proceedings of the Third Materials Engineering Conference, New York, New York, November 13-14, 1994.

2. Fisher J. W. and R. J. Dexter, *High-Performance Steels for America's Bridges*, Preceedings of the National Symposium on Steel Bridge Construction, AISC, Atlanta, Ga., November 11, 1993; also in Welding Journal, January 1994, pp 37-43.

3. Dexter, R. J., M. Le-Wu Lu and J. W. Fisher, *Application of High-Performance Steel New and Retrofit Structures*; Infrastructure: New Materials and Methods of Repair; Proceedings of the Third Materials Engineering Conference, New York, New York, November 13-14, 1994.

4. Shaw, M. J., Infrastructure...Repairs and Inspection, American Society of Civil Engineers, New York, NewYork, 1987.

5. Albrecht, P., *"Corrosion Control of Weathering Steel Bridges,"* Corrosion Forms & Control for Infrastructure, ASTM STP 1137, Chaker, V. ed., American Standards for Testing Materials, Philadelphia, Pennsylvania, October 1992.

6. CERF Report 94-5011, *Materials for Tomorrow's Infrastructure: A Ten Year Plan for Deploying High-Performance Construction Materials and Systems;*, CERF, Technical Report, Washington D.C., 1994.

7. Dexter, R. J., et al, *Design and Manufacturing Bases for Double-Hull Ships*, Proceedings of the Second (1992) International Offshore and Polar Engineering Conference, Vol. 1, pp 100-107, 1992.

8. Fisher, J. W., Fatigue and Fracture of Steel Bridges, Wiley Interscience, New York, New York, 1984.

9. Stout, R. D., and J. H. Gross, *ATLSS Studies on Chemical Composition and Processing of High Performance Steels*, Report to FHWA-AISI, ATLSS Report No. 95-04, March 1995.

10. Somers, B. R. and P.T. Thompson, *The Weldability of Some 690 MPa (100 ksi) Minimum Yield Strength, Low-Carbon, Low-Alloy, Thermal-Mechanical Control*

Processed Steels, International Symposium on Low-Carbon Steels for the 90's, ASMI and TMS, pp 549-563, October 1993.

11. Gross, J. H., R. D. Stout, and E. J. Czyryca, *Thermomechanical Processing of HY-130 Steel*, Welding Journal, Vol. 74, No. 4, PP 53-62, 1995.

12. Chrisbacher C. J., T. J. Todaro, J. H. Gross, and R. D. Stout, *Thermomechanical Processing of Low-Carbon High Yield-Strength Steels, International Symposium on High-Performance Steels for Structural Applications*, ASMI, Cleveland, Ohio, October 30 - November 2, 1995.

13. Todaro, T. J., Studies on the Chemical Composition and Thermo-Mechanical Processing of High Performance Steels, Lehigh University Master's Thesis, Bethlehem, PA, 1993.

14. Wilson, A. D., E. G. Hamburg, D. J. Colvin, S. W. Thompson and G. Krauss, *"Properties and Microstructures of Copper Precipitation Aged Plate Steels,"* Microalloyed HSLA Steels-Conference Proceedings, ASM International, 1988, pp.259-275.

15. E. J. Czyryca, R. E. Link, R. J. Wong, D. A. Aylor, T. W. Montemarano, and J. P.Gudas, *"Development and Certification of HSLA-100 Steel for Naval Ship Construction,"* Naval Engineering Journal, May 1990, pp. 63-81.

16. Montemarano, B. P. Sack, J. P. Gudas, M. G. Vasilaros and H. H. Vanderveldt, *"High-Strength Low Alloy Steels in Naval Construction,"* Journal of Ship Production, Vol. 2, No. 3, August 1986, pp. 145-162.

17. Graville, B.A., *"Cold Cracking in Welds in HSLA Steels"*, Welding of HSLA (Microalloyed) Structural Steels, ASM, Rome, Italy, November 9-12, 1976.

18. Wilson, A. D., E. G. Hamburg and J. H. Bucher disscussion of J.C. West paper *"The Benefits of a Modified Chemistry, High Strength, Low Alloy Steel"*, Journal of Ship Production, Vol. 3, No. 2, May 1987, pp 114-115.

19. Speich, G. R., and T. M. Scoonover, *"Continuous-Cooling-Transformation Behavior of HSLA-80 (A710) Steel"*, presented TMS AIME Symposium on Processing, Microstructure and Properties of HSLA steels, November 1987, Pittsburgh.

20. Proceedings of the International Conference on *Processing, Microstructure, and Properties of Microalloyed and Other Modern High-Strength Low-Alloy Steels*, Edited by A. J. DeArdo, ISS, June 3-6, 1994.

21. Proceedings of the International Symposium on *Low-Carbon Steels for the 90's*, Edited by R. Asfahani and G. Tither, ASMI and TMS, November 18-21, 1993.

22. Research on *Modern High-Strength Low-Alloy Steels*, Bulletin 373, Welding Research Council, June 1992.

23. Stout, R. D., Weldability of Steels, 4th ed., Welding Research Council, New York, New York, 1987.

24. *Guide to Weldability and Metallurgy of Welding of Steels Processed by Thermomechanical Rolling or by Accelerated Cooling*, Subcommittee IXA, International Institute of Welding, Paper No. IX-1649-91, 1991.

25. Lundin, C. D., et al, *Weldability of Low-Carbon Microalloyed Steels for Marine Structures*, Bulletin 359, Welding Research Council, December 1990.

26. Proceedings of International Conference on The Metallurgy, Welding, and Qualification of Microalloyed (HSLA) Steel Weldments, Edited by Hickey, Howden, and Randall, AWS, November 6-8, 1990.

27. Hertzberg, R. W., Deformation and Fracture Mechanics of Engineering Materials, 2nd Ed., John Wiley and Sons, New York, New York, 1989.

28. Schrader, A., and A. Rose, De Ferri Metallographia- Metallographic Atlas of Iron, Steels, and Cast Irons II, W.B. Saunders Company, Philadelphia, PA, 1966.

29. Samuels L. E., Optical Microscopy of Carbon Steels, ASM, Metals Park, Ohio, 1980.

30. Le May, I and L McDonald Schetky, Copper In Iron and Steel, John Wiley & Sons, New York, 1982.

Vita

The author was born to Novel Jean Taplin-Magee in the vast "city of angels" South Central Los Angeles, California on August 13, 1969. Sibilings are older brother Reginald Bernard Taplin and older sister Geraldine Denise Taplin. As an art and science major he graduated from Westchester High School in June 1987. In December of 1993, the author received a Bachelor of Science degree in Industrial Engineering from California State University at Northridge. Currently, he attends Lehigh University in candidacy for the degree of Master of Science in Materials Science and Engineering. Funded by the NSF and the Oak Ridge Institute for Science and Education (ORISE) he works as an ATLSS Graduate Research Scholar under the guidance of Dr. Robert D. Stout and Dr. John H. Gross.

END OF
TITLE